Petroleomics

From crude oil to asphaltenes

Dr. Matthias Witt, Senior Scientist MRMS, Bruker Daltonics GmbH & Co. KG, Bremen, Germany

Content

Introduction

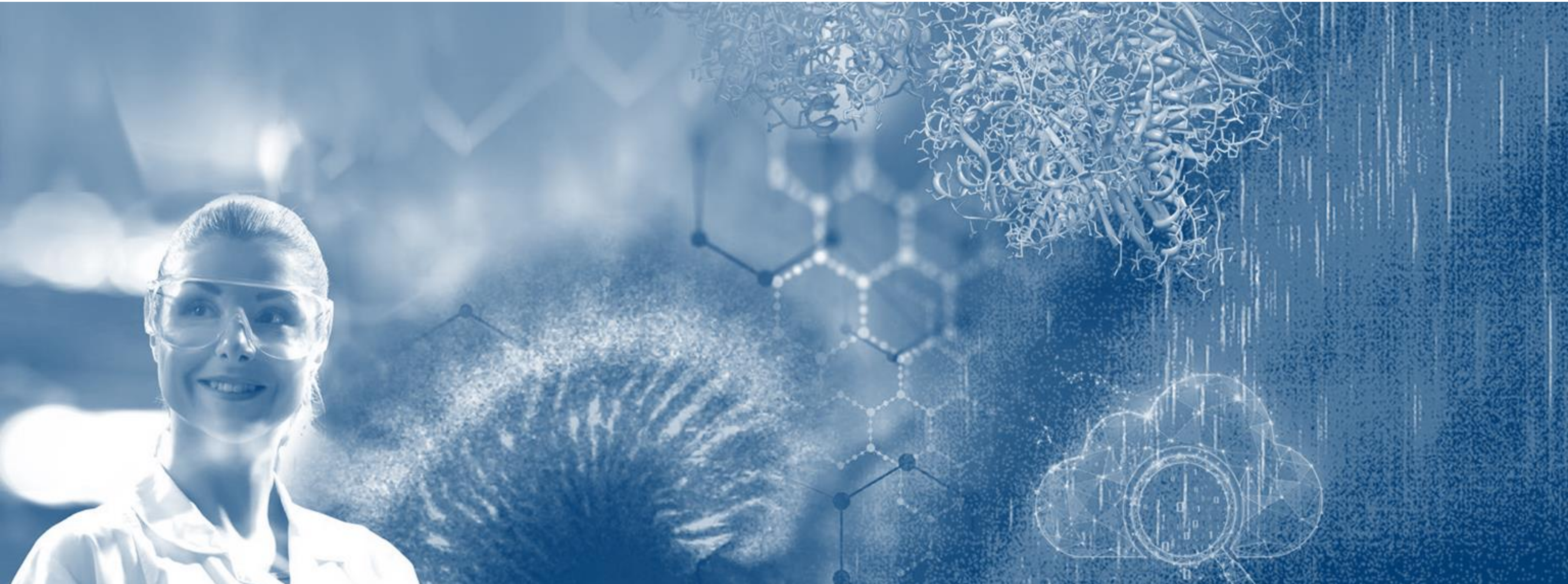

Introduction

Upstream, Midstream and Downstream

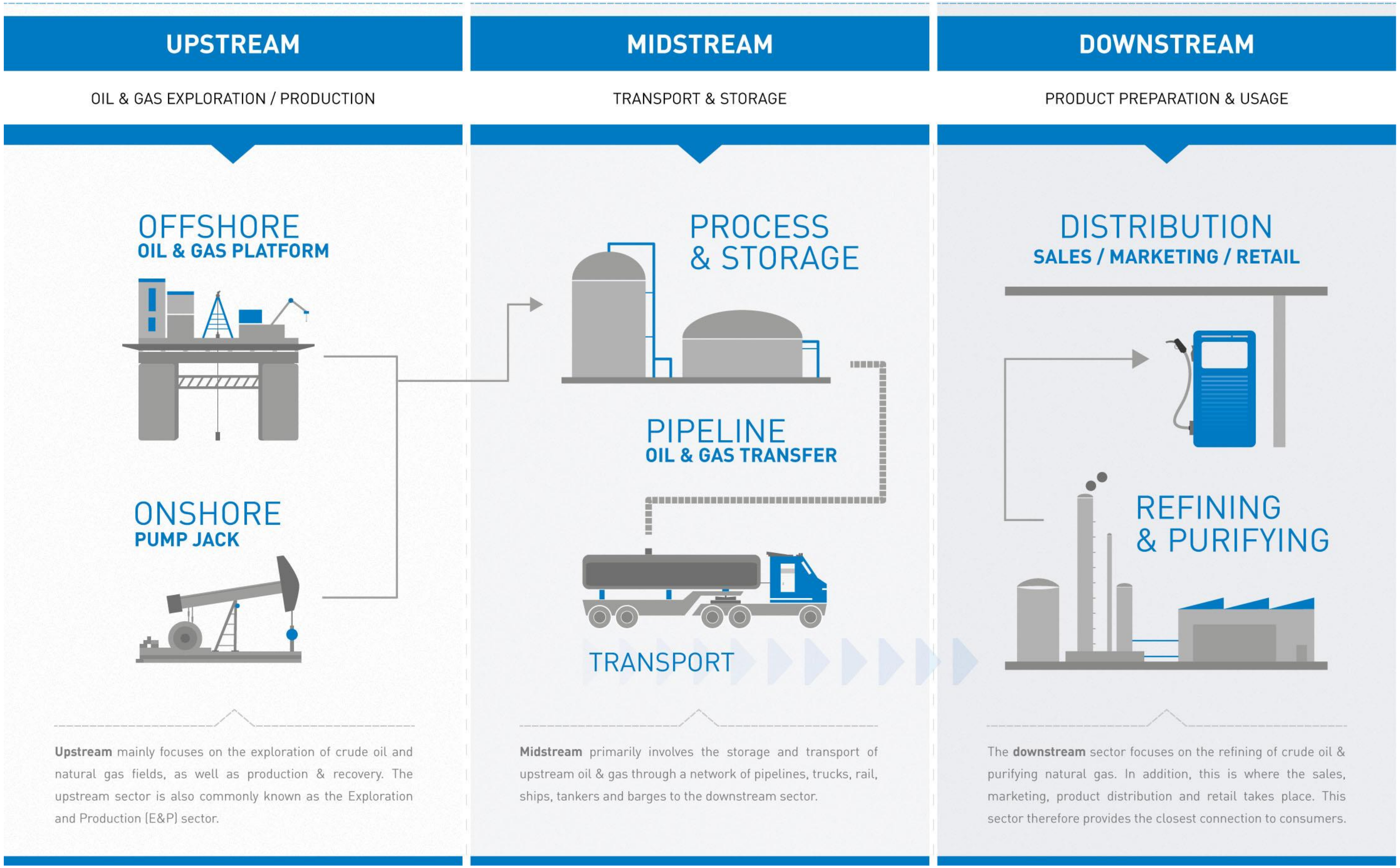

https://www.ecom-ex.com/de/loesungen/branchen/oel-und-gasindustrie/

Introduction

Petroleum products – different cuts

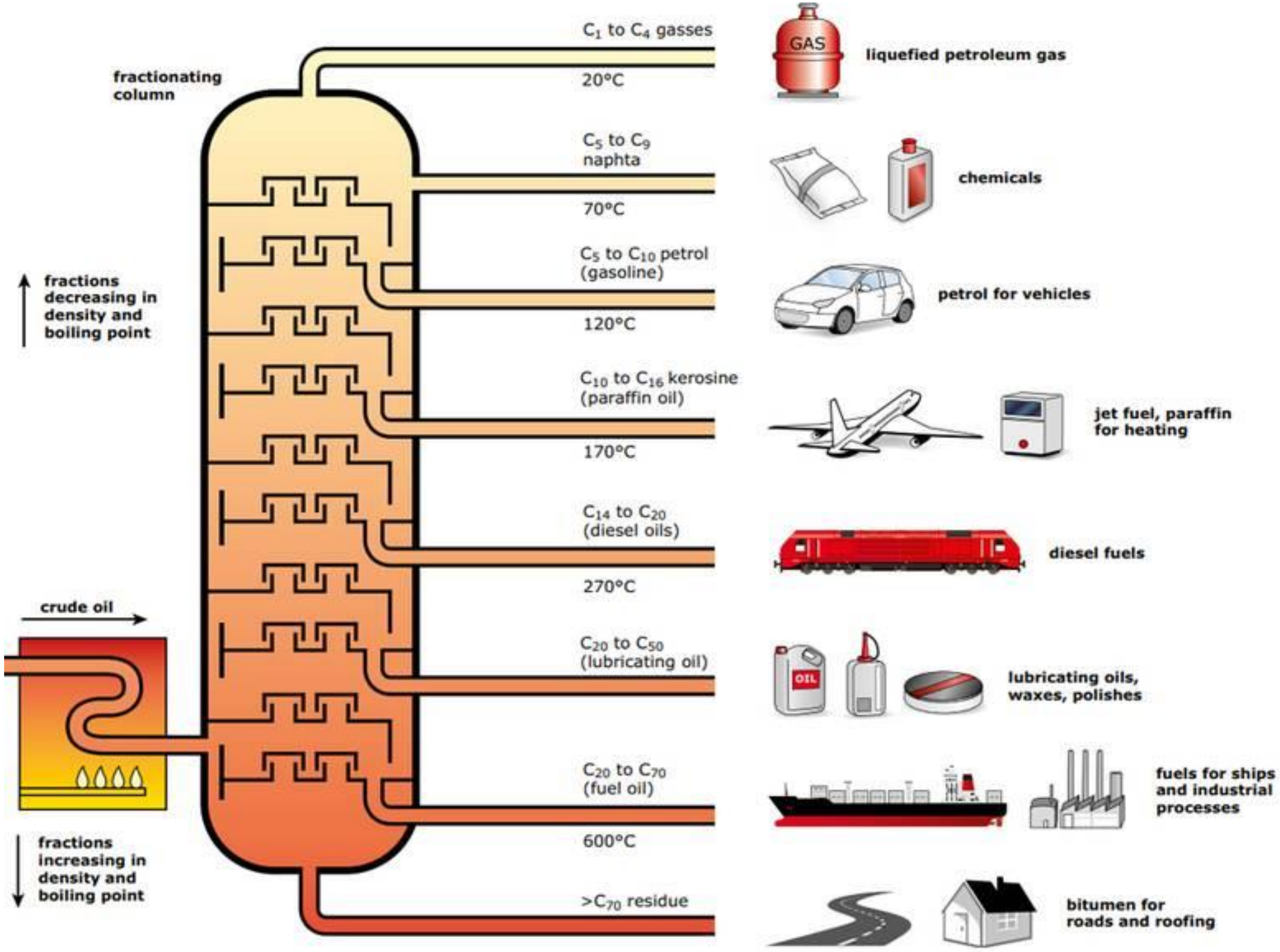

Introduction

Effect of molecular structure on boiling point

Boduszynski Continuum Model

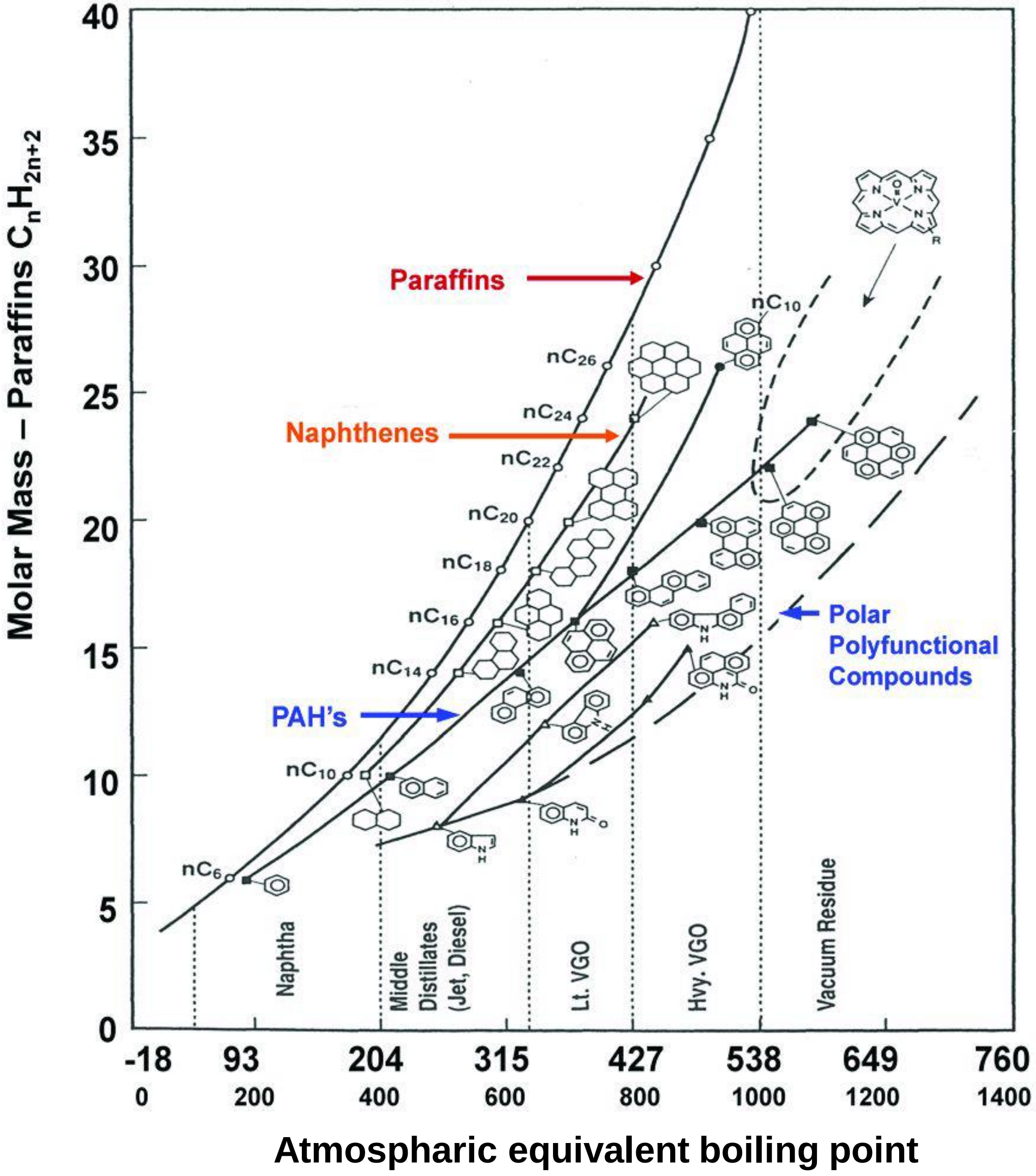

M. Boduszynski, Energy & Fuels 1987, 1, 2-11. *(1st paper in E&F)*

Introduction

SARA Fractionation

K. Akbarzadeh et al., Oilfield Review, Asphaltenes - Problematic but Rich in Potential, 2007.

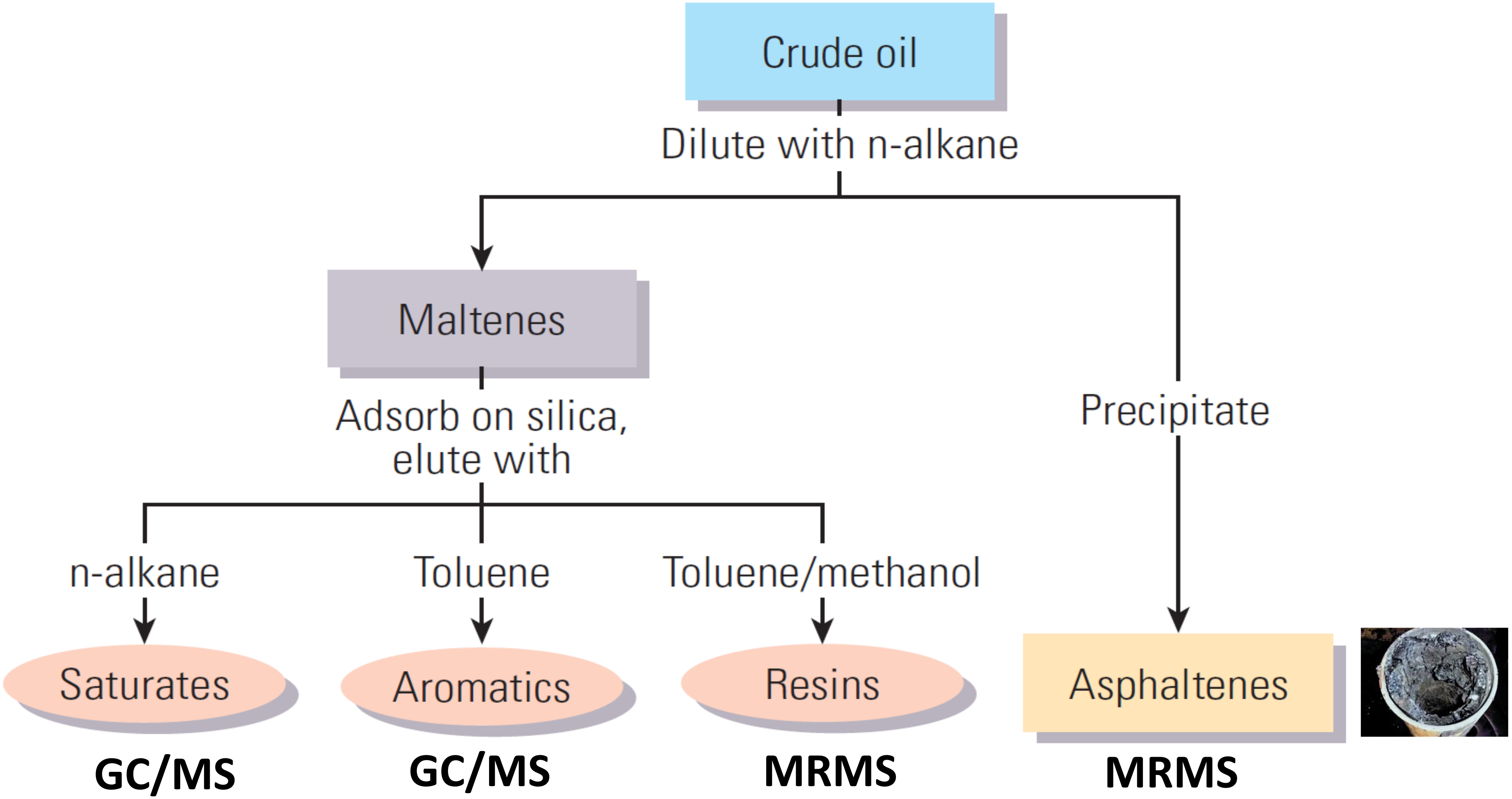

Introduction

Mass resolution and mass accuracy

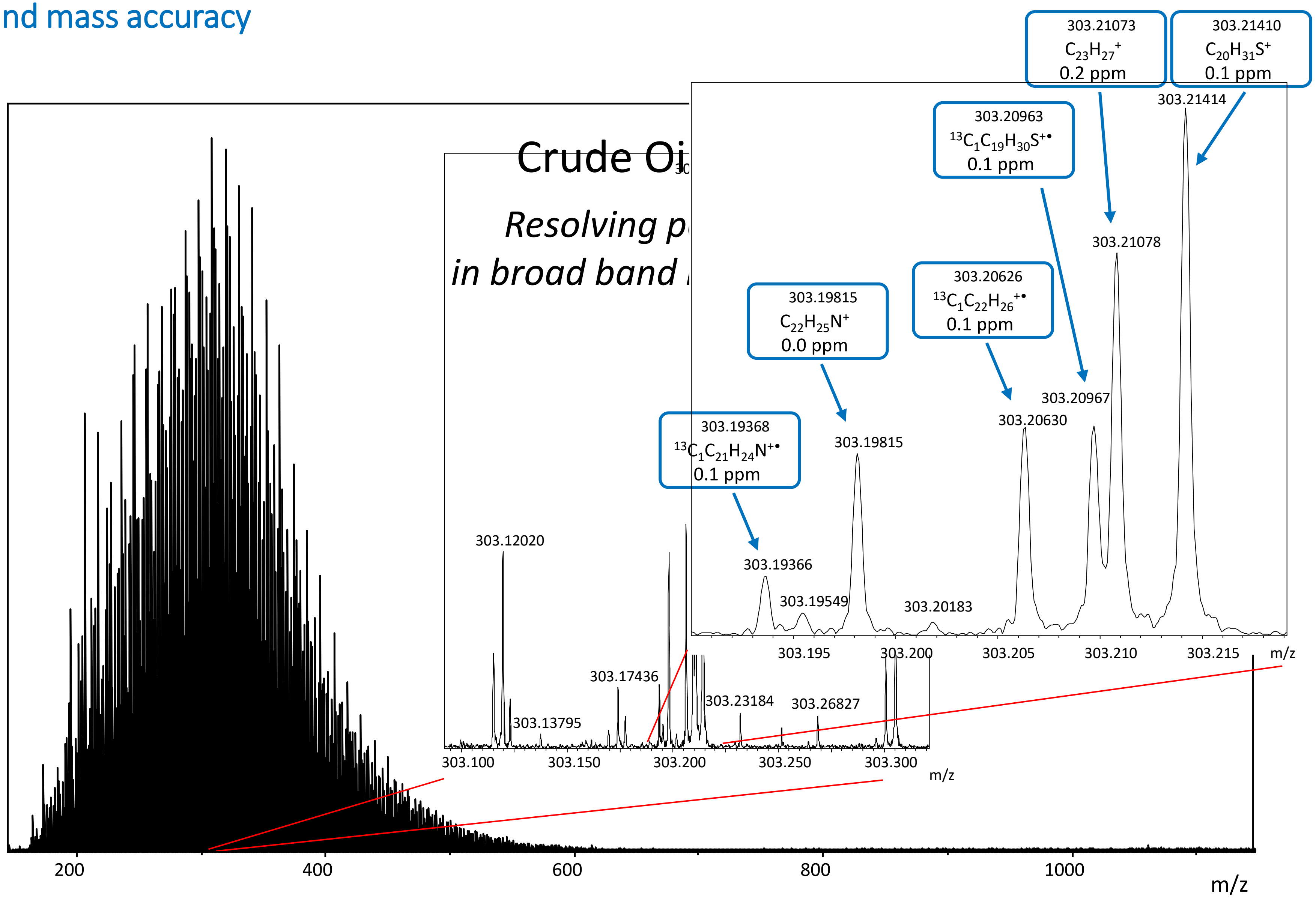

Introduction

Isotopic fine structure (IFS)

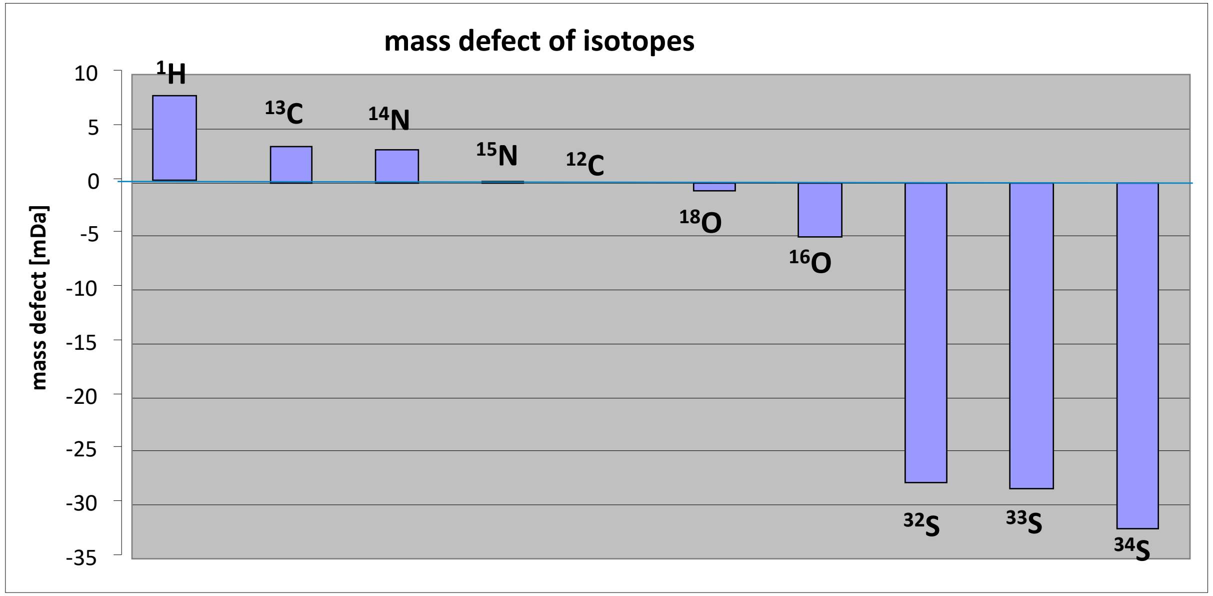

Δm (C_3;SH_4): 3.4 mDa

Δm ($^{13}C_2$;CN): 3.6 mDa

Δm (^{13}C;CH): 4.5 mDa

Δm (C_4H;$^{13}CSH_4$): 1.1 mDa

Δm(^{32}S;^{34}S) = 1.9959 Da

Δm($^{12}C_2$;$^{13}C_2$) = 2.0067 Da

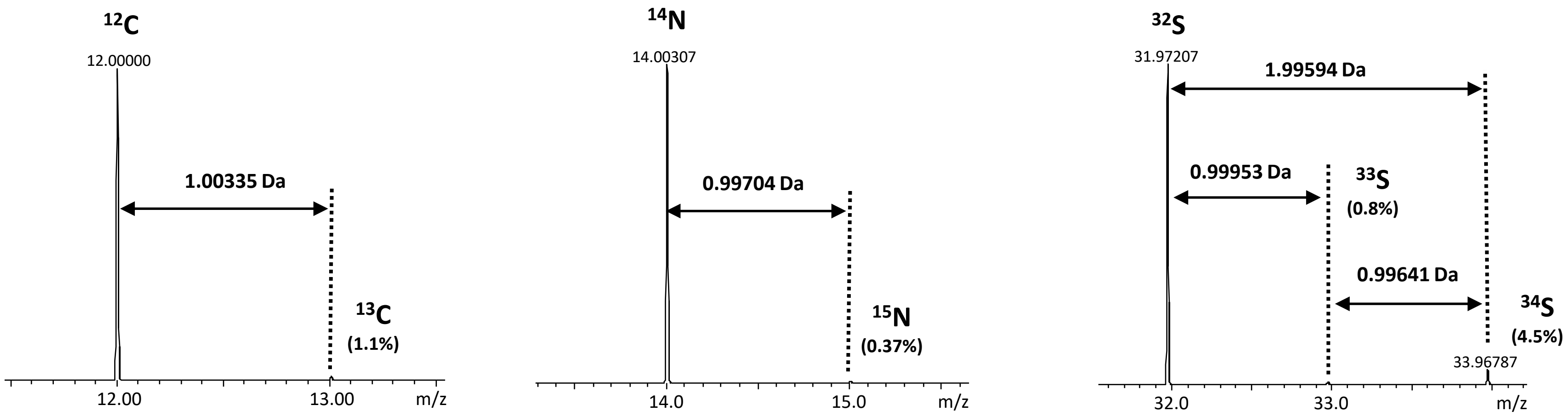

Introduction

Processing workflow in Petroleomics using PetroOrg

Internal recalibration

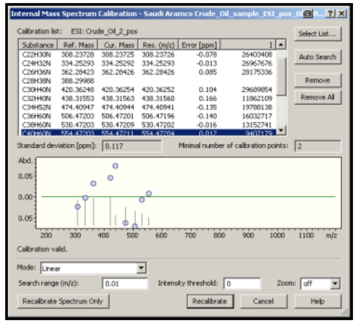

Export mass spectrum

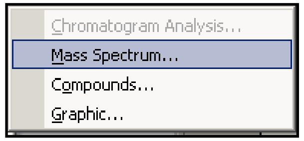

PetroOrg software Molecular Formula calculation

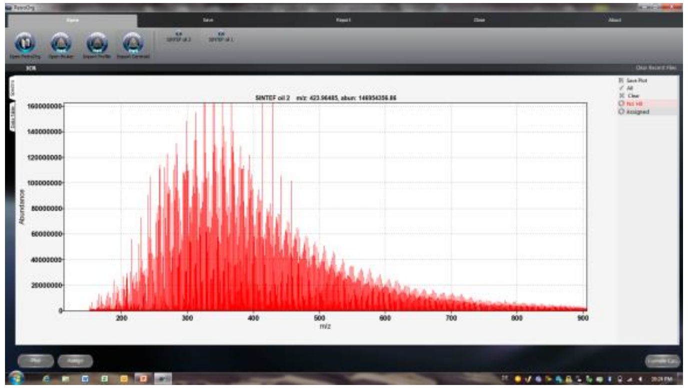

Mass spectrum

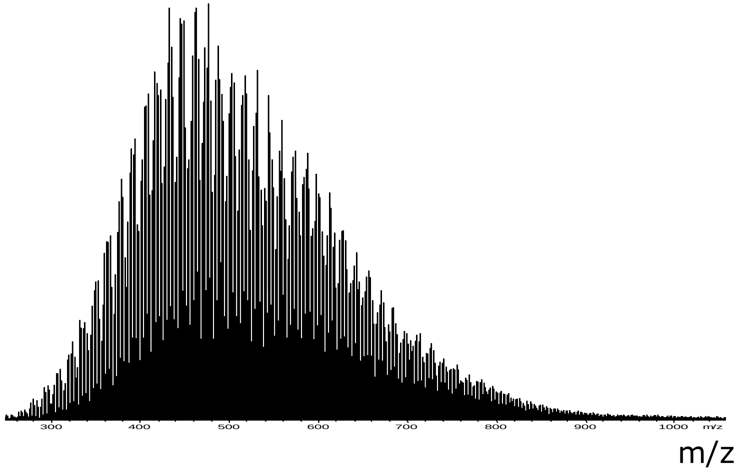

Class distribution plot

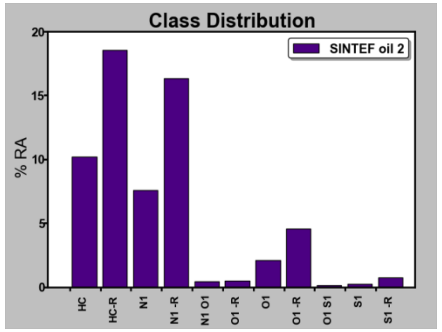

DBE vs. C plot

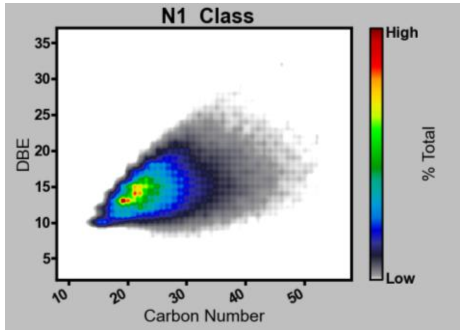

Introduction

Processing workflow in Petroleomics using PetroOrg

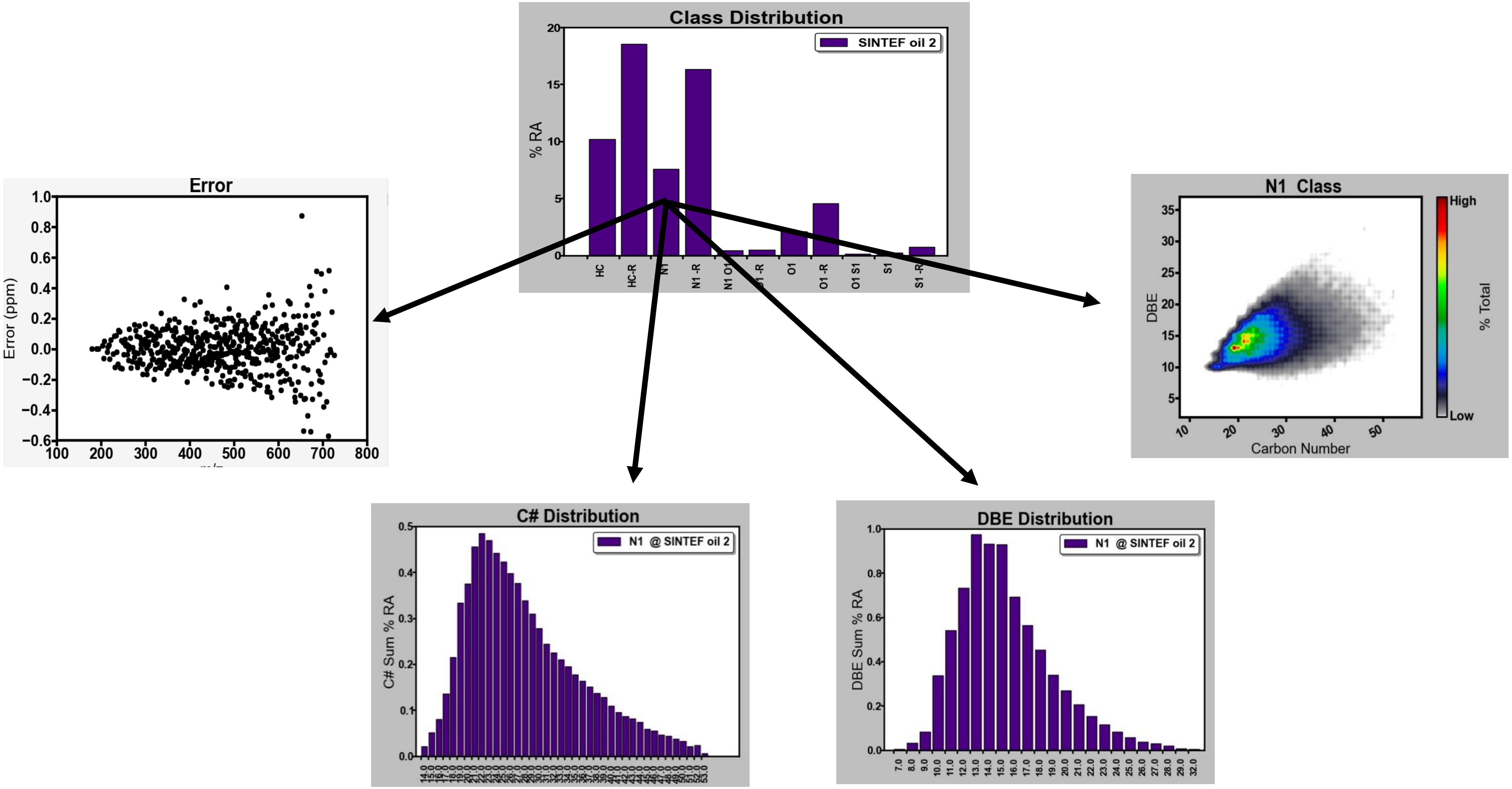

Introduction

Ionization methods for Petroleomics

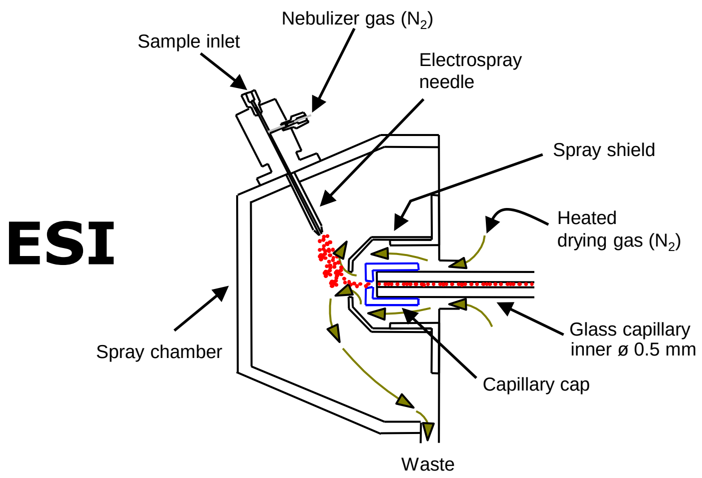

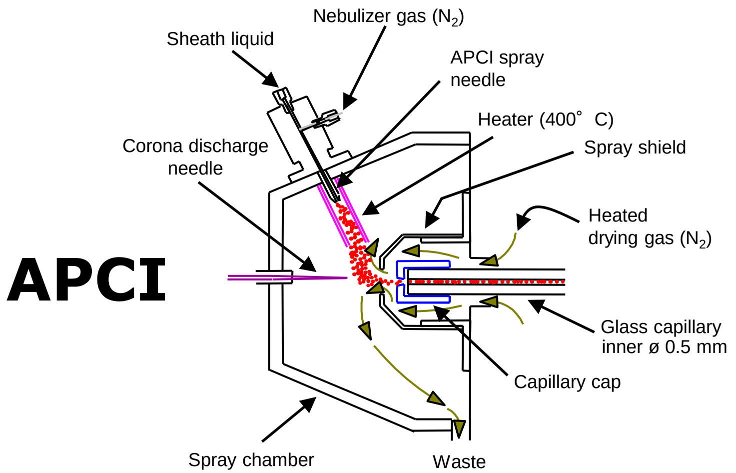

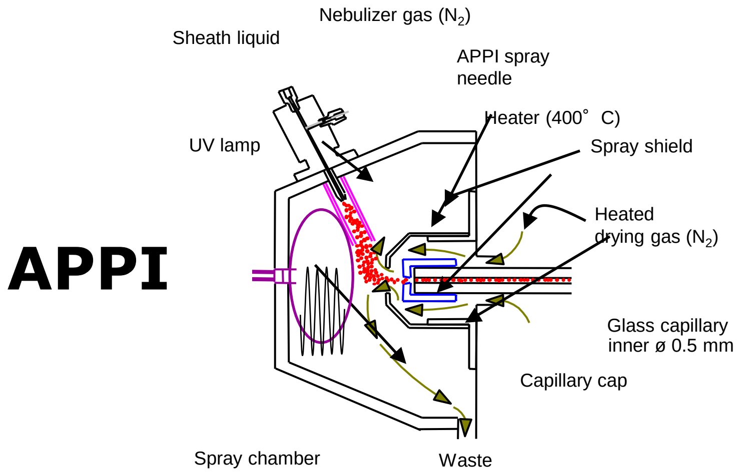

Introduction

Effect of Ionization methods – positive ion mode

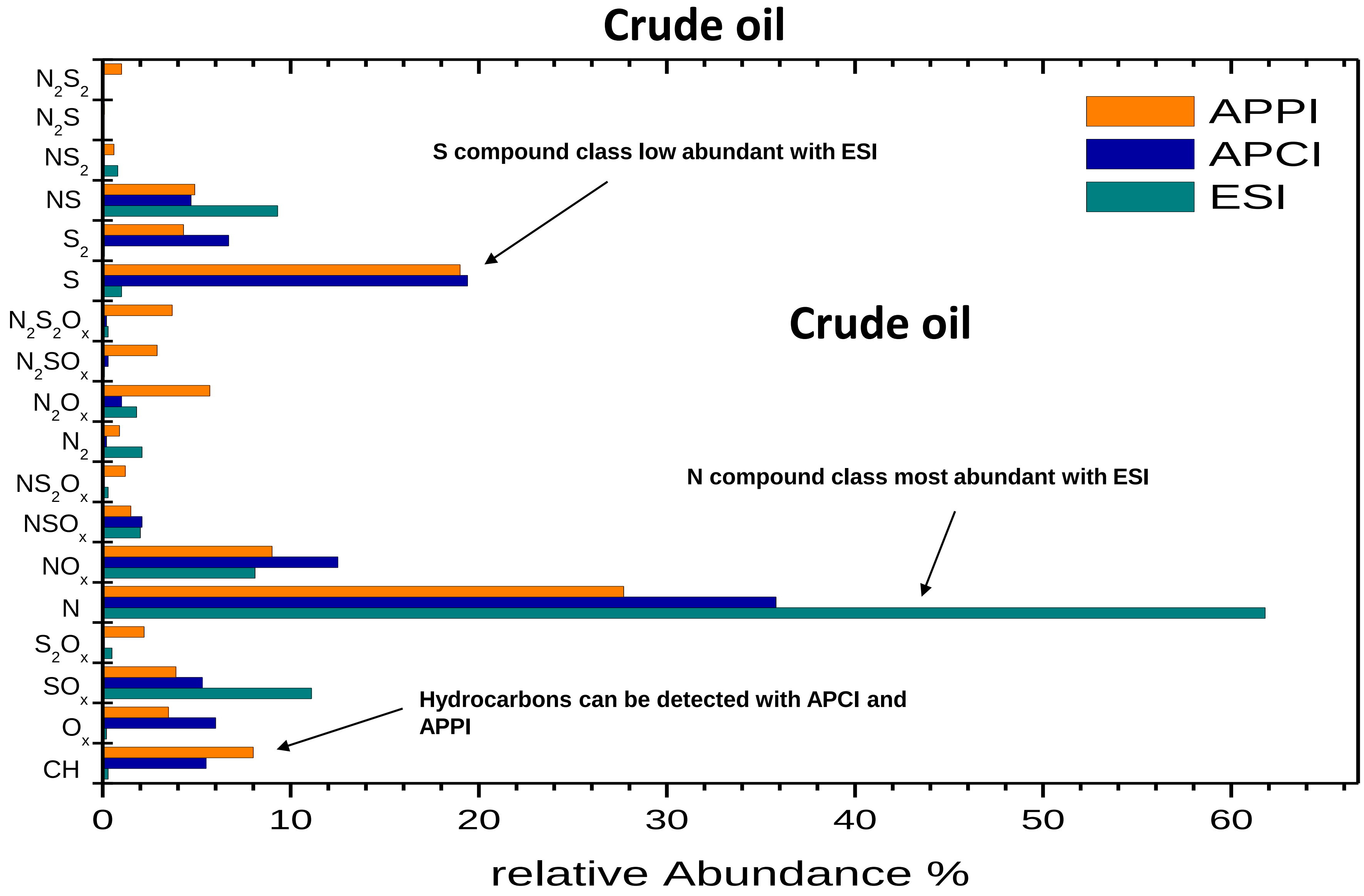

Introduction

Effect of Ionization methods – negative ion mode

Crude oil

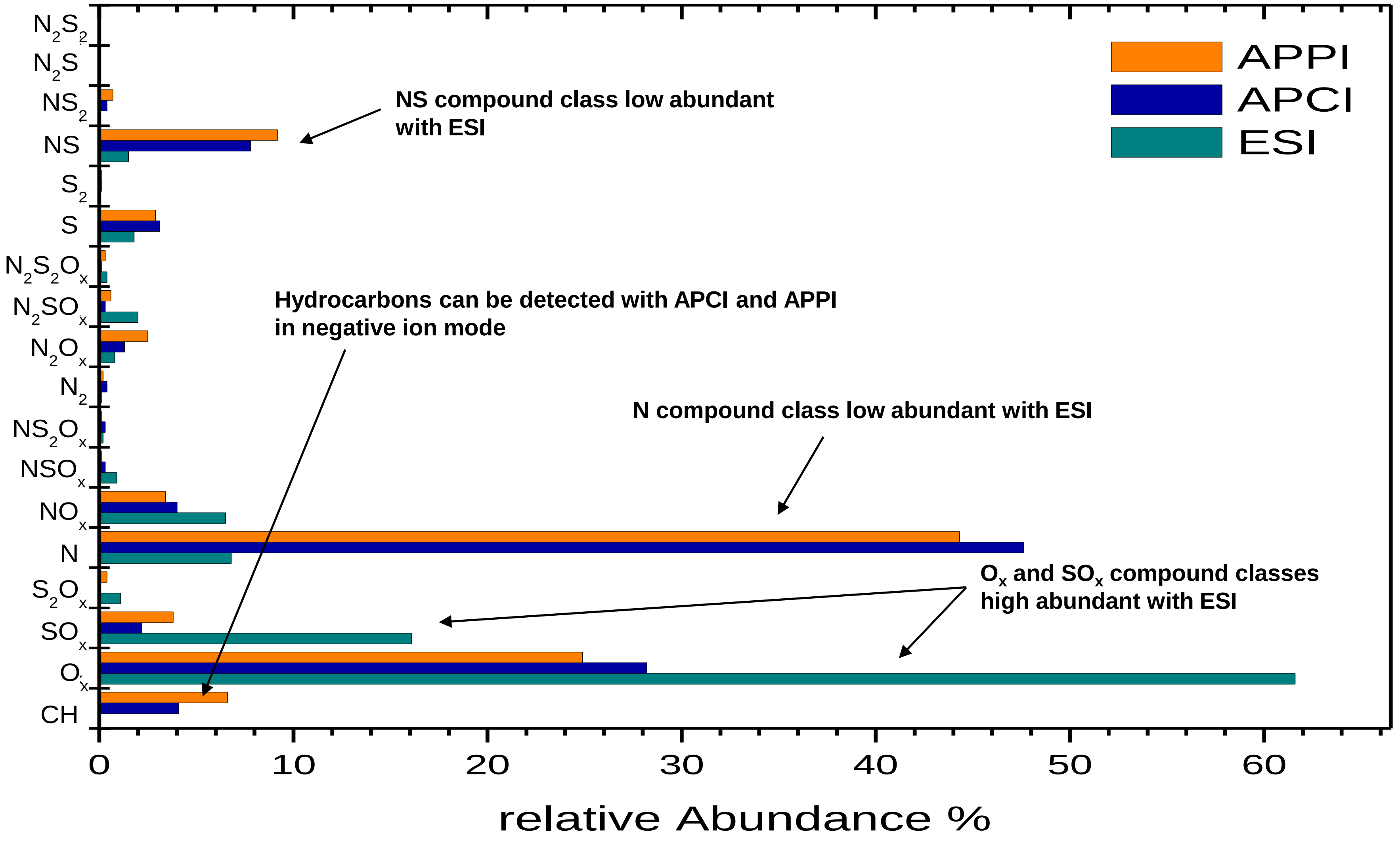

Introduction

Ionization method for Petroleomics

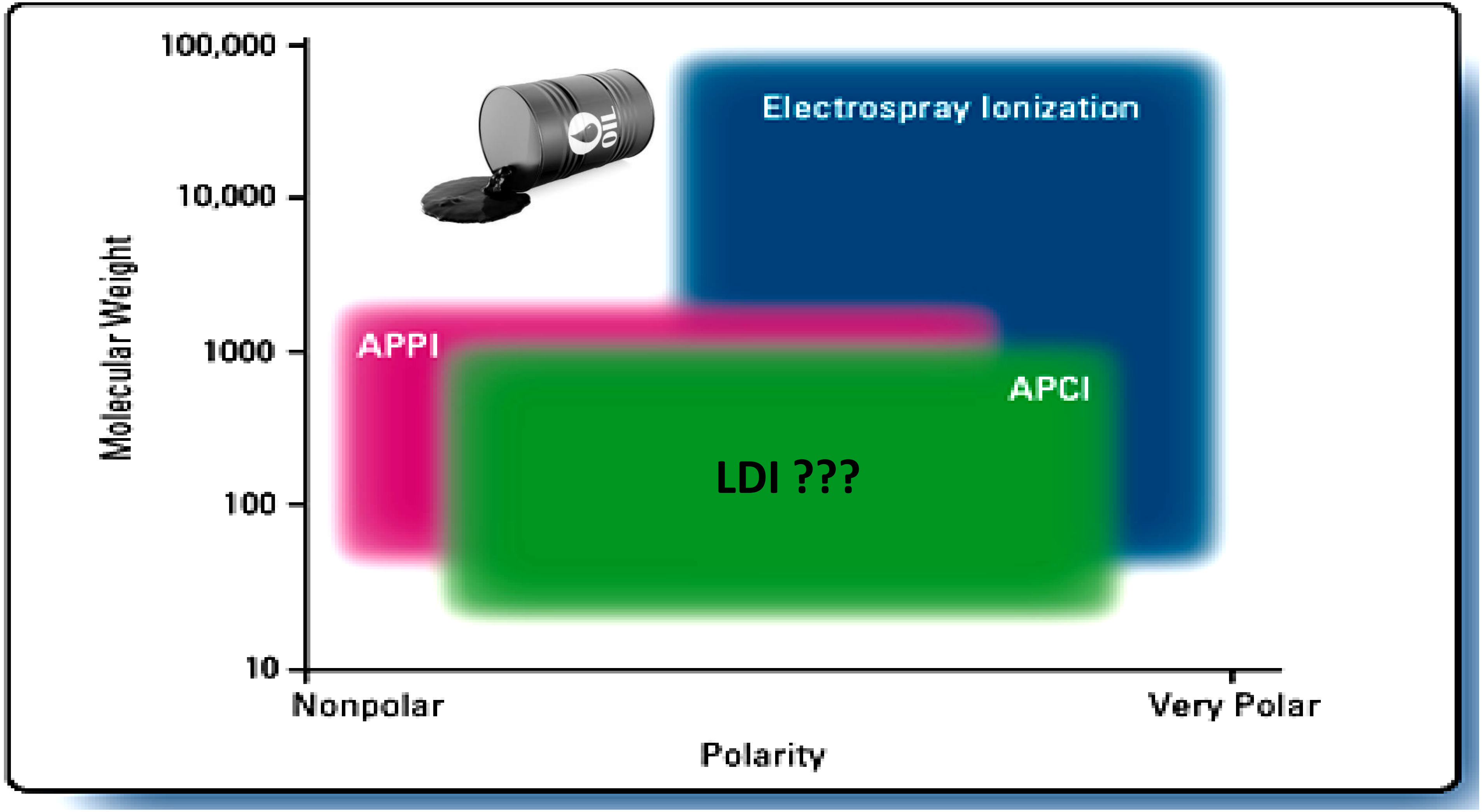

LDI in Petroleomics

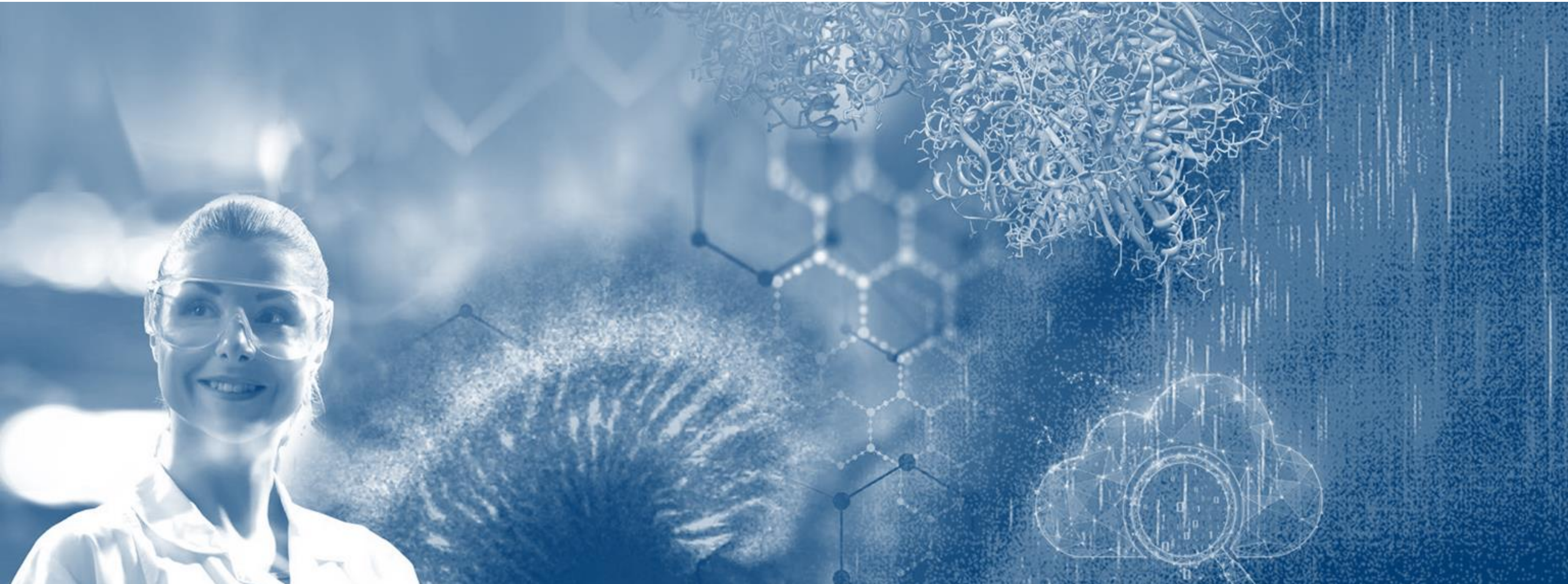

LDI of Crude Oil

LDI at 355 nm with Nd:YAG laser

Properties of Crude Oils Used in This Study

	source	origin	S (ppm)[a]	N (ppm)[b]	TAN[c]
crude no. 1	Napo	Ecuador	20 100	4 011	0.18
crude no. 2	Qinhuangdao	China	2 500	4 405	3.15
crude no. 3	Doba	Congo	1 100	1 884	4.26

Correlation of oxygen containing classes (O_1 and O_2) with TAN in negative ion mode

Negative ion mode

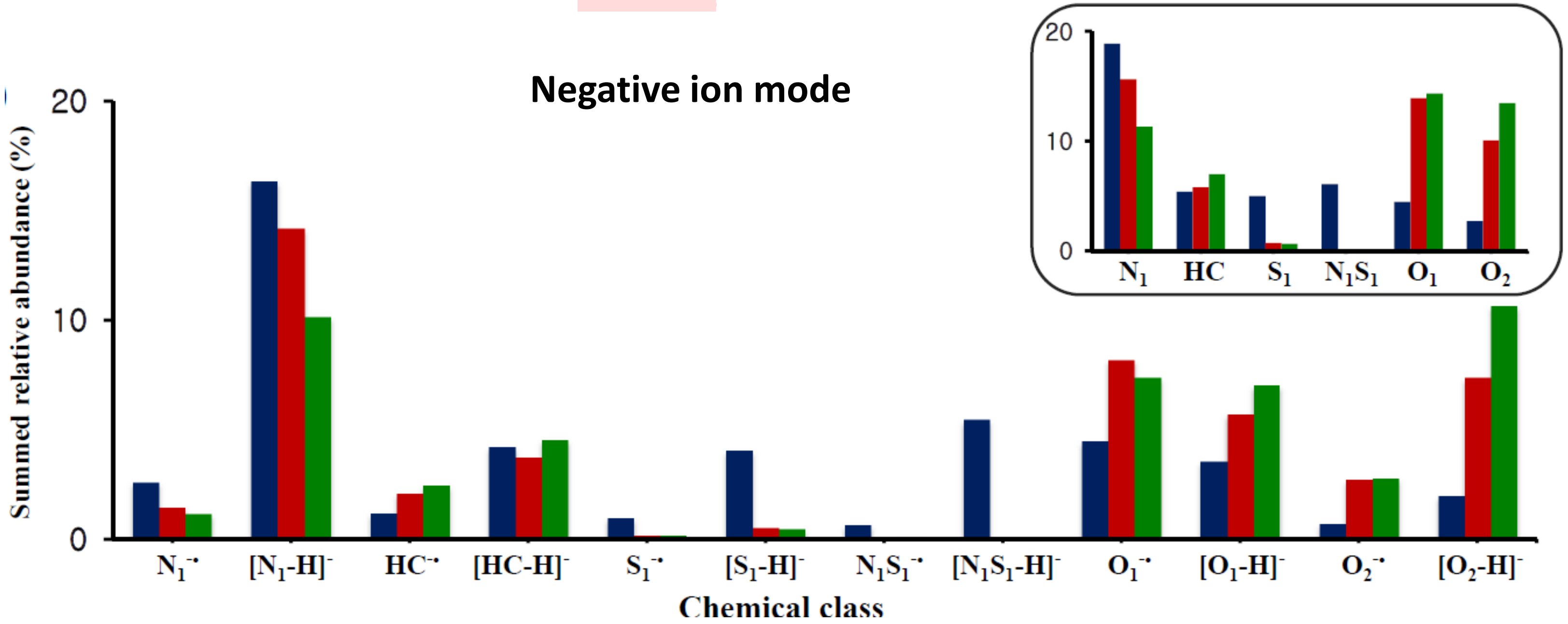

Cho, Y.; Witt, M.; Kim, H.K., Kim S. *Anal. Chem.* **2012**, *84*, 8587–8594.

LDI of Crude Oil

LDI at 355 nm with Nd:YAG laser

a) Crude #1 **TAN: 0.18**

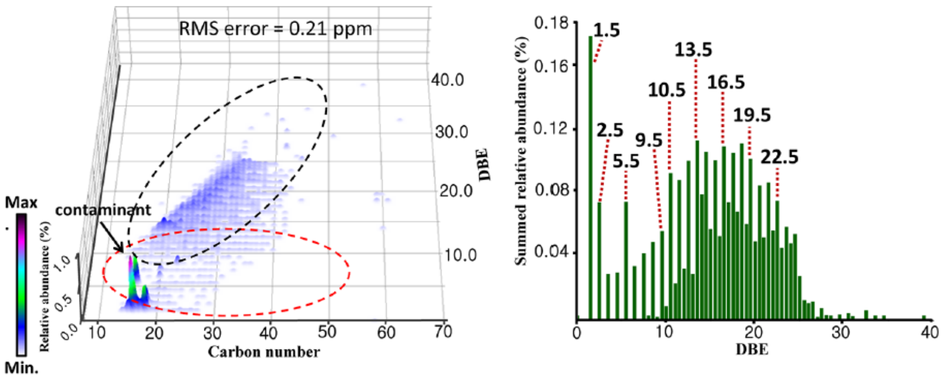

b) Crude #2 **TAN: 3.15**

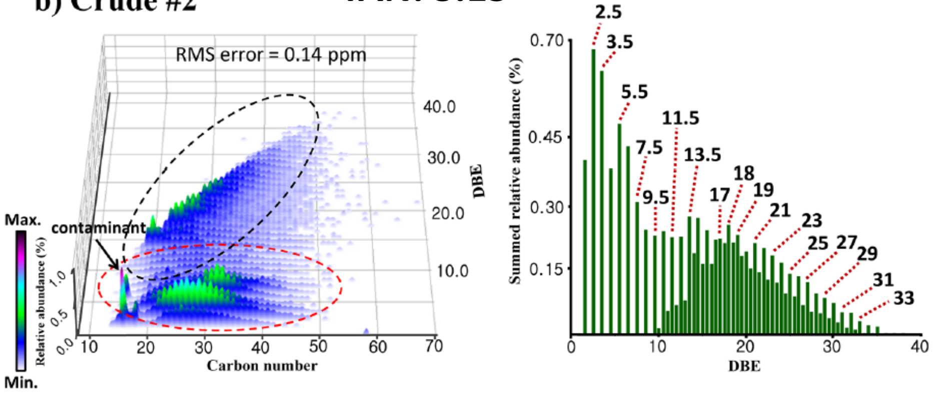

c) Crude #3 **TAN: 4.26**

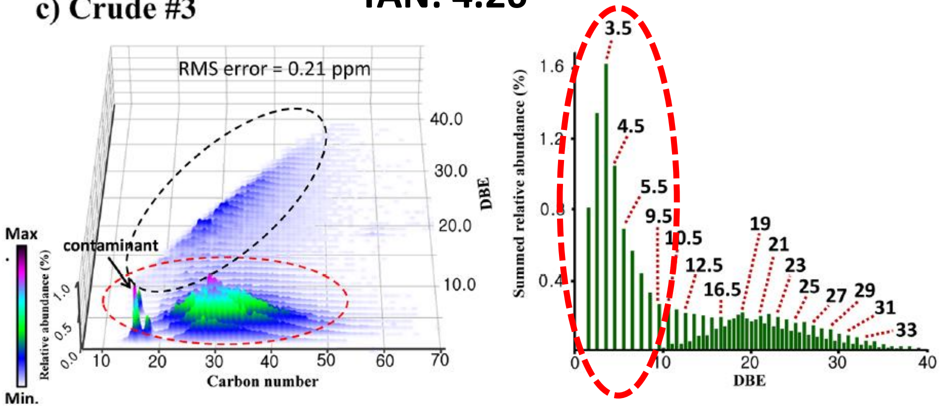

Cho, Y.; Witt, M.; Kim, H.K., Kim S. *Anal. Chem.* **2012**, *84*, 8587–8594.

Detection of Metalloporphyrins by LDI

LDI of crude oil on stainless steel target

Detection of vanadyl porphyrins

a)

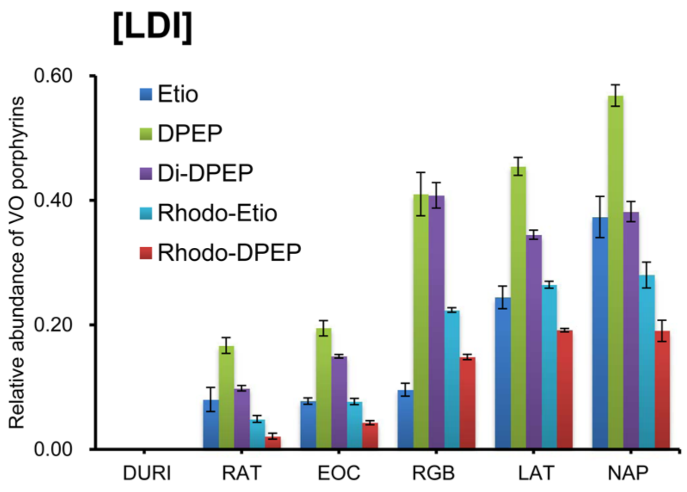

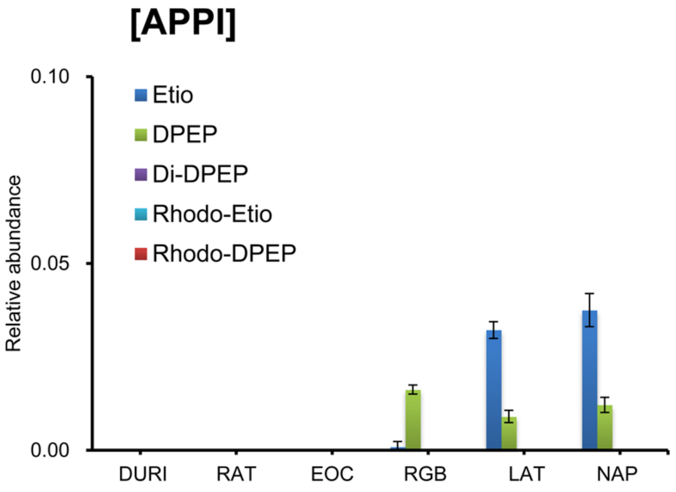

abbreviation	V (ppm)[e]	Ni (ppm)[f]
NAP	329.8	129.0
LAT	308.7	128.6
RGB	93.5	71.0
EOC	54.6	21.4
RAT	43.8	21.7
Duri	1.3	49.1

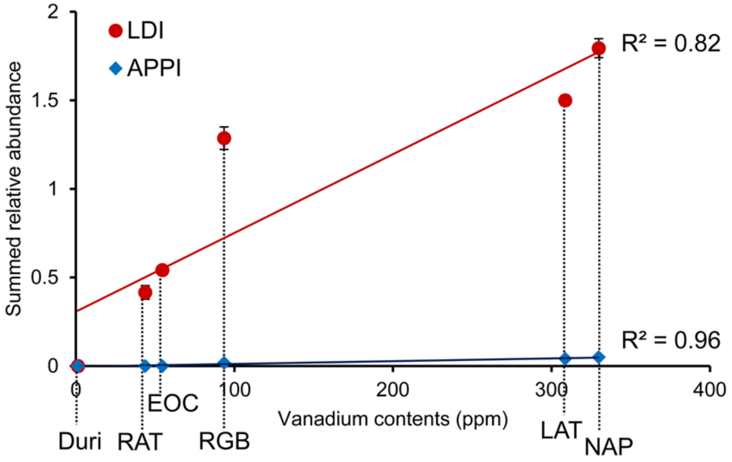

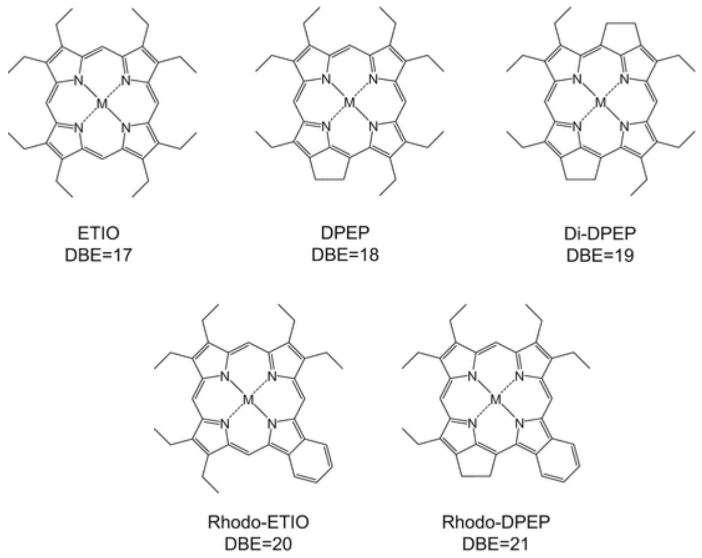

Vanadyl: M = V=O

Cho, Y.; Witt, M.; Jin, J.M., Kim, Y.H., Nho, N.-S., Kim; S. Energy Fuels 2014, 28, 6699-6706.

LDI *vs* APPI

Comparison of ionization methods

LDI is more sensitive to nitrogen containing compound classes

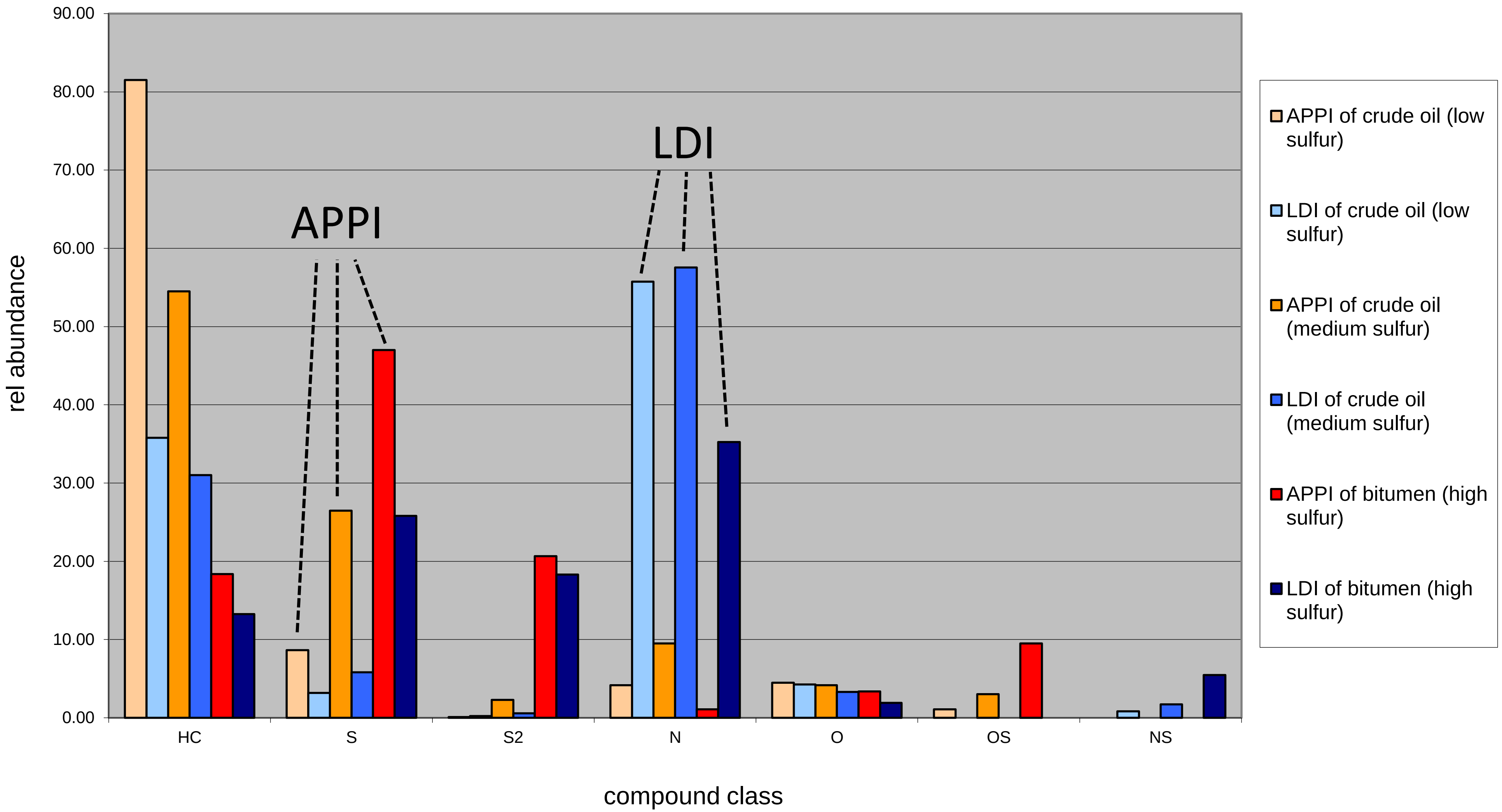

M. Witt, Petrophase Conference 2012.

LDI vs APPI

Comparison of ionization methods

Comparison of detected compounds in class S_1 in a crude oil by APPI and LDI

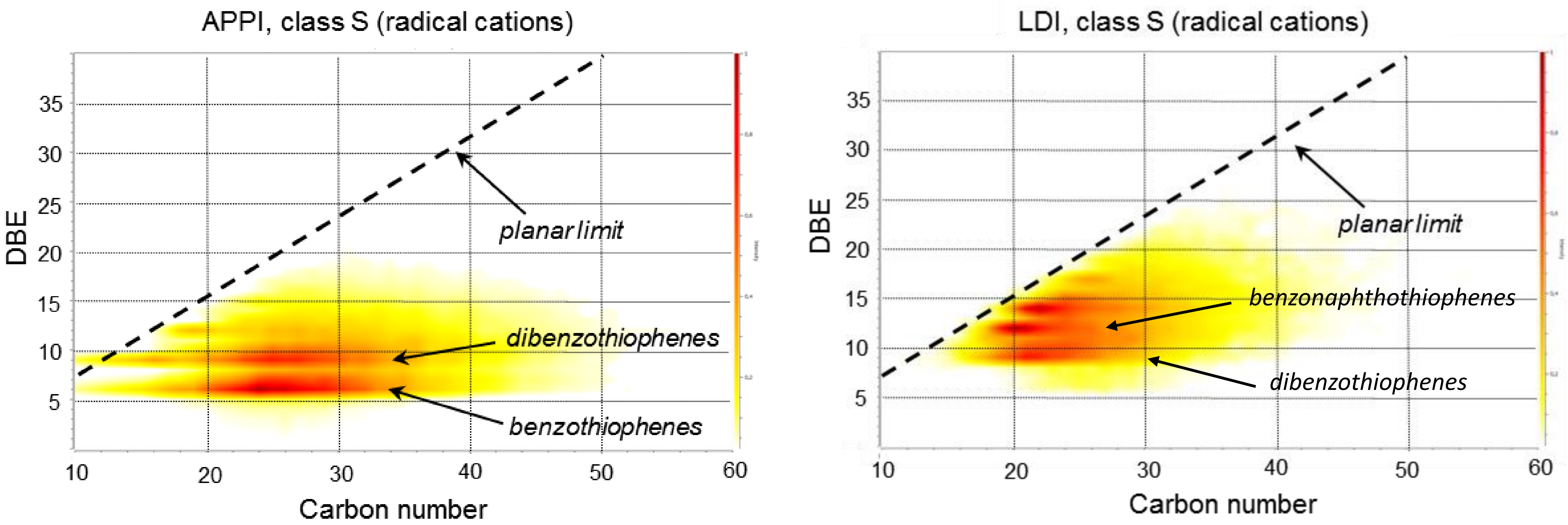

LDI is more sensitive to highly aromatic compounds!

Thin Layer Chromatography

Experimental setup

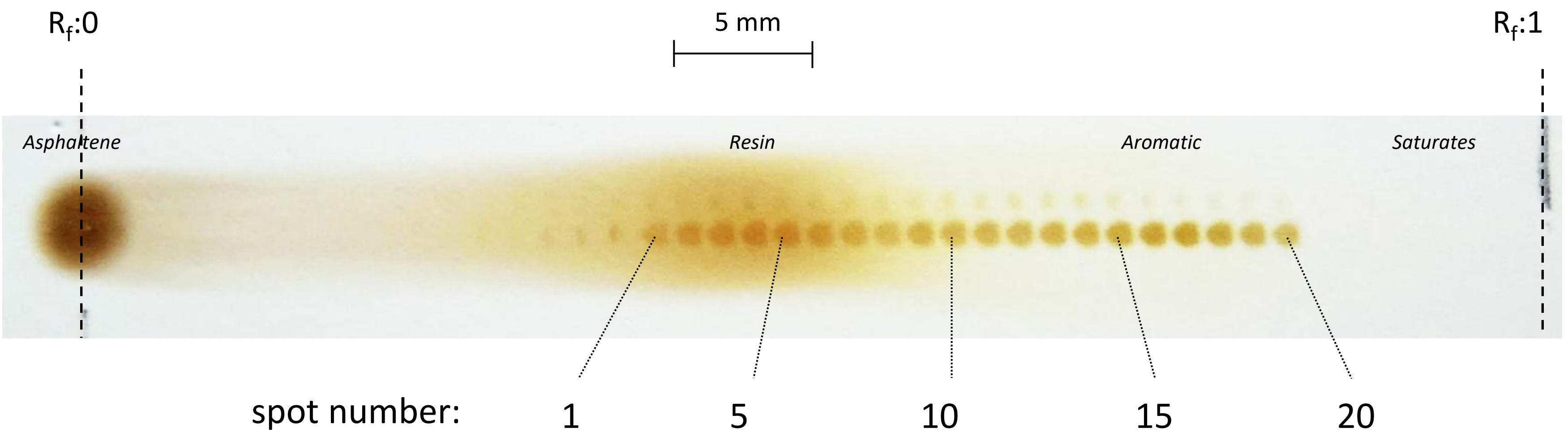

- Spot diameter: 1.0 mm
- Lateral difference between spots: 1.2 mm
- 3 µL of a 1:5 solution of crude oil dissolved in DCM deposited on the TLC plate
- mobile phase: n-heptane:i-propanol 95:5
- stationary phase: TLC silica 60 F254 (Merck 1.05539.00001) 5 × 7.5 cm sheet

Similar measurements were done by Smith et. al., Energy Fuels, 2014.

Thin Layer Chromatography

LDI spectra of different spot numbers

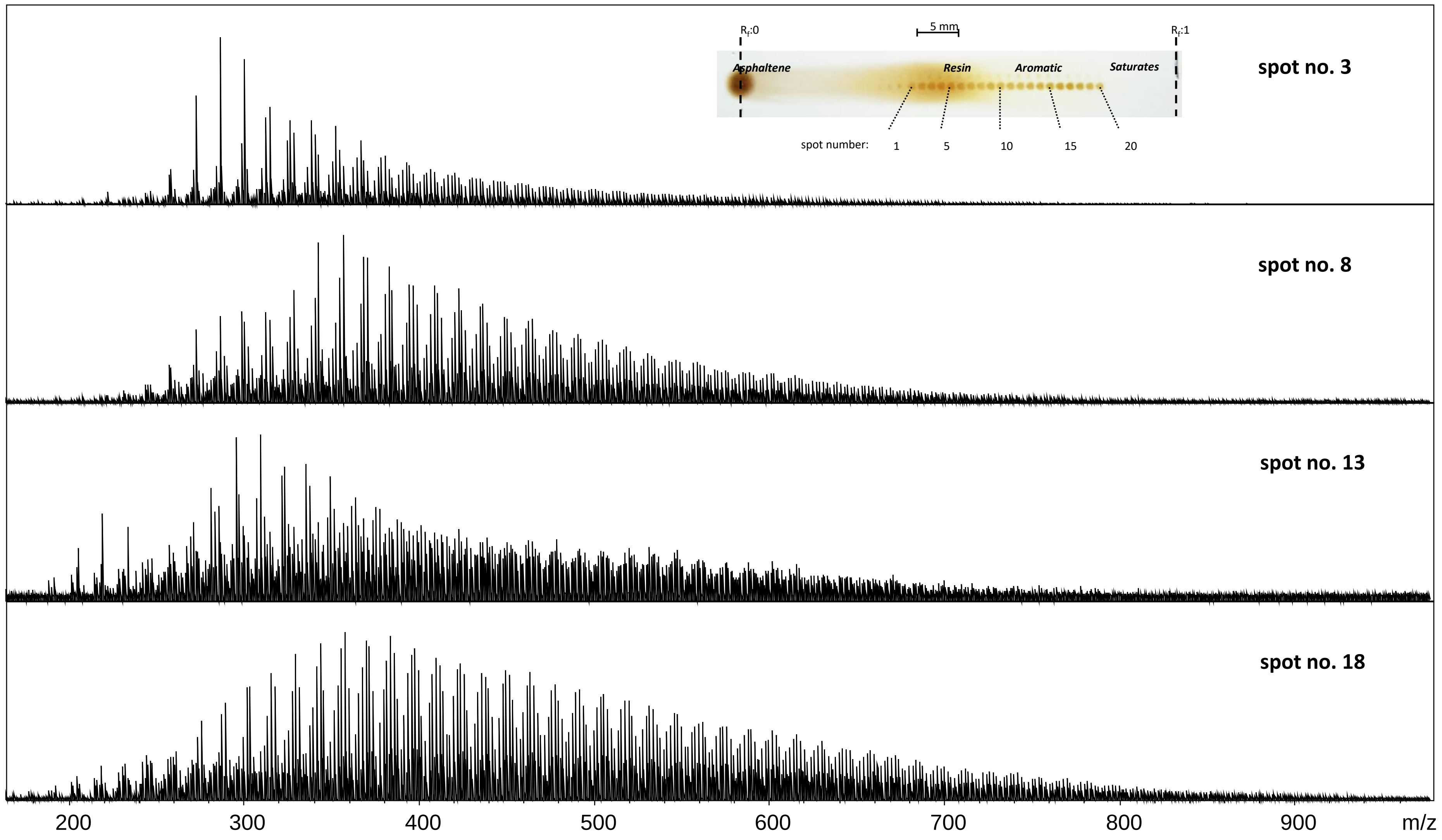

Thin Layer Chromatography

Relative abundance of compound classes

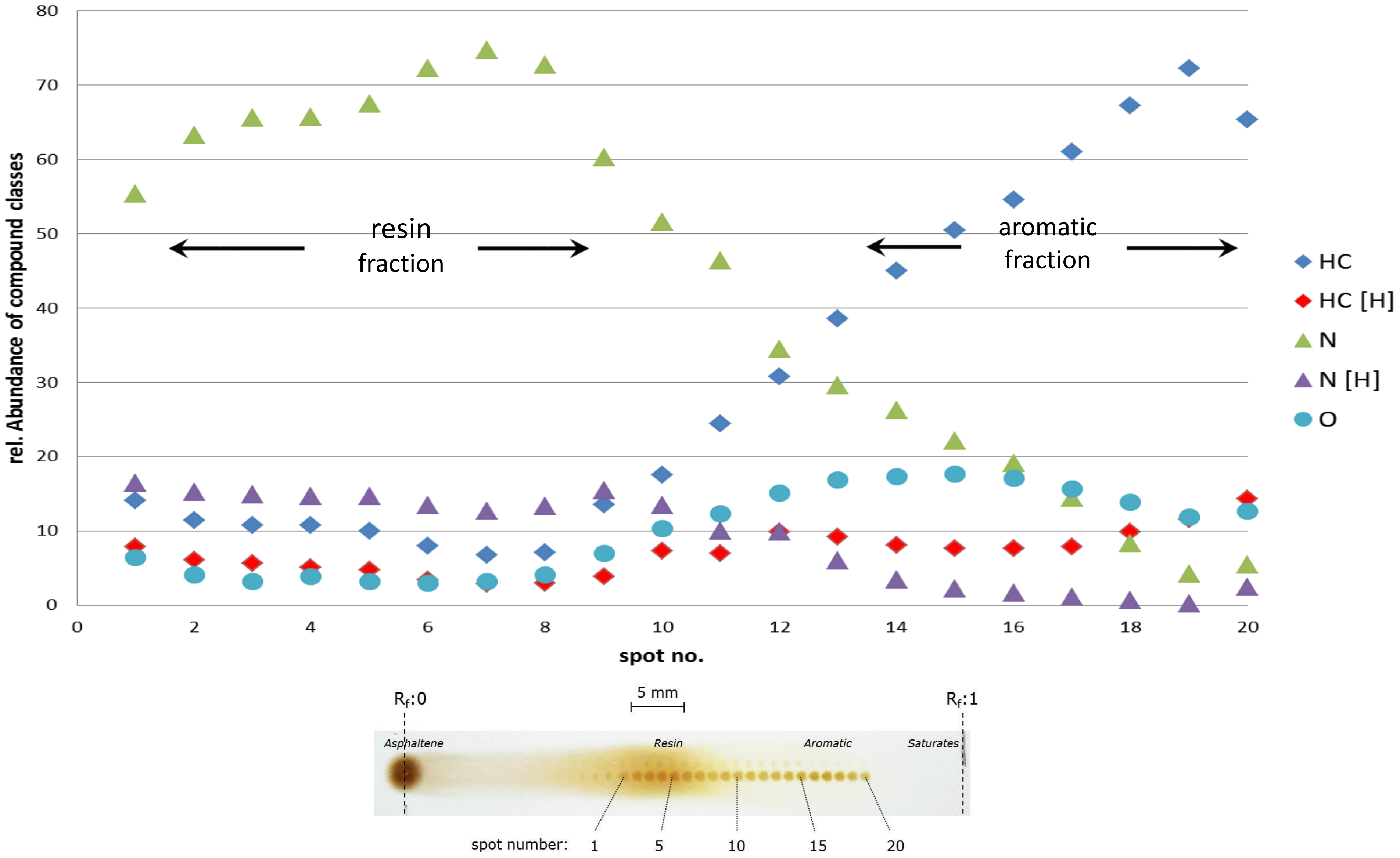

Thin Layer Chromatography

Aromaticity of resin fractions: class N_1

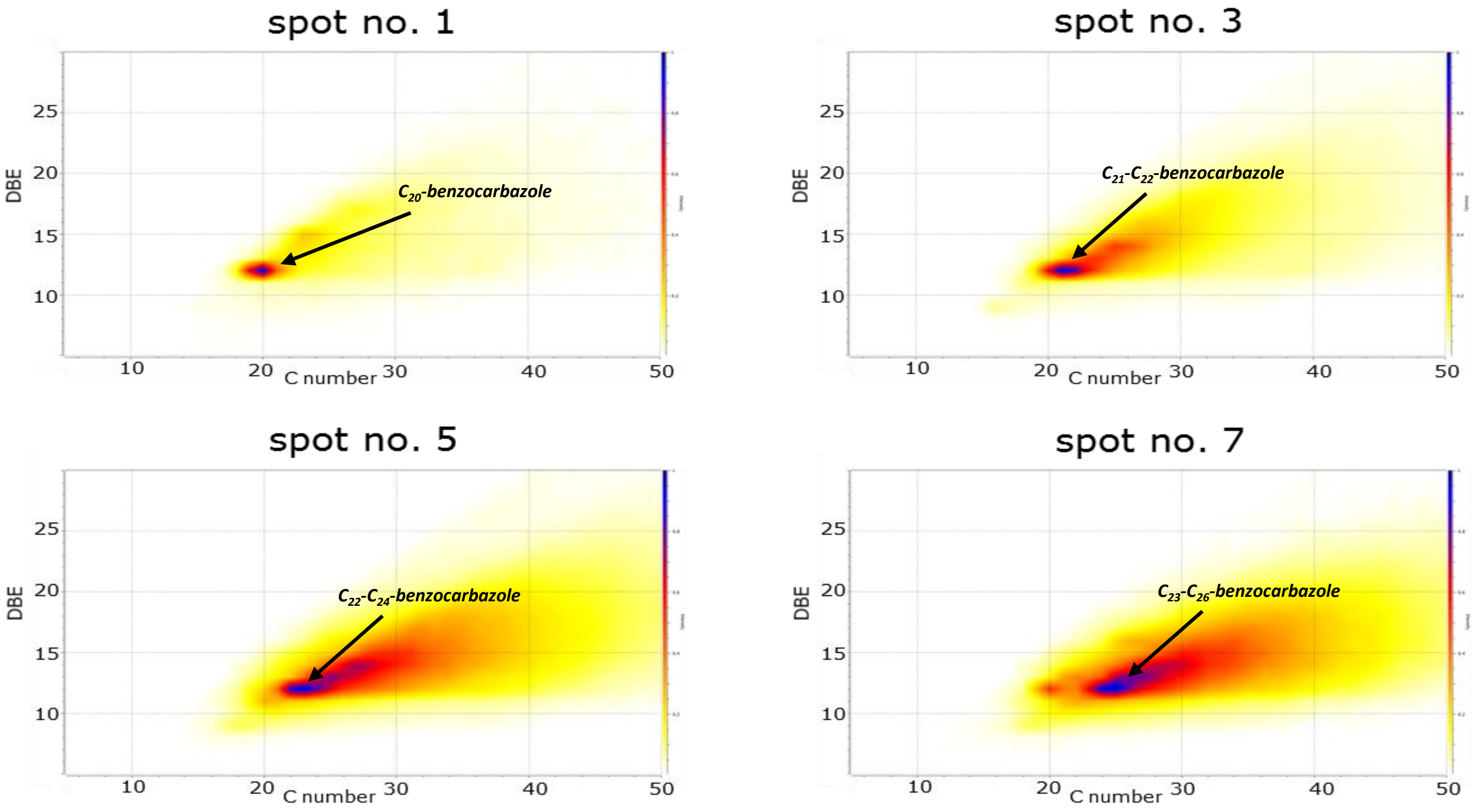

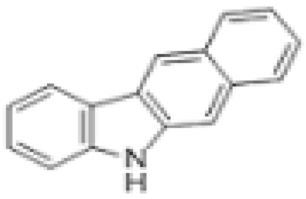

benzocarbazole

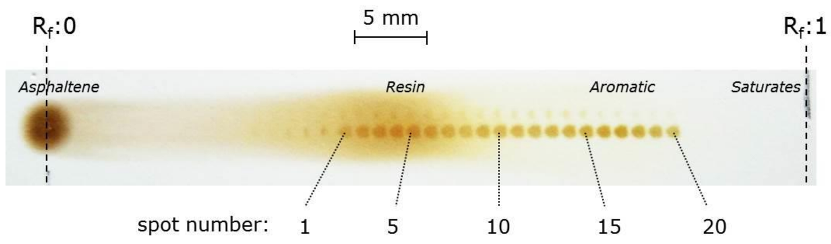

Can we quickly tell samples apart by LDI?

LDI of different crude oil samples

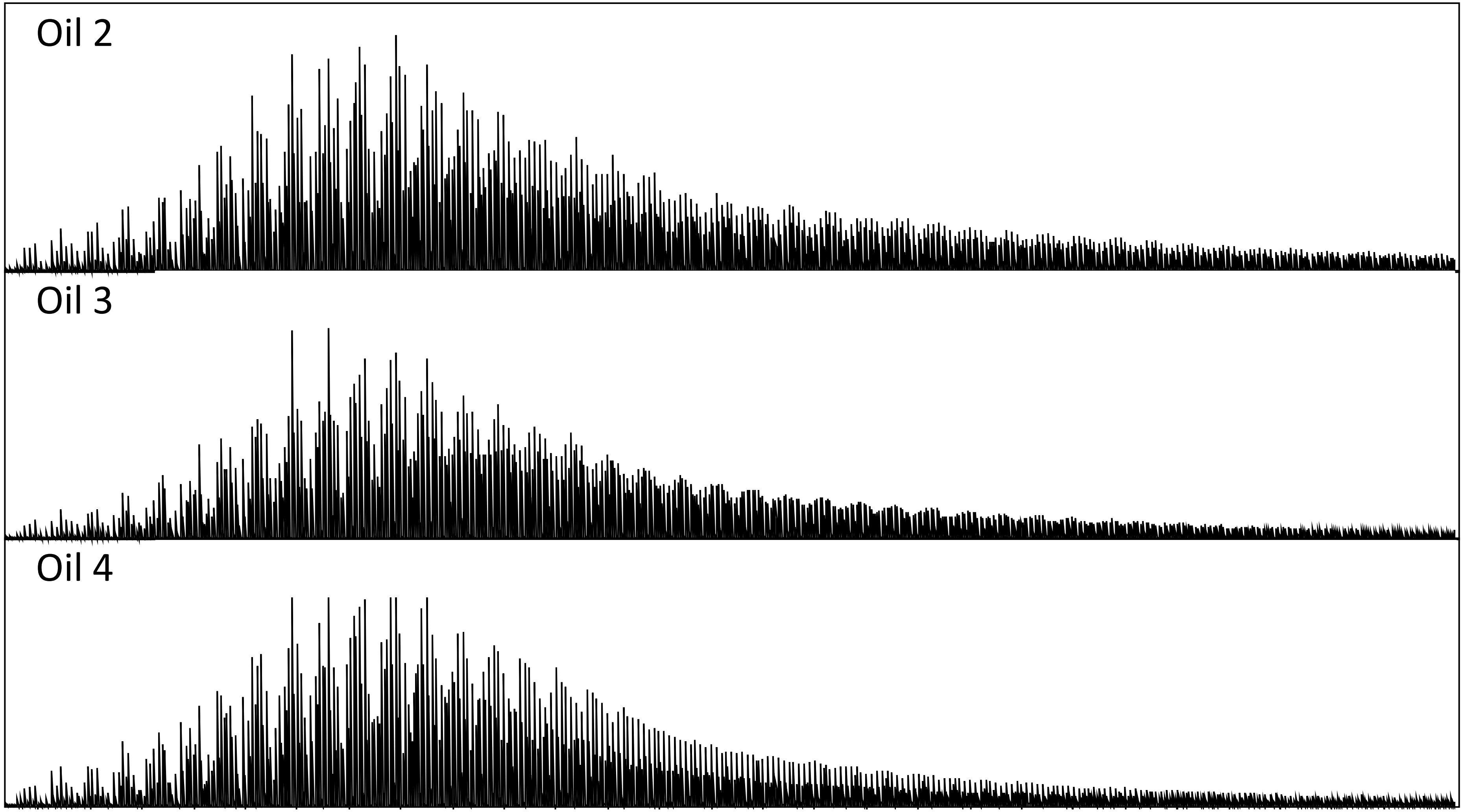

*Samples have been kindly provided by Dr. Kolbjørn (SINTEF, Trondheim, Norway)

Can we quickly tell samples apart by LDI?

LDI of different crude oil samples

Oil 8 and 8a: identical oils from different bottles
Oil 9a: Oil 9 one day in ion source at 3 mbar

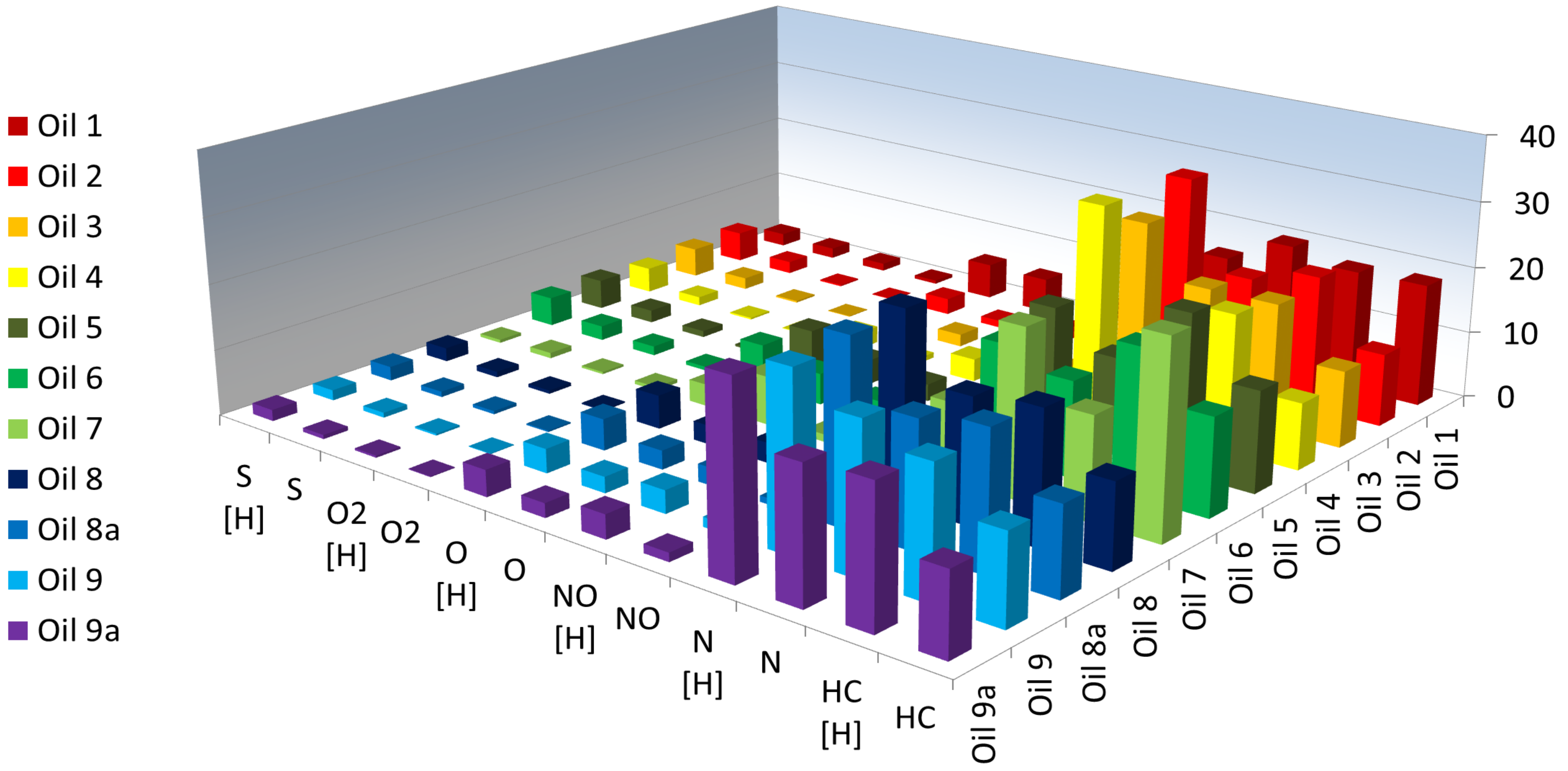

*Samples have been kindly provided by Dr. Kolbjørn (SINTEF, Trondheim, Norway)

Can we quickly tell samples apart by LDI?

Reproducibility of LDI measurements

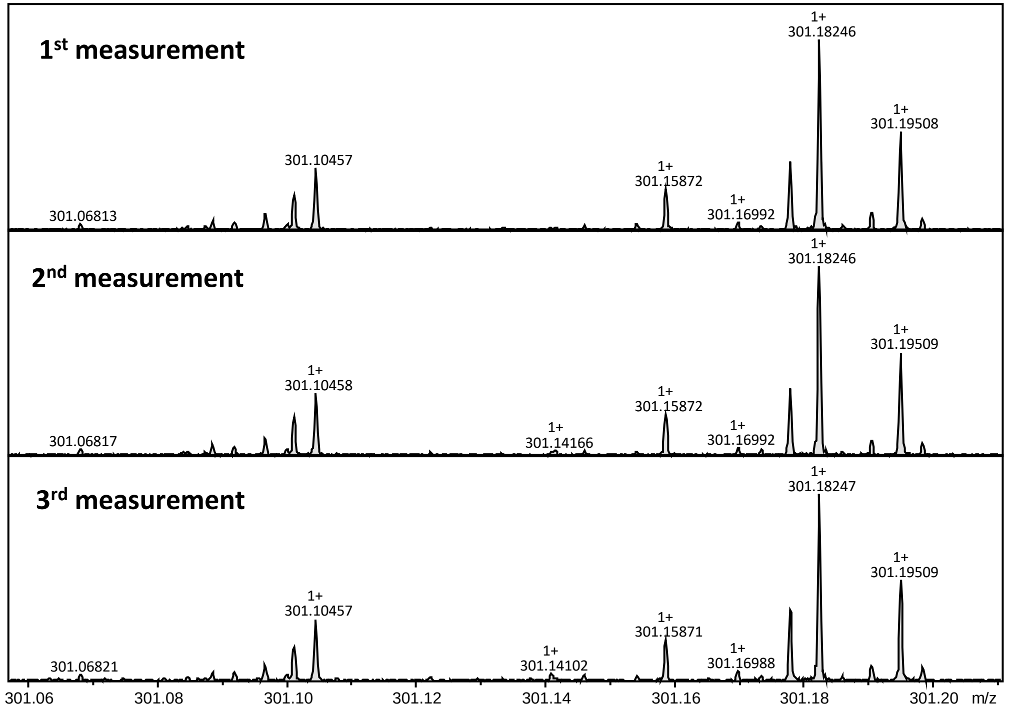

Class	Oil 8 rep1	Oil 8 rep2	Oil 8 rep3	Oil 8 rep4	Oil 8 rep5	Std. deviation [%]
HC	12.97	12.17	12.83	13.04	12.25	**3.3**
HC [H]	20.24	19.67	20.36	20.44	19.87	**1.6**
N	18.62	18.28	18.25	18.21	18.22	**0.9**
N [H]	27.27	28.74	27.47	27.24	28.56	**2.6**
O	2.82	2.62	2.76	2.71	2.61	**3.3**
O [H]	4.72	4.86	4.72	4.71	4.83	**1.5**
S [H]	2.14	2.08	2.15	2.14	2.11	**1.4**

*Samples have been kindly provided by Dr. Kolbjørn (SINTEF, Trondheim, Norway)

Principle Component Analysis

Reproducibility of LDI measurements

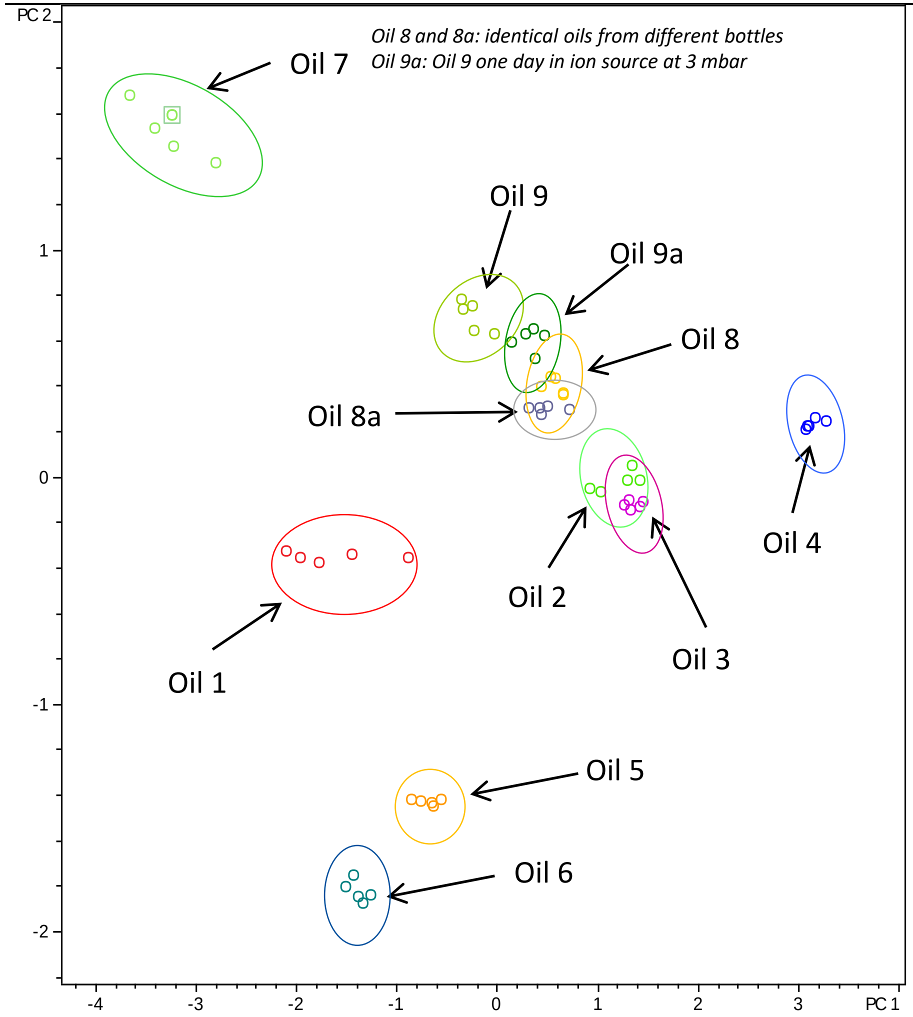

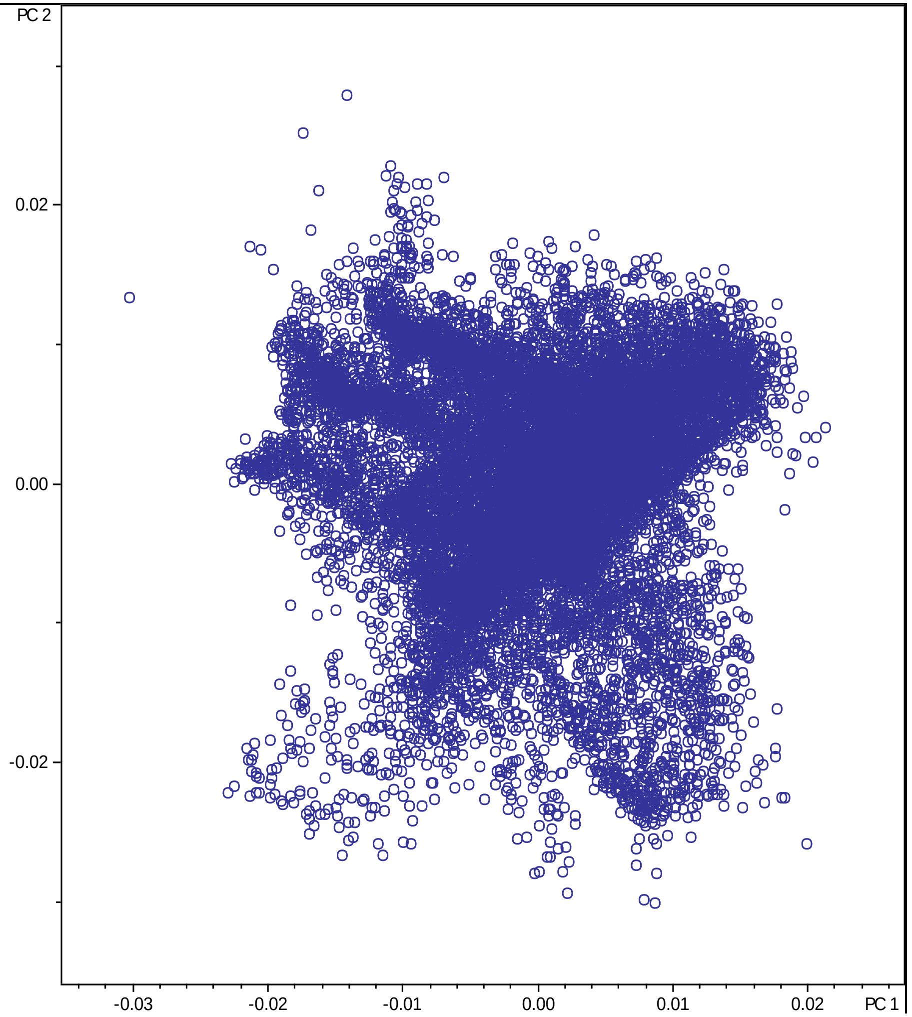

*Samples have been kindly provided by Dr. Kolbjørn (SINTEF, Trondheim, Norway)

Oil mixtures

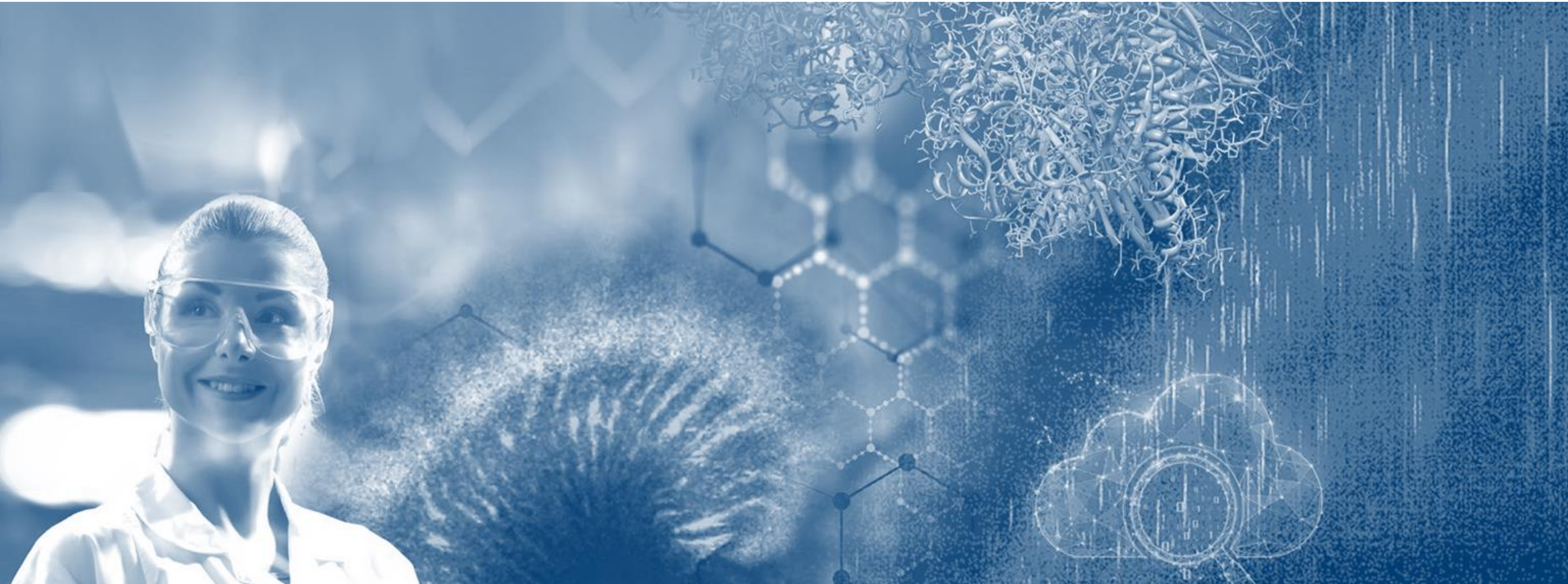

Ternary Oil Mixtures

Compound classes of 3 different crude oils from North sea

M. Witt, W. Timm, *Energy Fuels 2016, 30, 5, 3707-3713.*

Compound classes plot

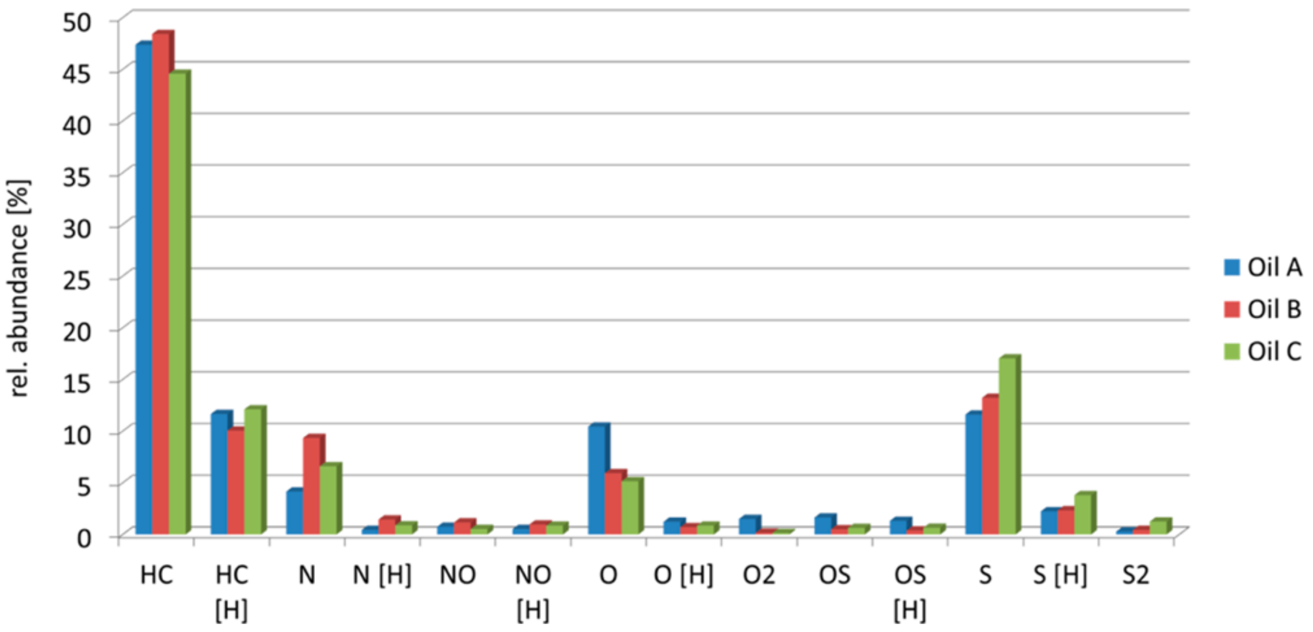

NNLS method

	measured (%)	actual (%)	relative error (%)
mixture 1: oil A	32.4	33.3	2.8
mixture 1: oil B	36.0	33.3	8.1
mixture 1: oil C	31.6	33.3	5.2
mixture 2: oil A	15.6	10.0	56.2
mixture 2: oil B	10.0	10.0	0.3
mixture 2: oil C	74.4	80.0	7.1
mixture 3: oil A	39.0	45.0	13.4
mixture 3: oil B	38.1	35.0	8.9
mixture 3: oil C	22.9	20.0	14.5

NNLS: non-negative least square

Ternary Oil Mixtures

Principle component analysis (PCA)

M. Witt, W. Timm, *Energy Fuels 2016, 30, 5, 3707-3713.*

Pure oils and defined mixtures

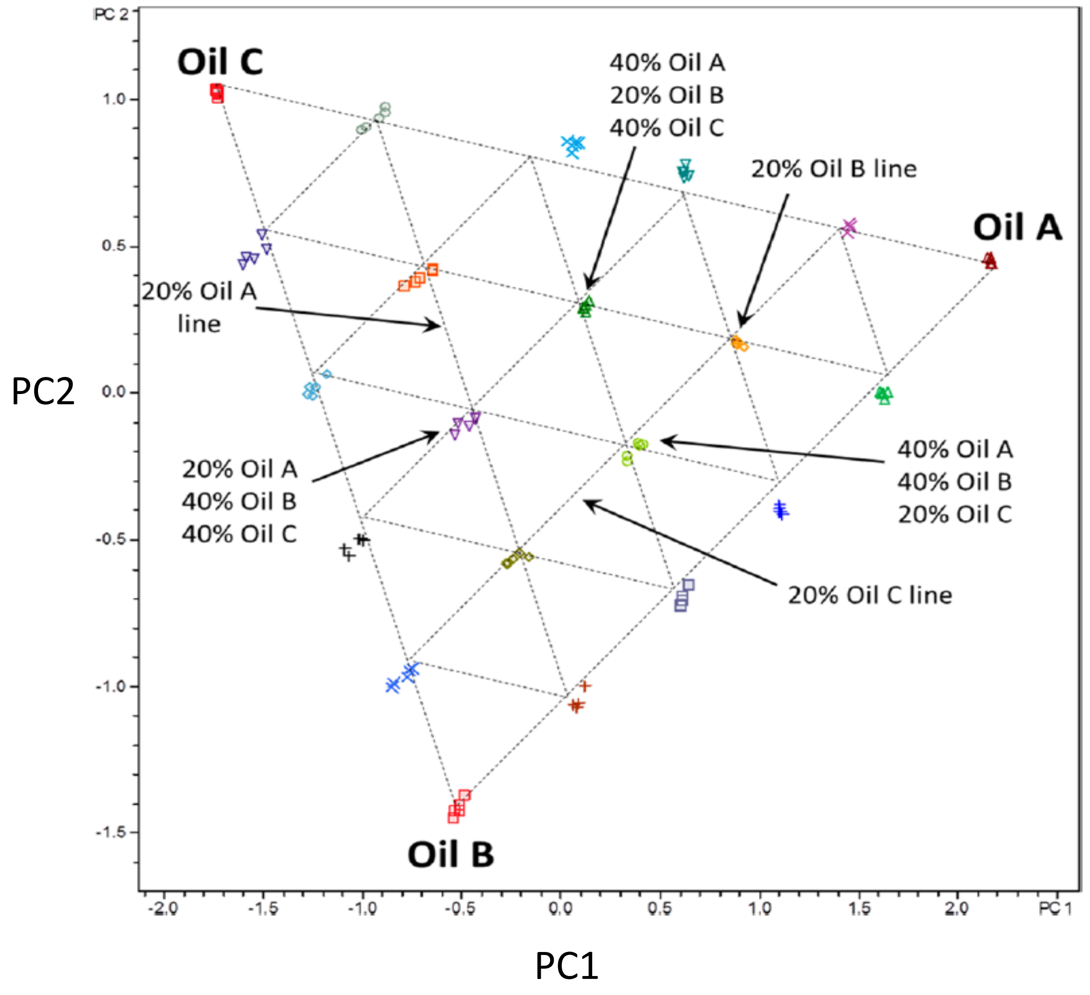

Calculation of mixtures based on PCA of defined mixtures

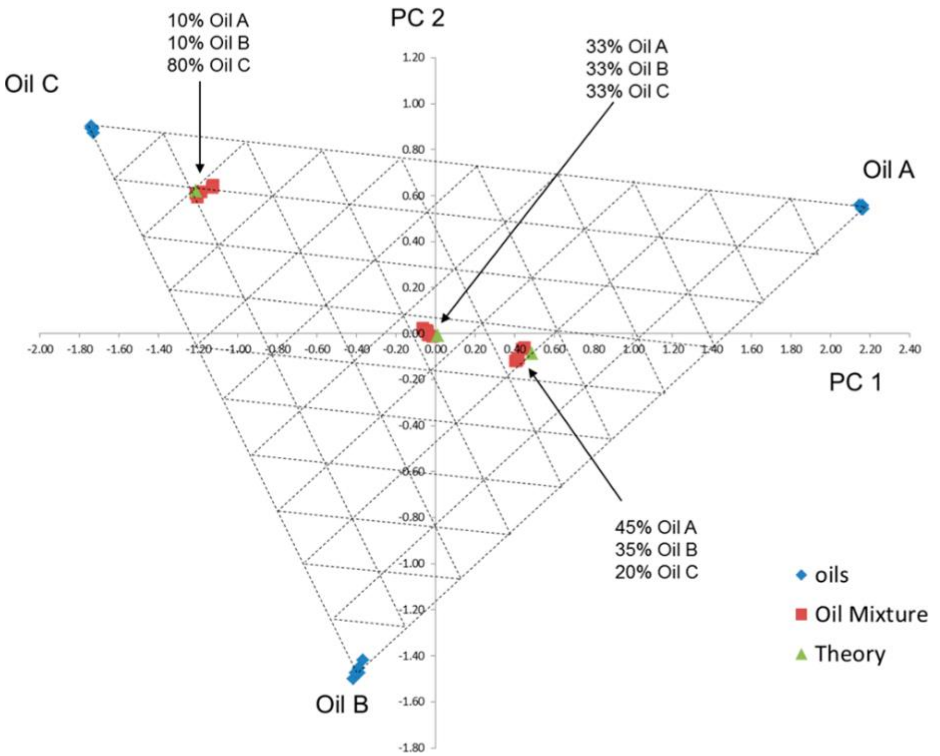

Ternary Oil Mixtures

Determination of mixture ratios using PCA and vector analysis

M. Witt, W. Timm, *Energy Fuels 2016, 30, 5, 3707-3713.*

Calculation of Relative Percentages of Three Ternary Oil Mixtures Using **Vector Analysis** of the Ternary Diagram Calculated with the PC1 versus PC2 of the **PCA Scoring Plot**

				PCA	NNLS
	measured (%)	actual (%)	absolute error (%)	relative error (%)	relative error (%)
mixture 1: oil A	32.1	33.3	1.2	3.5	2.8
mixture 1: oil B	32.9	33.3	0.4	1.3	8.1
mixture 1: oil C	34.9	33.3	1.6	4.7	5.2
mixture 2: oil A	11.1	10.0	1.1	10.7	56.2
mixture 2: oil B	9.8	10.0	0.2	1.6	0.3
mixture 2: oil C	79.1	80.0	0.9	1.1	7.1
mixture 3: oil A	43.2	45.0	1.8	3.9	13.4
mixture 3: oil B	35.5	35.0	0.5	1.5	8.9
mixture 3: oil C	21.2	20.0	1.2	6.2	14.5

Asphaltene fractions

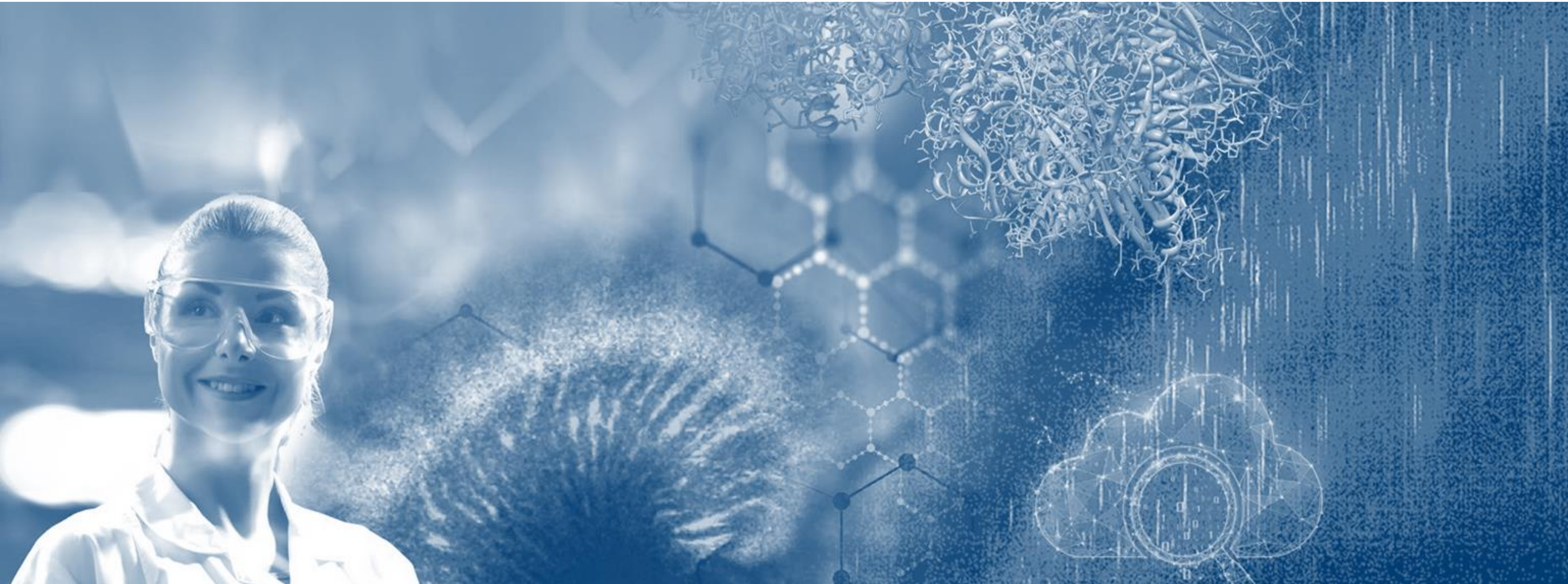

Asphaltene fractions

Fractions based on solubility in different solvent

E. Rogel, M. Witt, *Energy & Fuels* 2016, 30, 915-923.

APPI positive ion mode

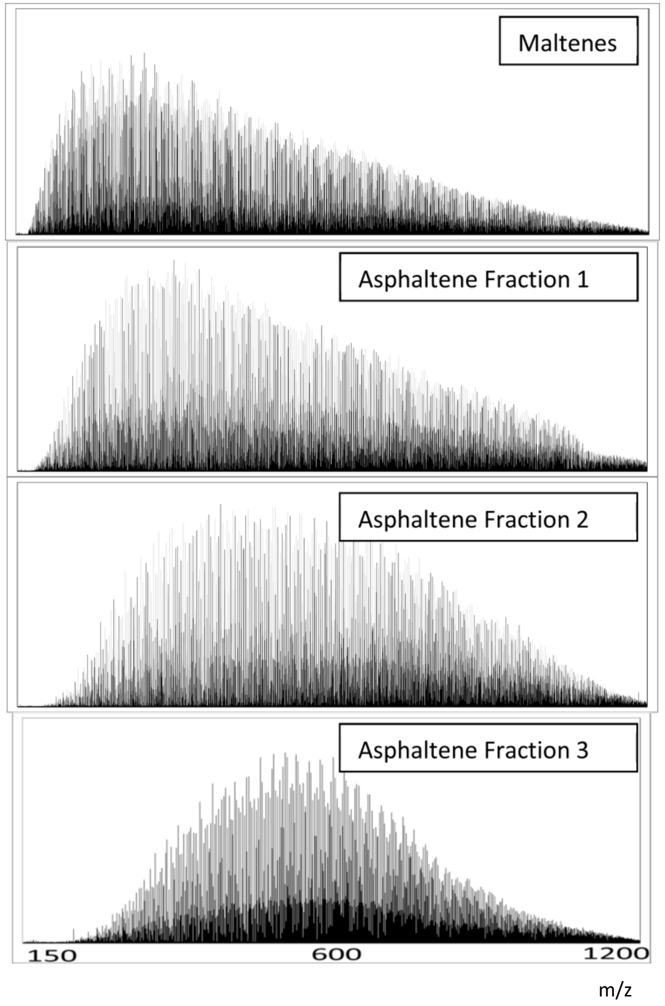

Maltene: Heptane solubles

Fraction 1: 15:85 CH_2Cl_2/n-heptane

Fraction 2: 30:70 CH_2Cl_2/n-heptane

Fraction 3: CH_2Cl_2 solubles

Asphaltene fractions

Fractions based on solubility in different solvent

E. Rogel, M. Witt, *Energy & Fuels* 2016, 30, 915-923.

Compound classes

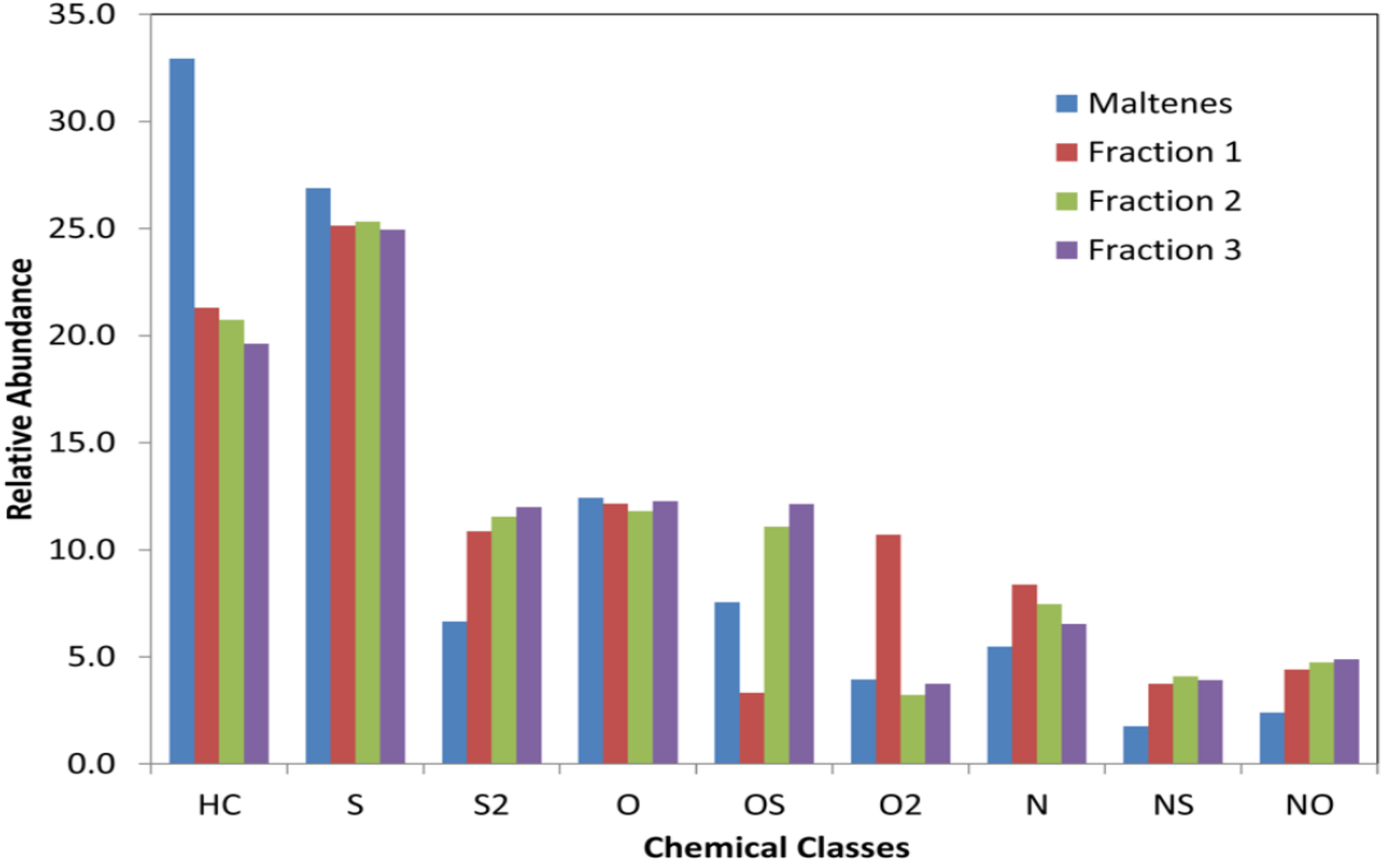

Asphaltene fractions

Fractions based on solubility in different solvent

E. Rogel, M. Witt, *Energy & Fuels* 2016, 30, 915-923.

Fractions: DBE and C number abundance plot

DBE

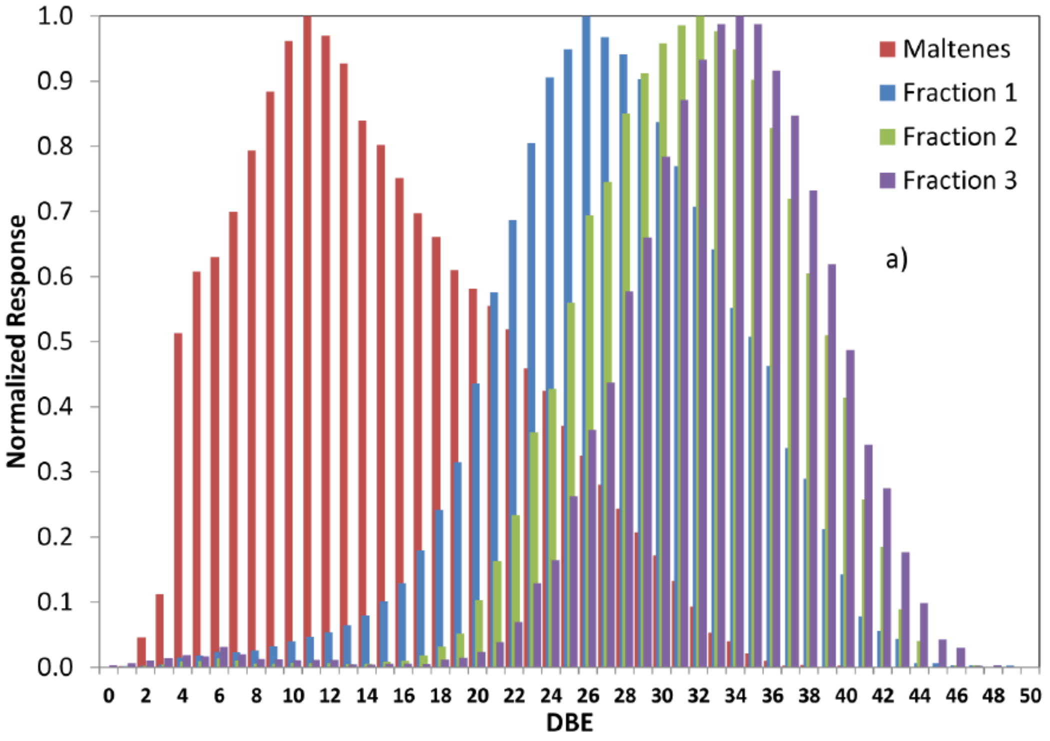

Carbon number

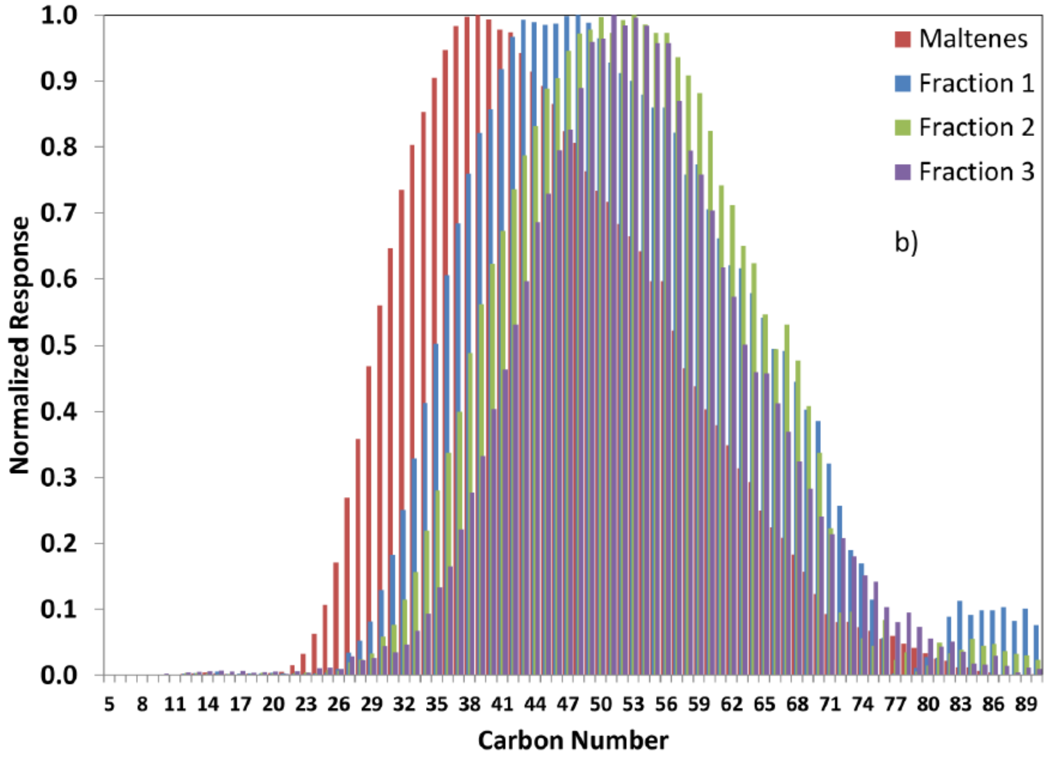

Asphaltene fractions

Fractions based on solubility in different solvent

E. Rogel, M. Witt, *Energy & Fuels* 2016, 30, 915-923.

Fraction 2

Compound classes: DBE and carbon number

DBE

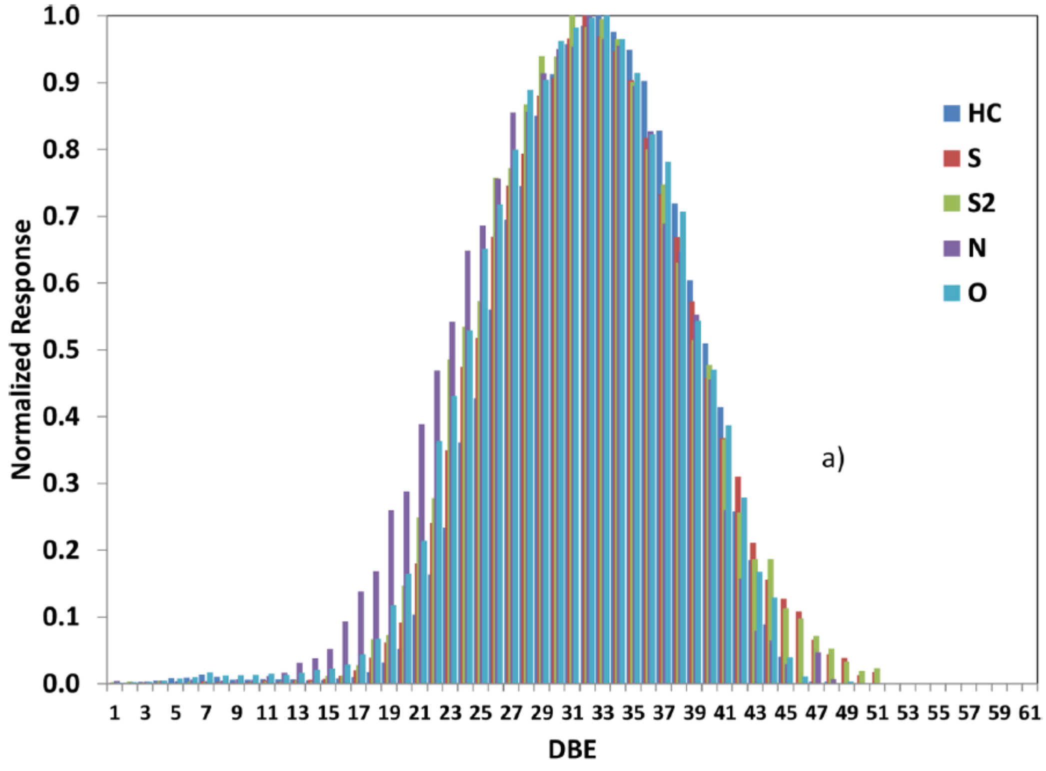

Carbon number

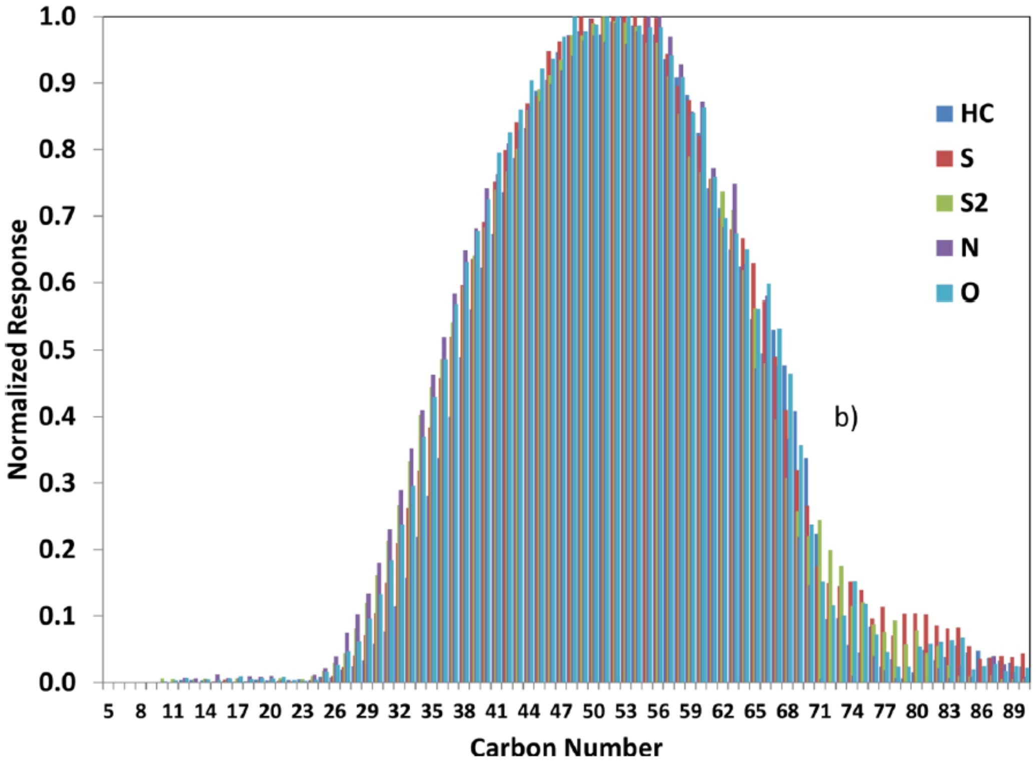

Asphaltene fractions

Precipitated at Different Solvent Power Conditions

E. Rogel, M. Witt, *Energy & Fuels* 2018, 32, 2653-2660.

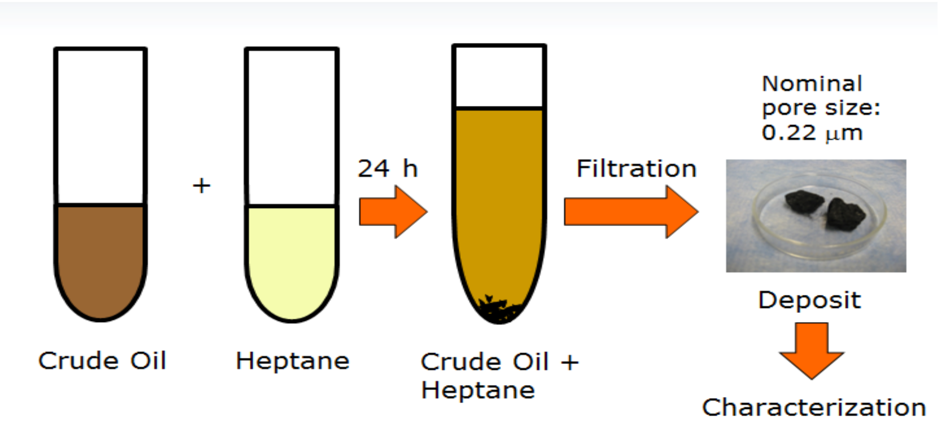

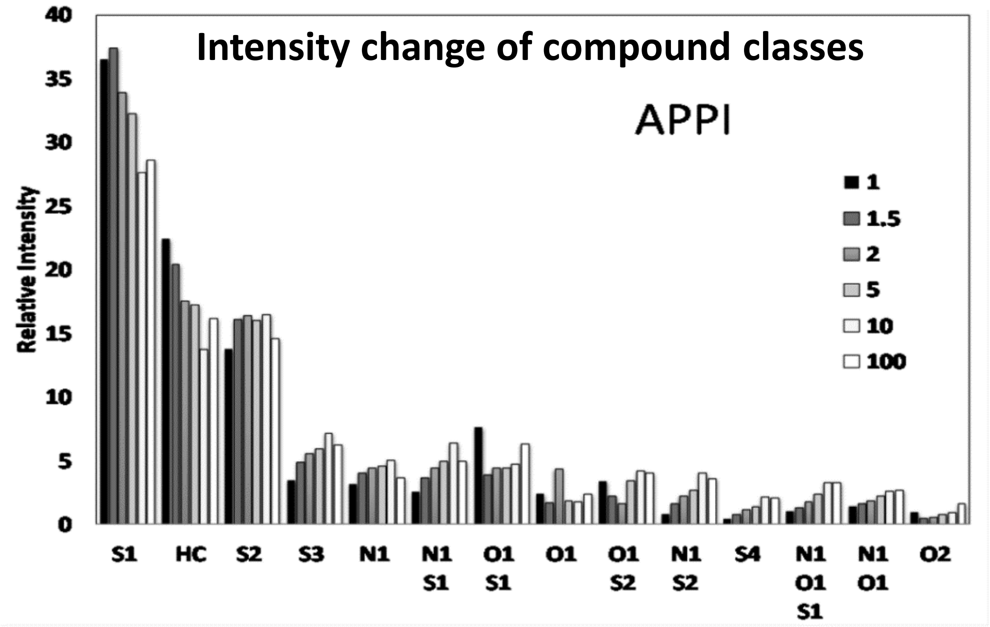

HCOR	C (wt %)	H (wt %)	H/C molar ratio
1	82.86	11.01	1.59
1.5	83.58	10.41	1.49
2	84.08	10.00	1.43
5	80.94	8.72	1.29
10	81.35	8.41	1.24
100	80.33	8.04	1.20

HCOR: heptane crude oil ratio

Asphaltene fractions

Precipitated at Different Solvent Power Conditions

E. Rogel, M. Witt, *Energy & Fuels* 2018, 32, 2653-2660.

Change of DBE and Aromaticity

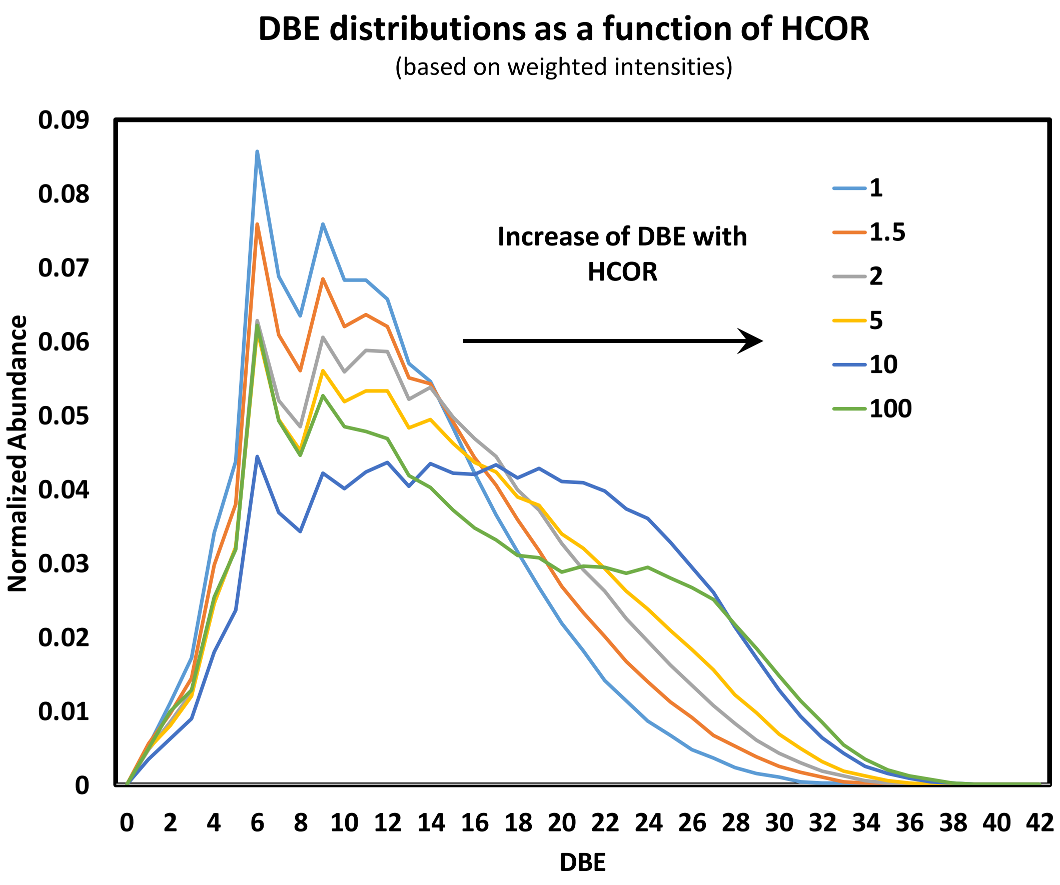

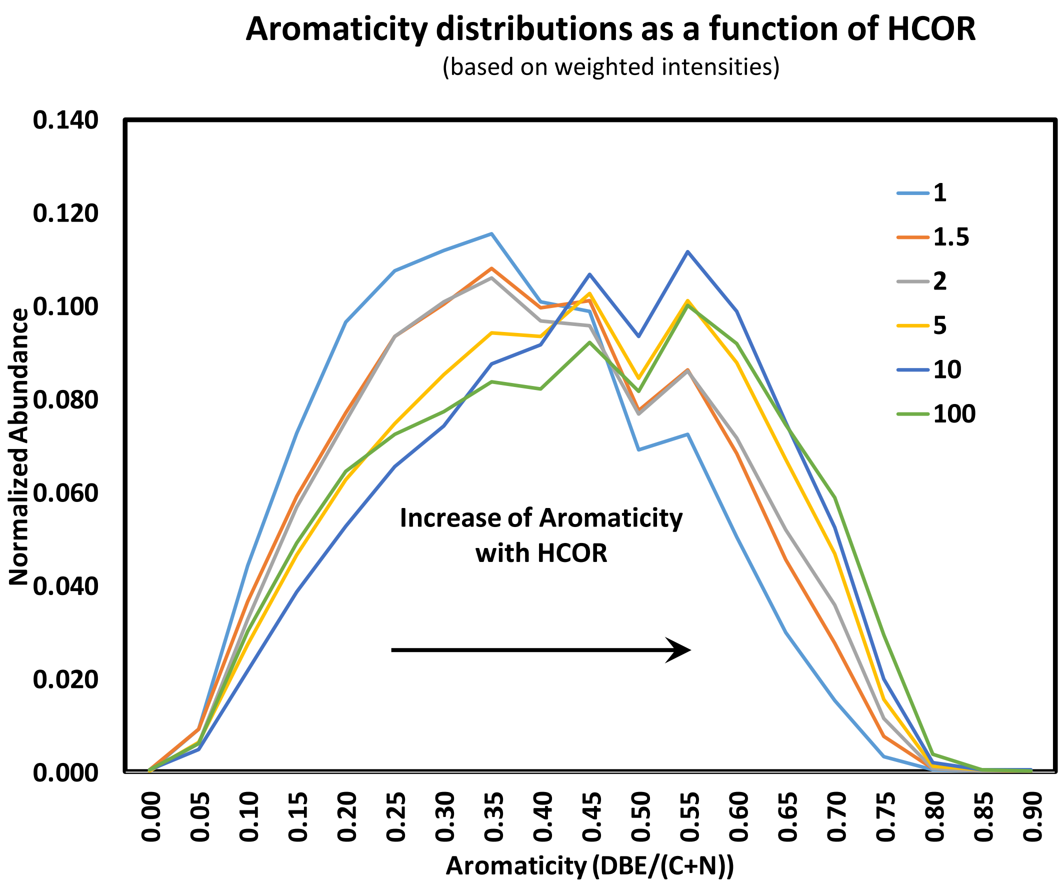

HCOR: heptane crude oil ratio

Asphaltene fractions

Precipitated at Different Solvent Power Conditions

E. Rogel, M. Witt, *Energy & Fuels* 2018, 32, 2653-2660.

DBE vs. C plots: Class HC

Distribution shifts with higher HCOR to higher DBE

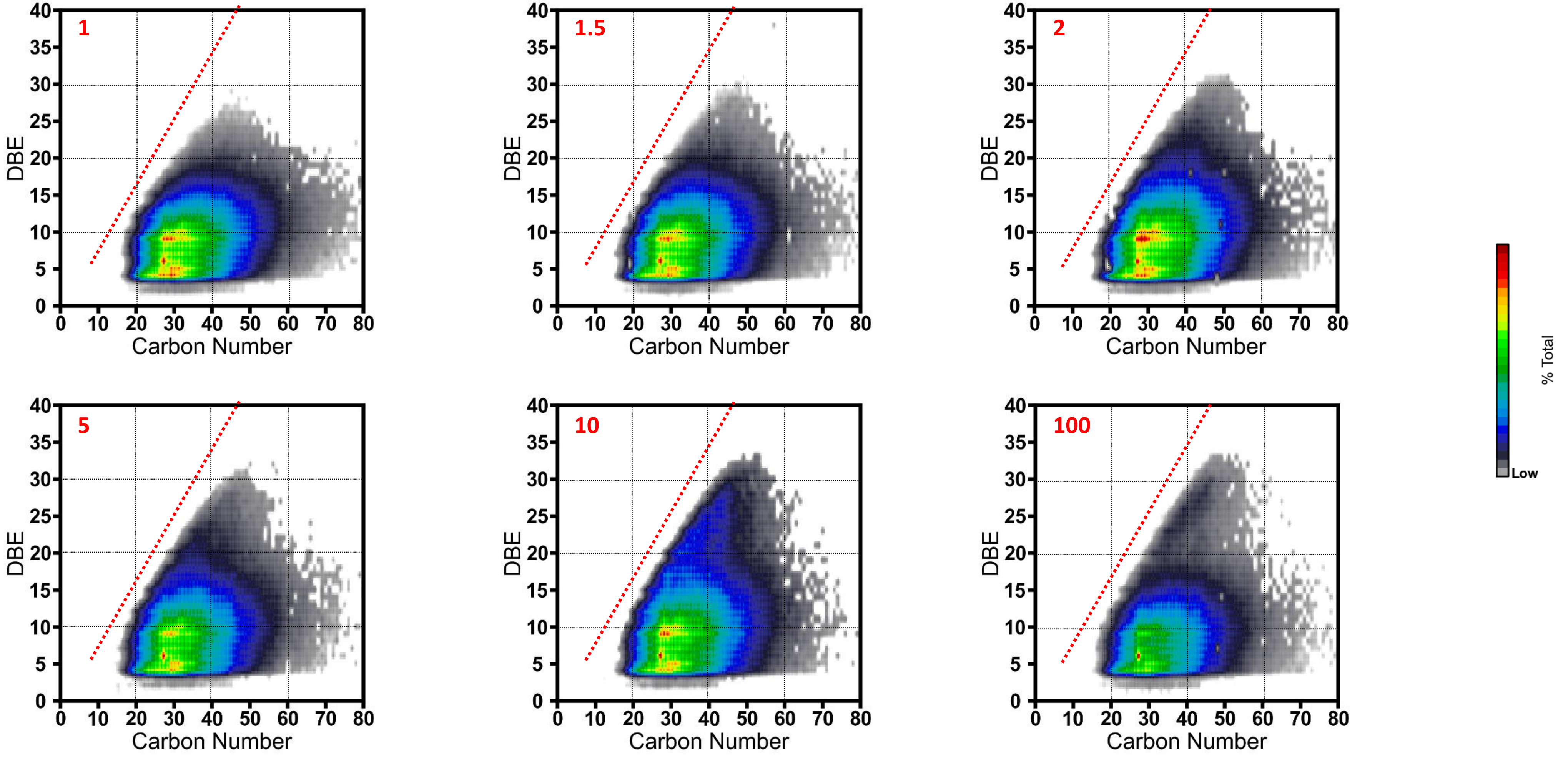

HCOR: heptane crude oil ratio

Asphaltene fractions

Precipitated at Different Solvent Power Conditions

E. Rogel, M. Witt, *Energy & Fuels* 2018, 32, 2653-2660.

DBE vs. C plots: Class S_1

Distribution shifts with higher HCOR to higher DBE

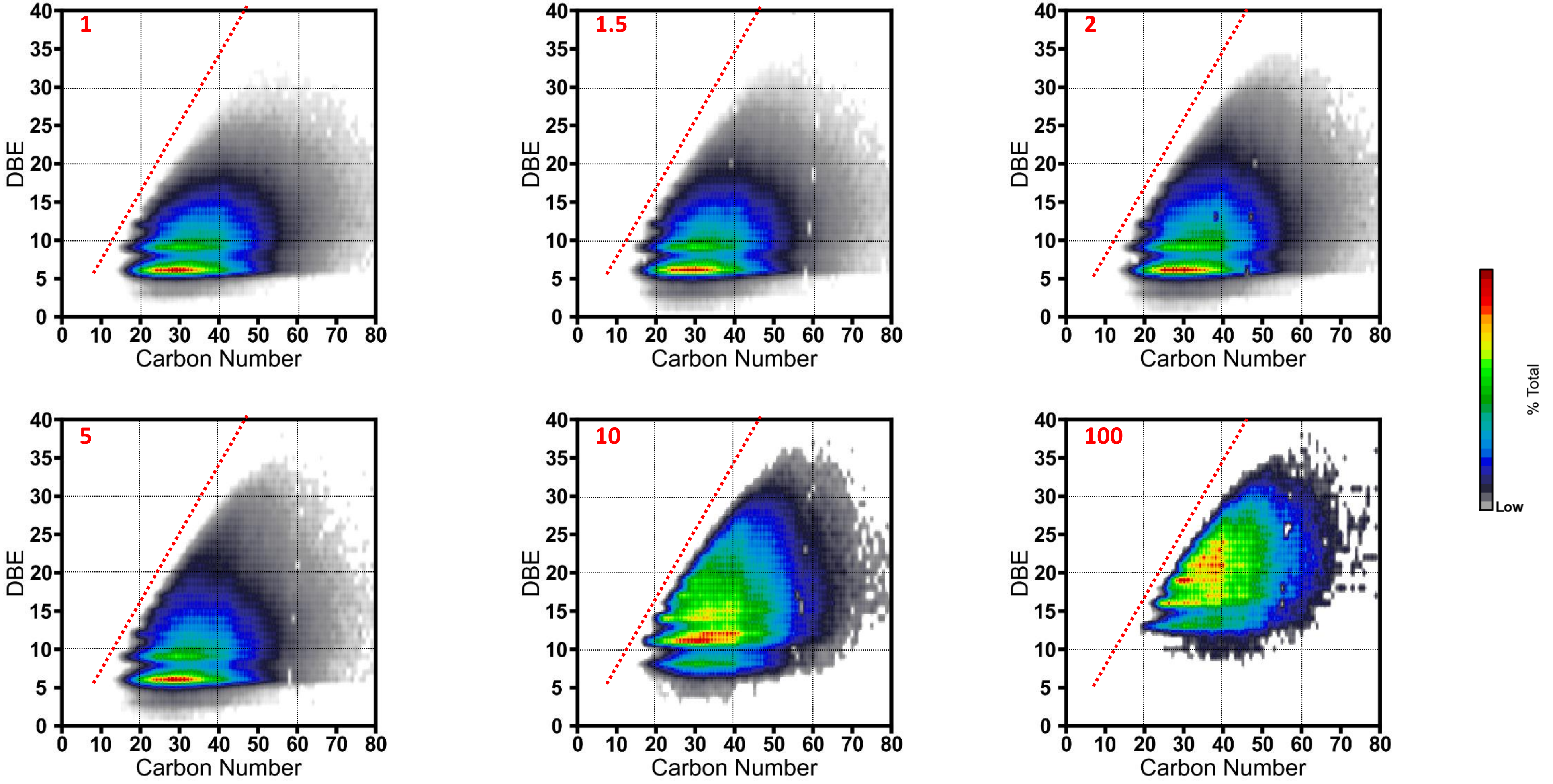

HCOR: heptane crude oil ratio

Asphaltene fractions

Precipitated at Different Solvent Power Conditions

E. Rogel, M. Witt, *Energy & Fuels* 2018, 32, 2653-2660.

No change in carbon distribution with HCOR

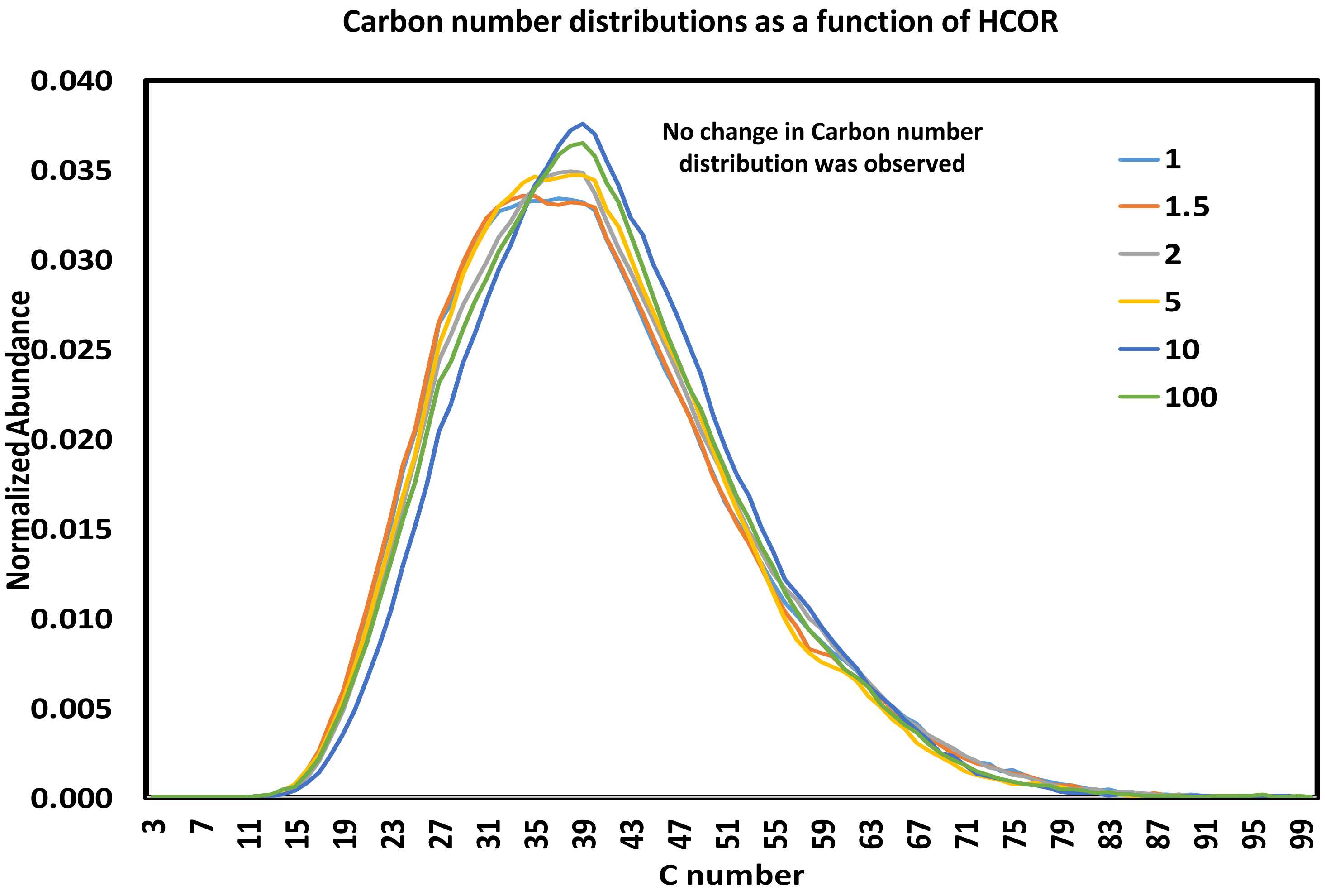

HCOR: heptane crude oil ratio

Asphaltene fractions

Precipitated at Different Solvent Power Conditions

E. Rogel, M. Witt, *Energy & Fuels* 2018, 32, 2653-2660.

Comparison of different aromaticity measurements: FT-IR, APPI FT-ICR MS and ^{1}H-NMR

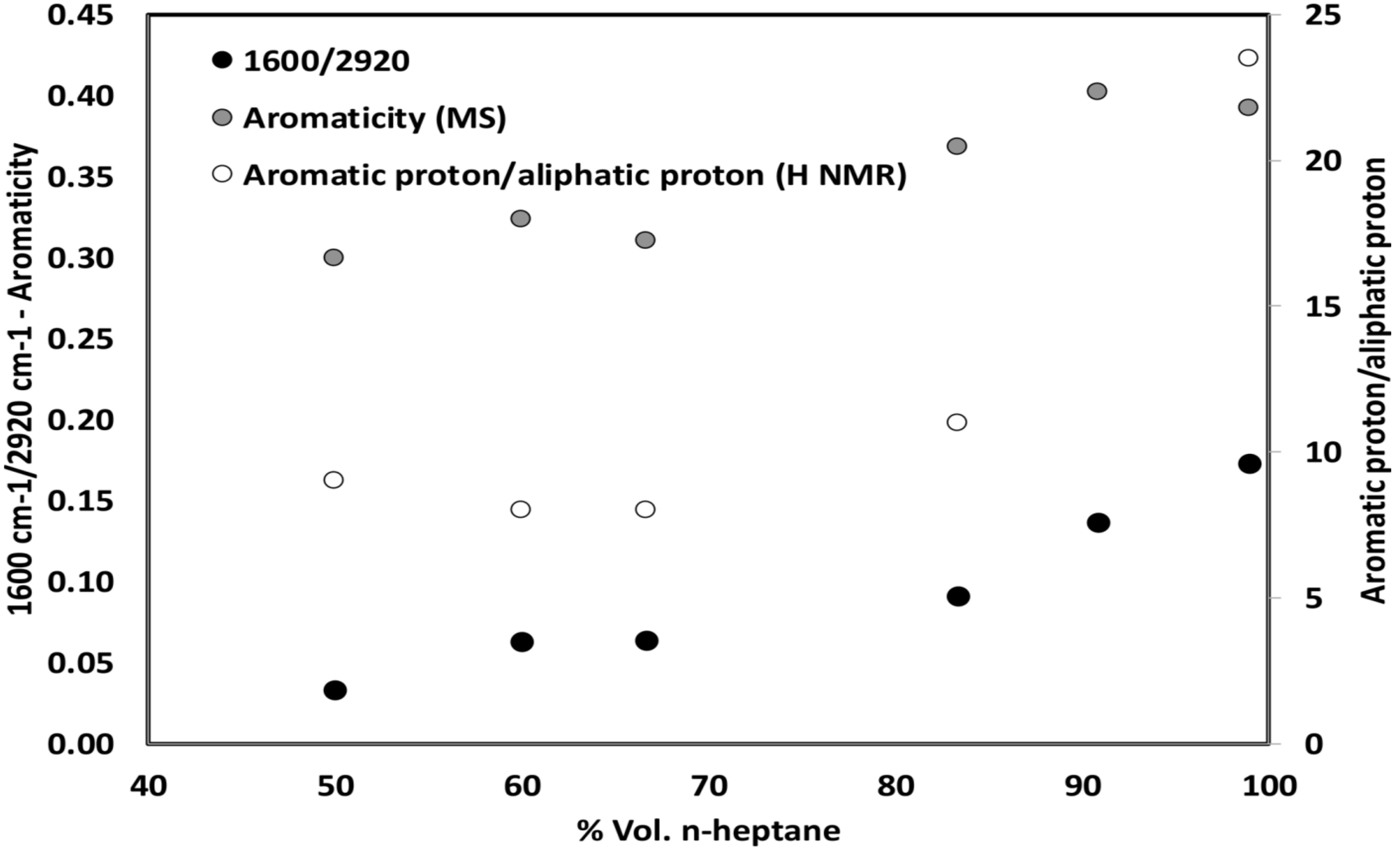

Asphaltene fractions

Precipitated at Different Solvent Power Conditions

E. Rogel, M. Witt, *Energy & Fuels* 2018, 32, 2653-2660.

Comparison of LDI and APPI with elemental analysis

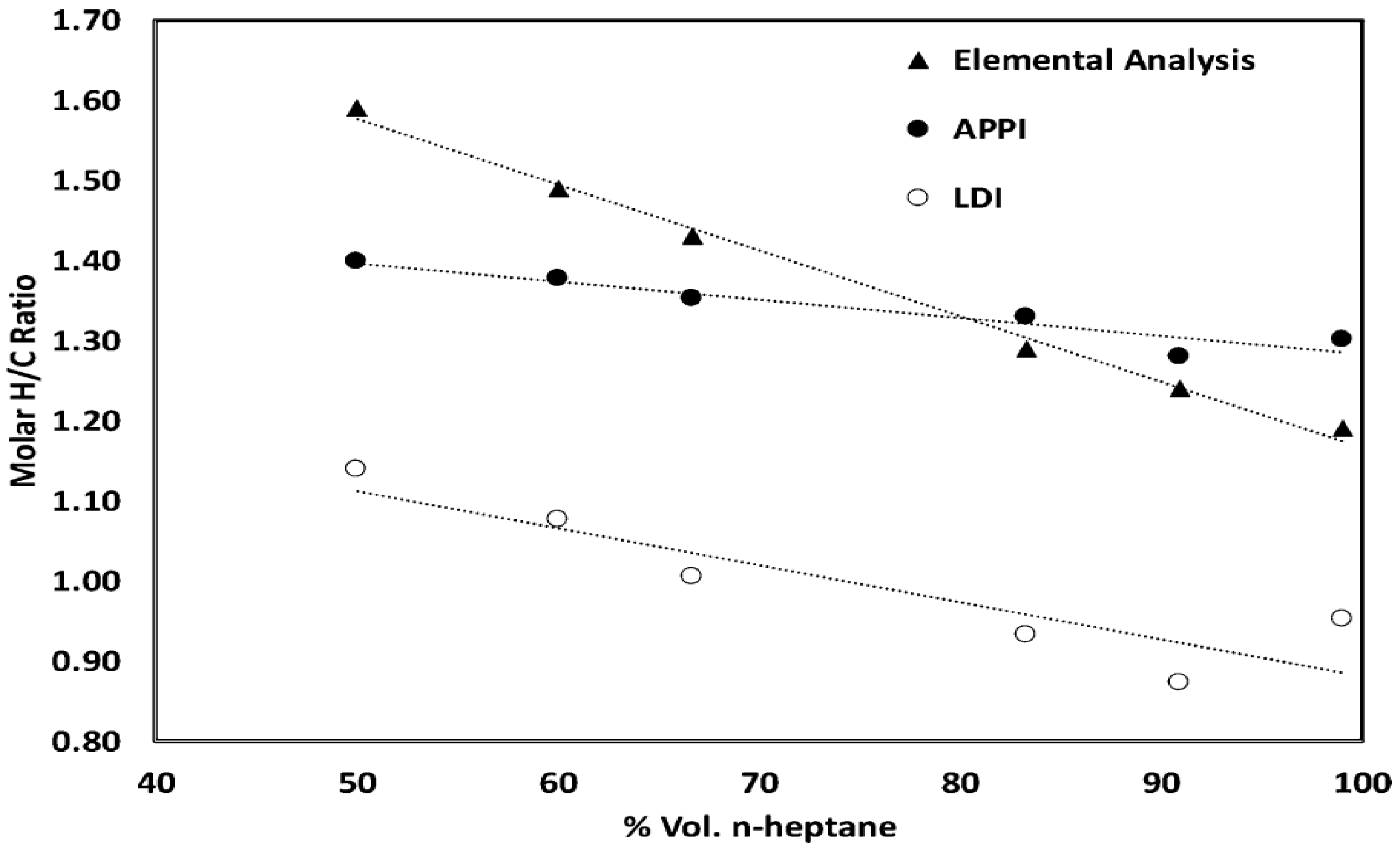

Asphaltene fractions

Precipitated at Different Solvent Power Conditions

E. Rogel, M. Witt, *Energy & Fuels* 2018, 32, 2653-2660.

Change of classes

Compositional distribution of unique species in the asphaltenes obtained at HCOR = 1 and 100

black: HCOR=1
grey: HCOR=100

a) DBE distribution

b) carbon distribution

c) hetero atom distribution

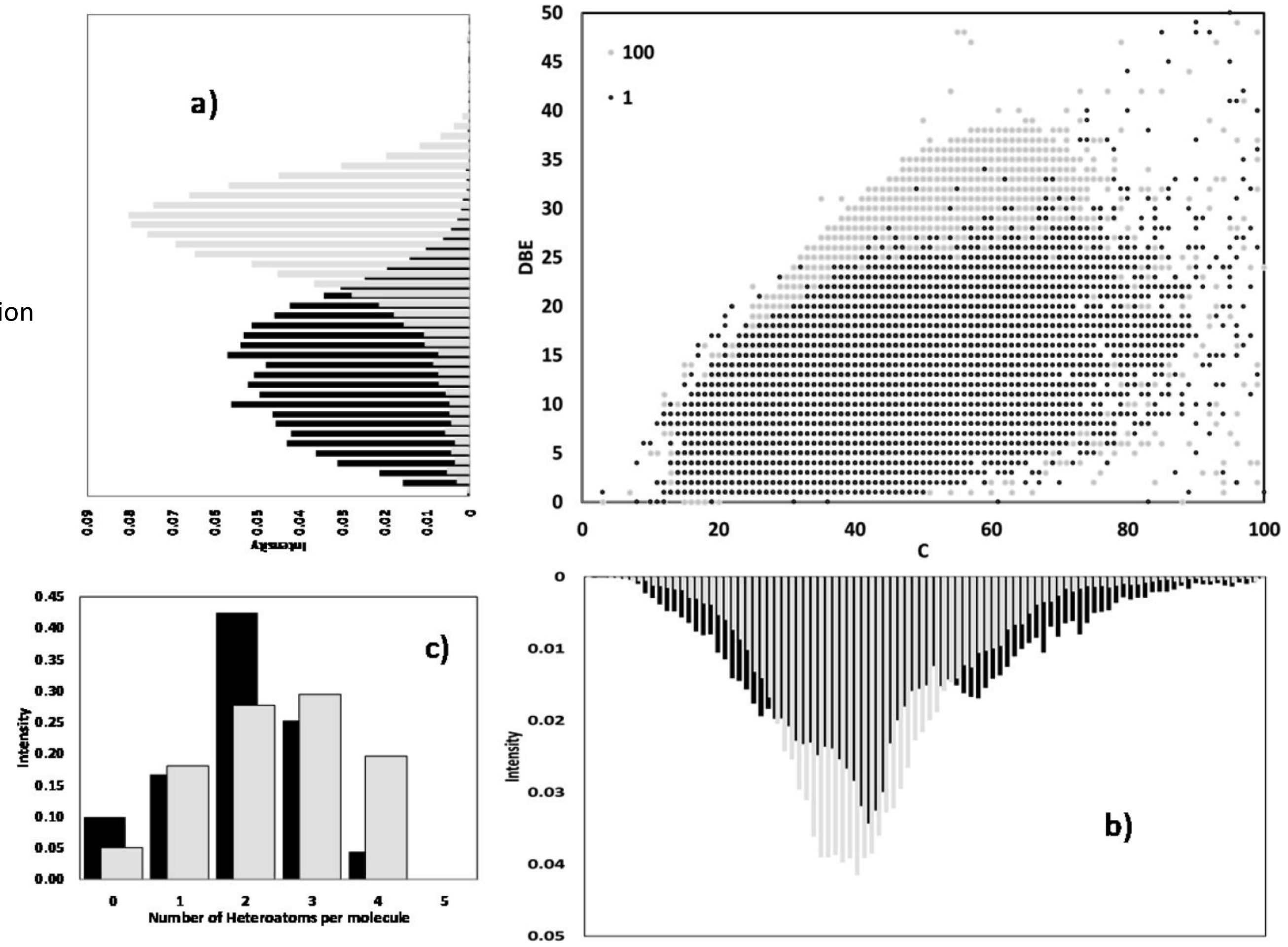

HCOR: heptane crude oil ratio

Asphaltene fractions

Time Effects on Precipitated Asphaltene

E. Rogel, M. Witt, *Energy & Fuels* 2019, 33, 9596−9603

Change of classes and hetero atom content

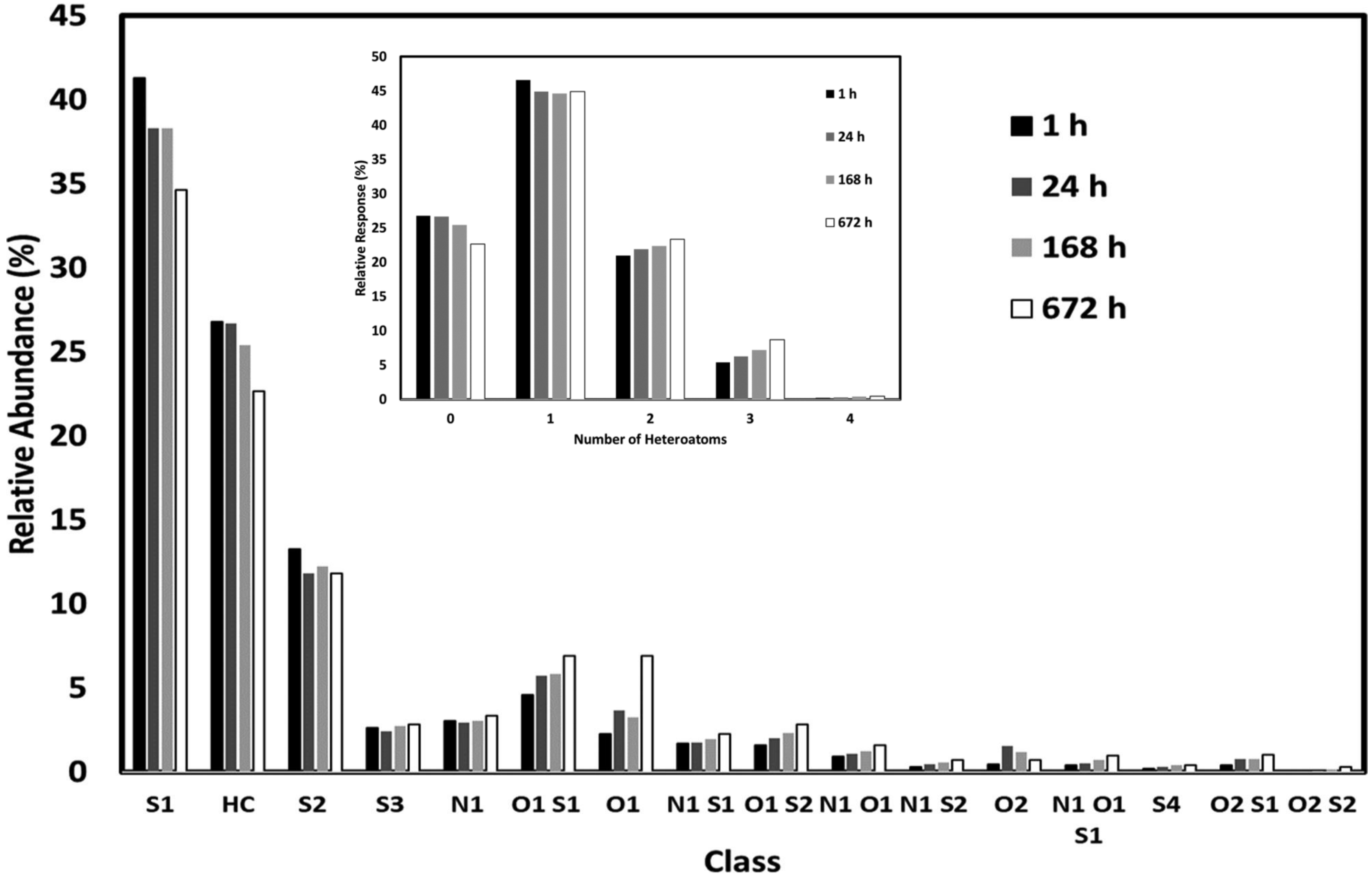

Time (h)	H/C ratio
1	1.54
24	1.43
168	1.42
672	1.38

heptane crude oil ratio 1:10

Asphaltene fractions

Time Effects on Precipitated Asphaltene

E. Rogel, M. Witt, *Energy & Fuels* 2019, 33, 9596−9603

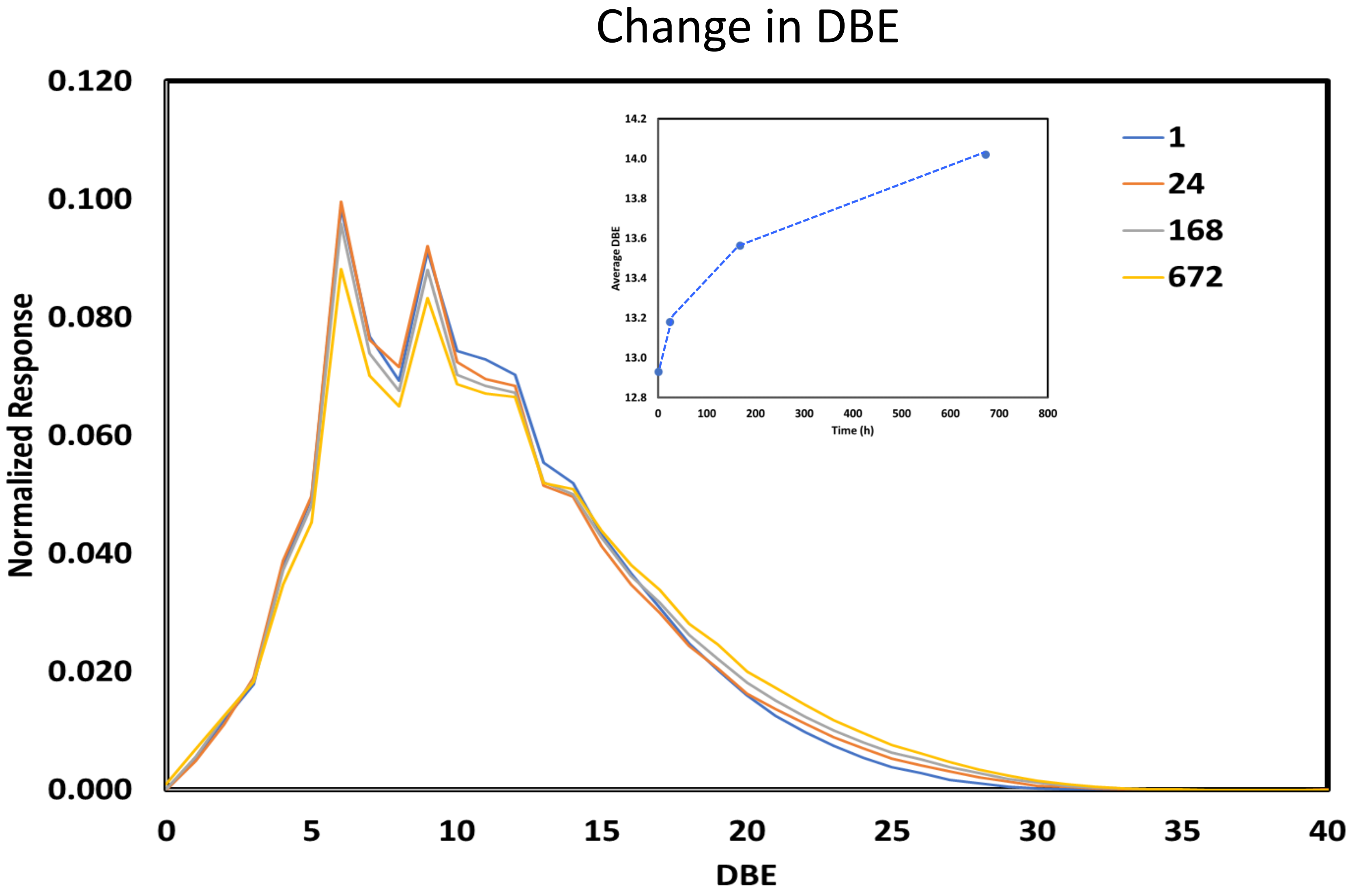

Time (h)	H/C ratio
1	1.54
24	1.43
168	1.42
672	1.38

heptane crude oil ratio 1:10

Asphaltene fractions

Time Effects on Precipitated Asphaltene

E. Rogel, M. Witt, *Energy & Fuels* 2019, 33, 9596−9603

Change in DBE

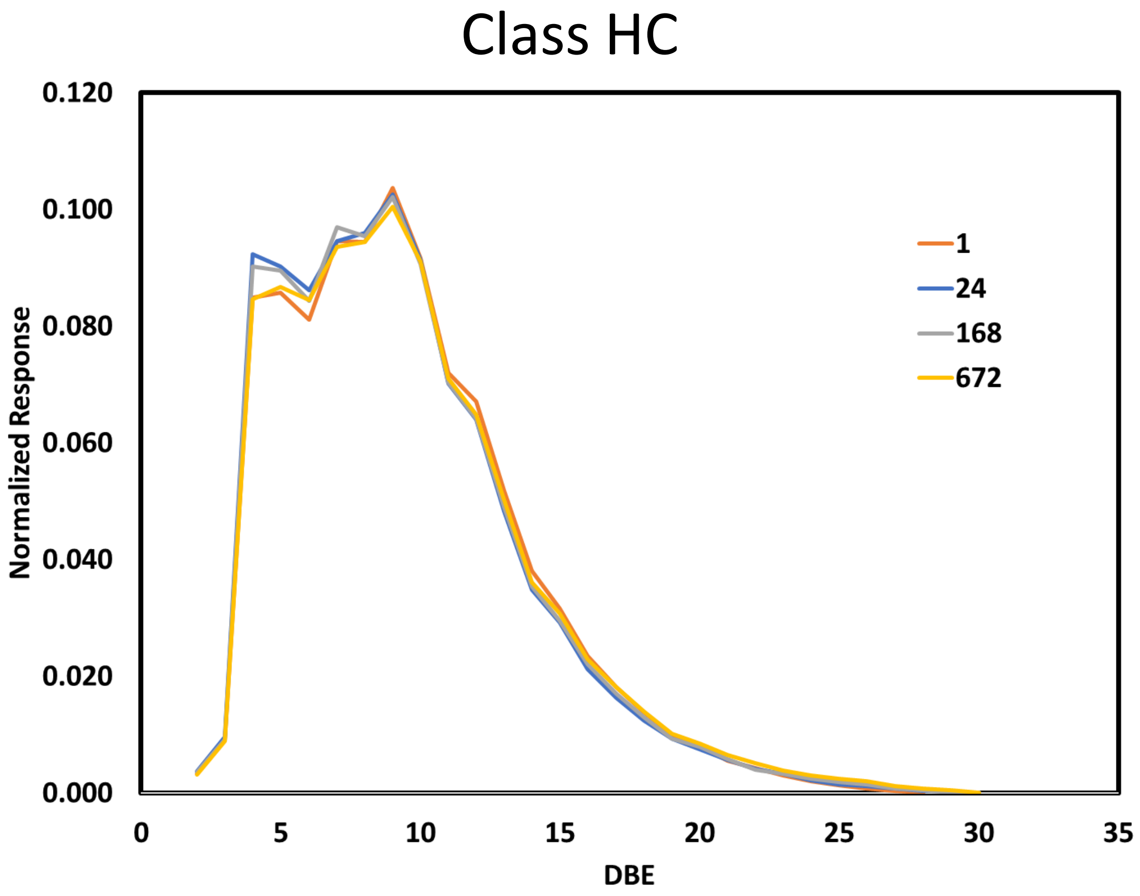

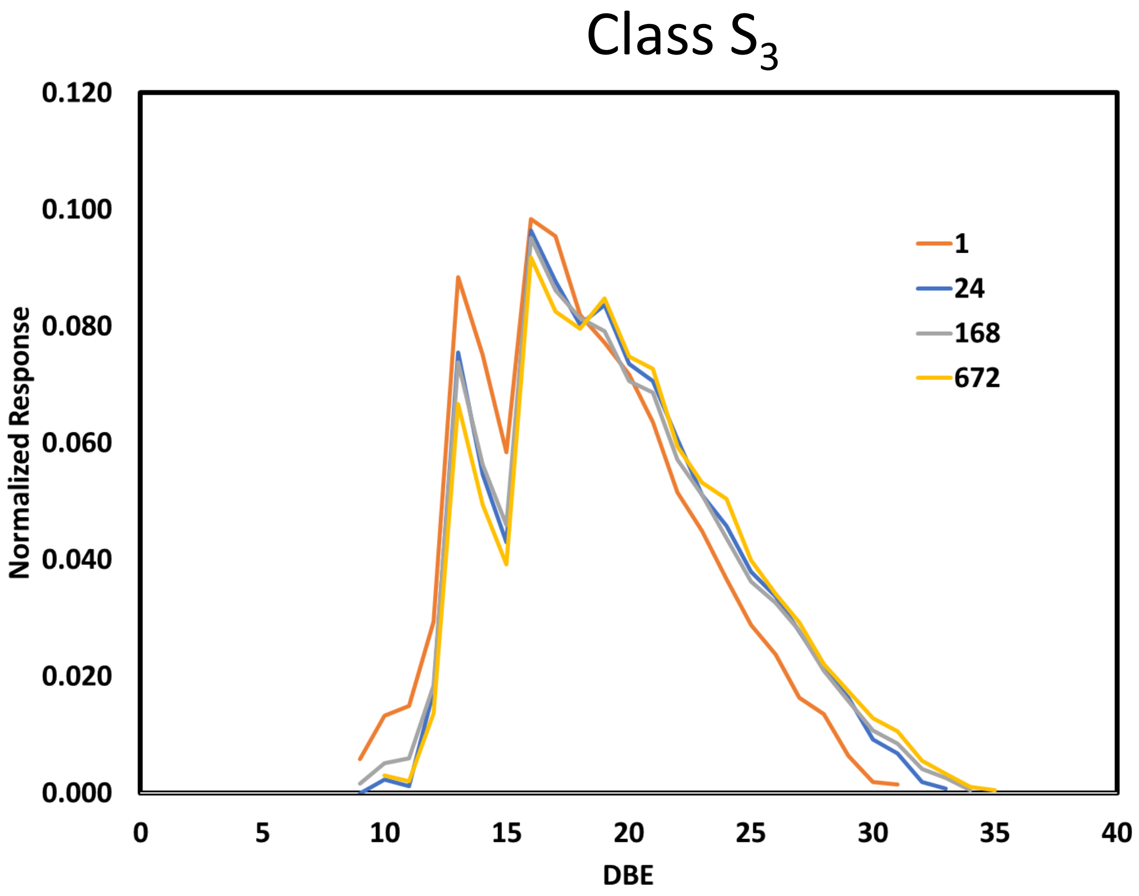

Asphaltene fractions

Time Effects on Precipitated Asphaltene

E. Rogel, M. Witt, *Energy & Fuels* 2019, 33, 9596−9603

Comparison of the compositional space for sulfur containing species that appear in the aged deposit (672 h) with the ones that go back to the fluid from the initially precipitated material (1 h)

▲ **Dissolved species**

○ **Precipitated species**

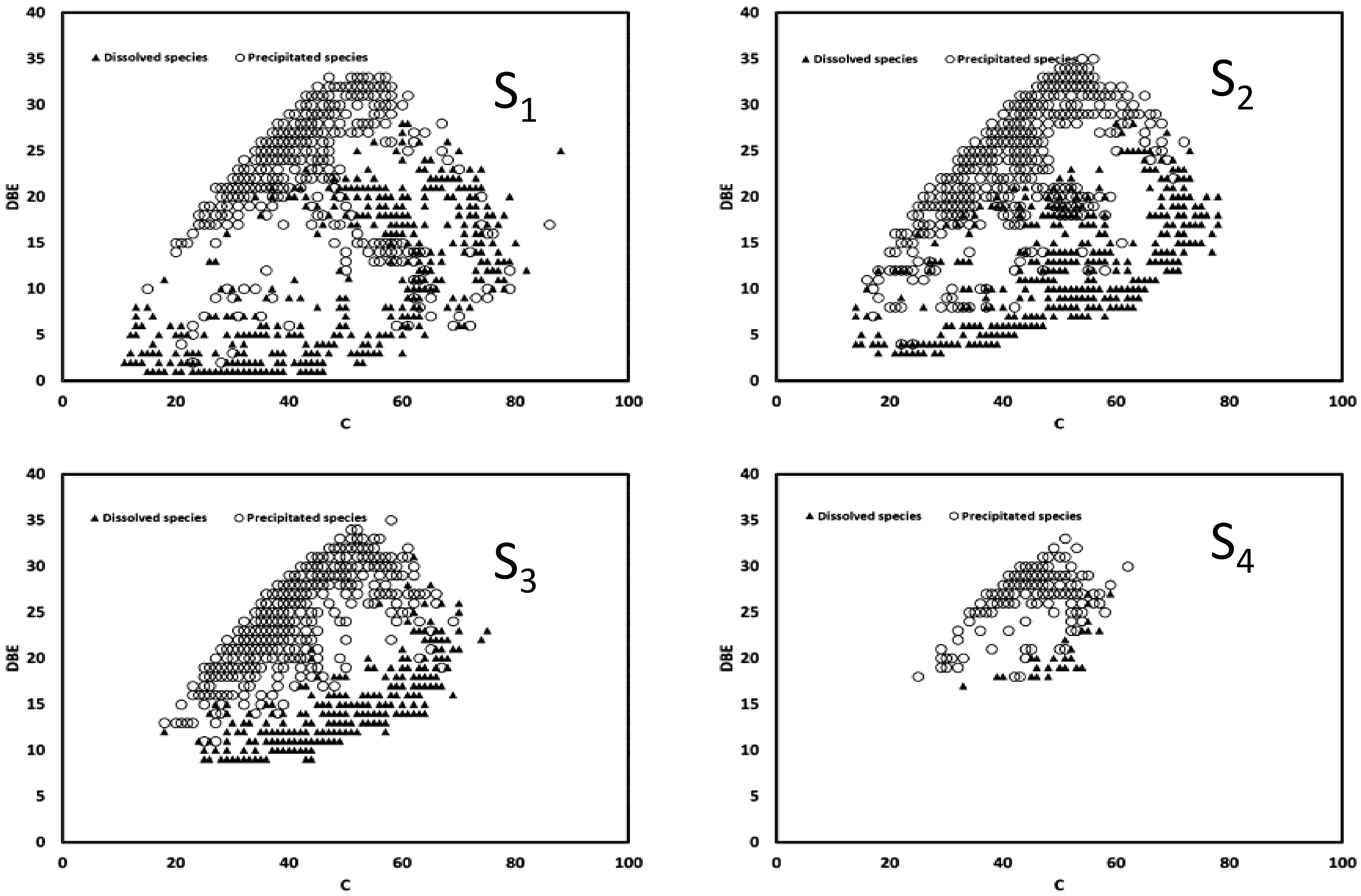

Hydroprocessing

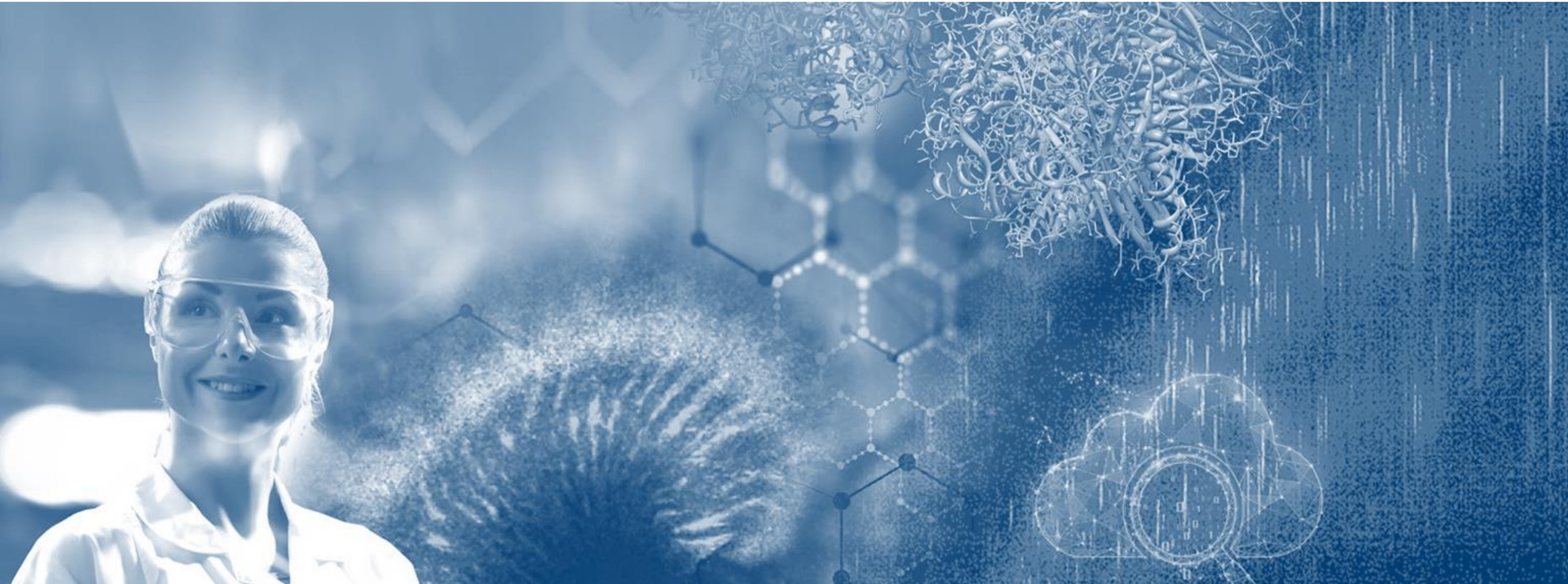

Hydroprocessing

Effect on compound classes

E. Rogel, M. Witt, *Energy & Fuels* 2017, 31, 3409-3416.

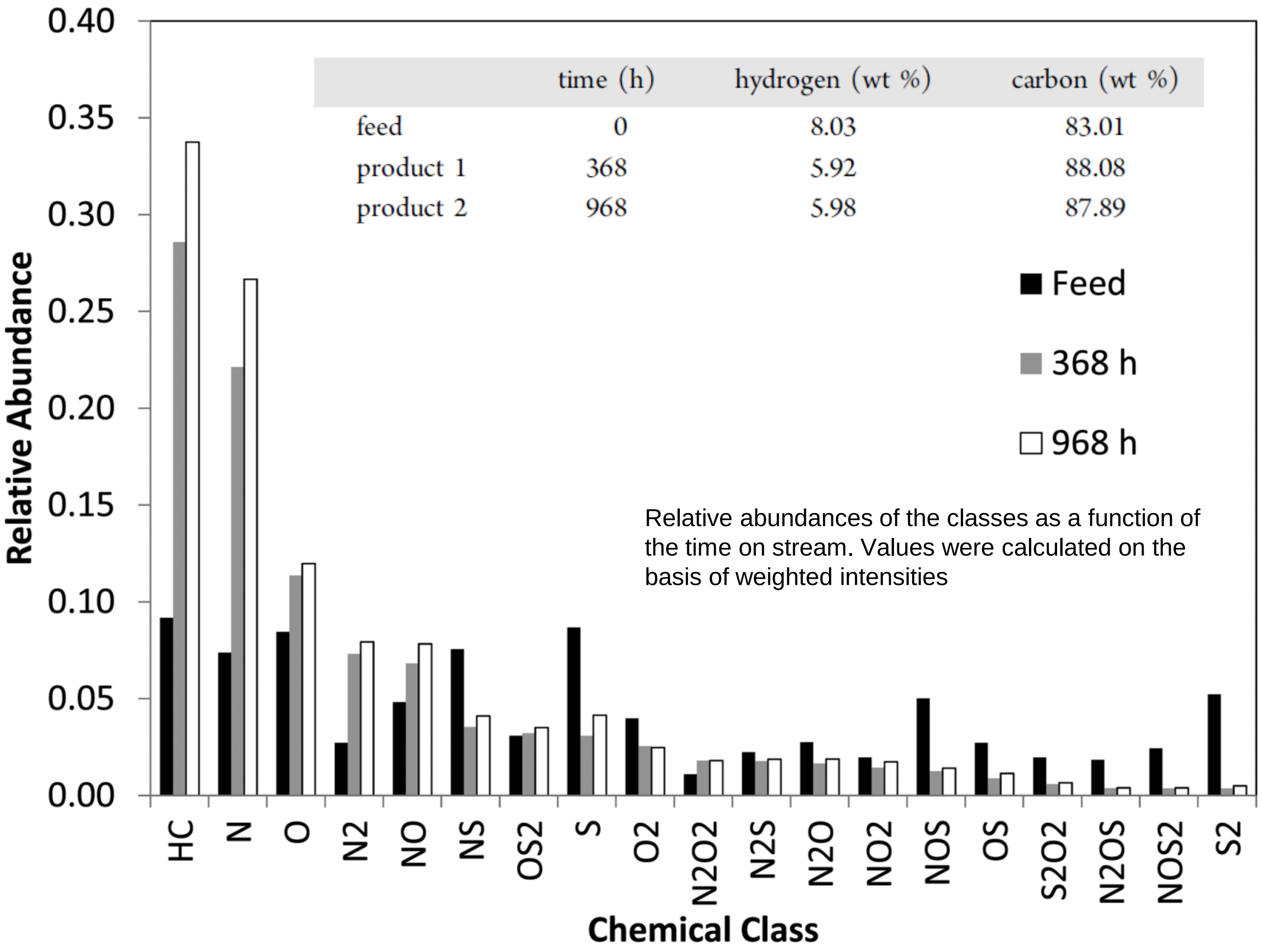

	time (h)	hydrogen (wt %)	carbon (wt %)
feed	0	8.03	83.01
product 1	368	5.92	88.08
product 2	968	5.98	87.89

Relative abundances of the classes as a function of the time on stream. Values were calculated on the basis of weighted intensities

Hydroprocessing

Effect on carbon distribution, aromaticity and hetero atom content

E. Rogel, M. Witt, *Energy & Fuels* 2017, 31, 3409-3416.

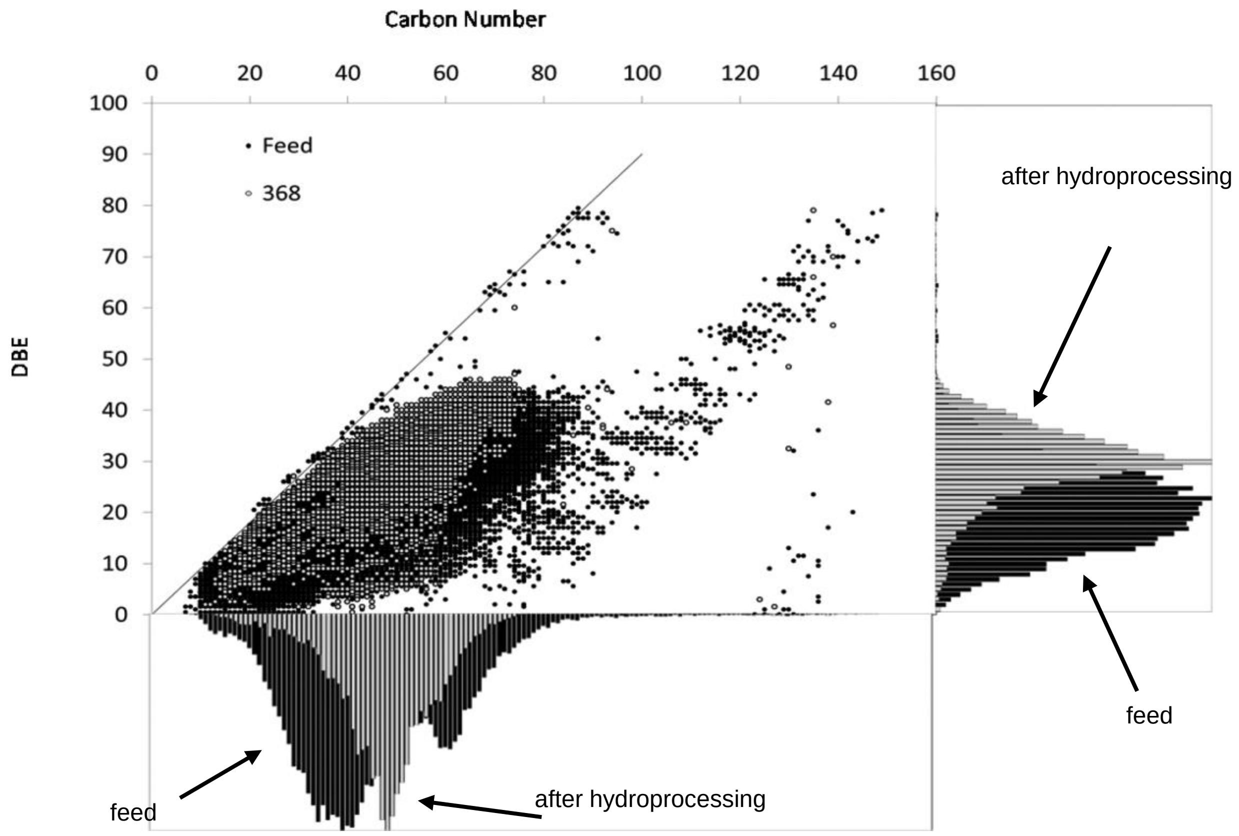

Comparison of the compositional space occupied by molecules that disappeared from the feed during processing to those that appeared in the products.

Heteroatom contents as a function of time on stream

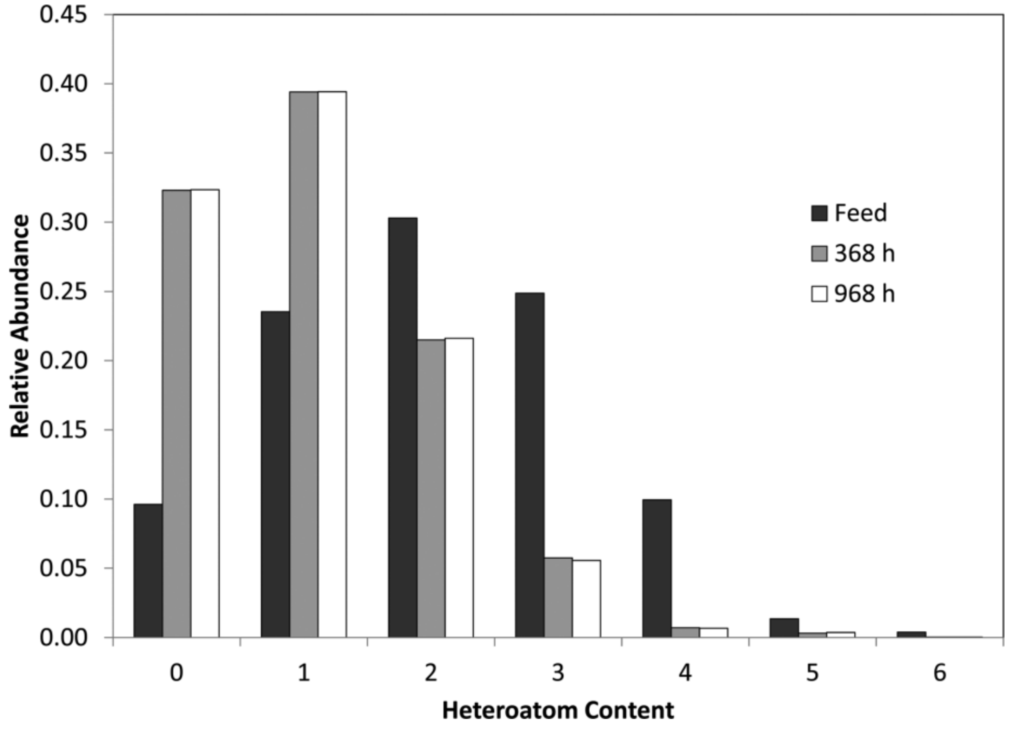

Hydroprocessing

Appearing and disappearing compound by hydroprocessing

E. Rogel, M. Witt, *Energy & Fuels* 2017, 31, 3409-3416.

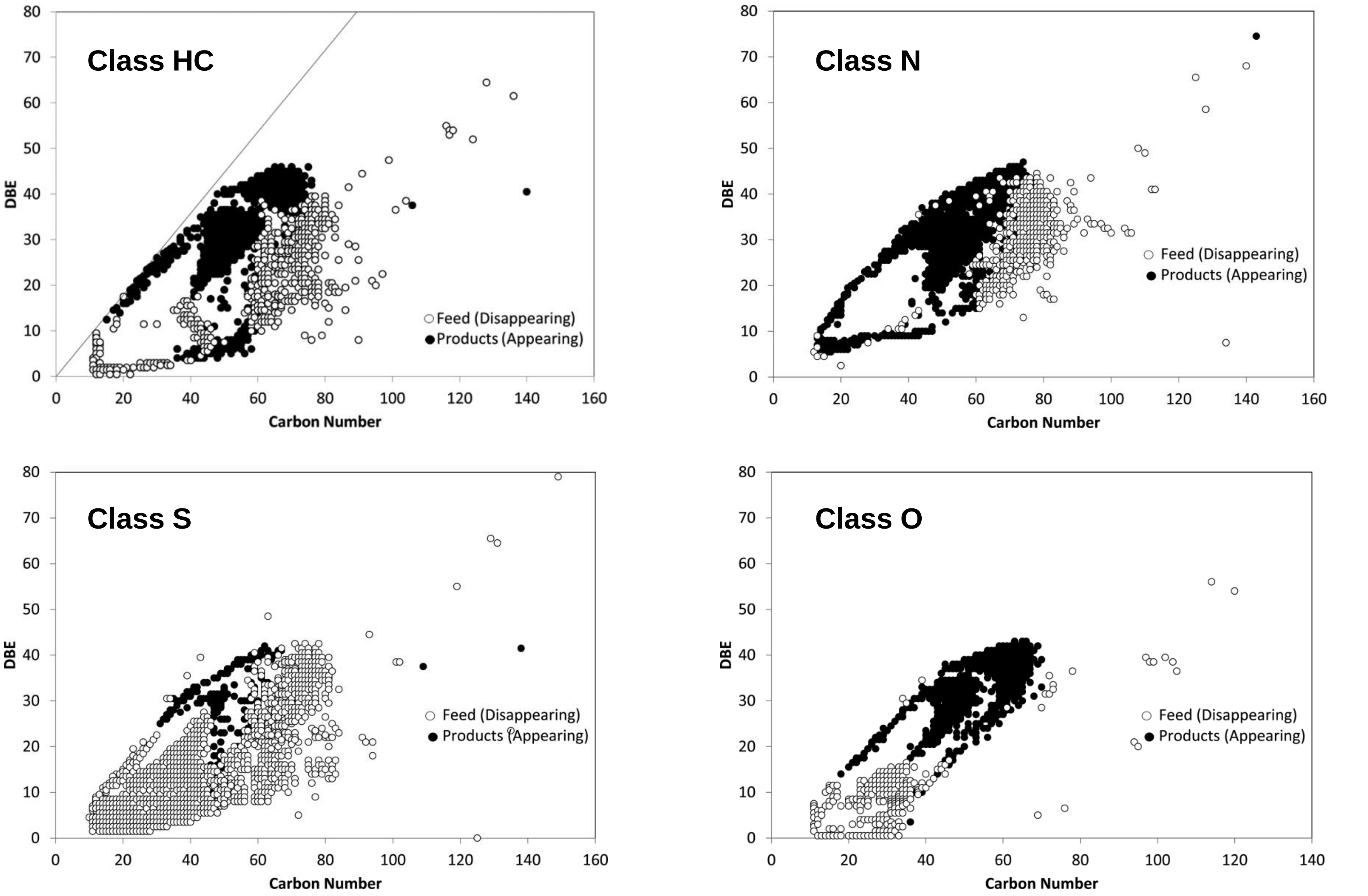

Compositional and Structural Continuum of Petroleum

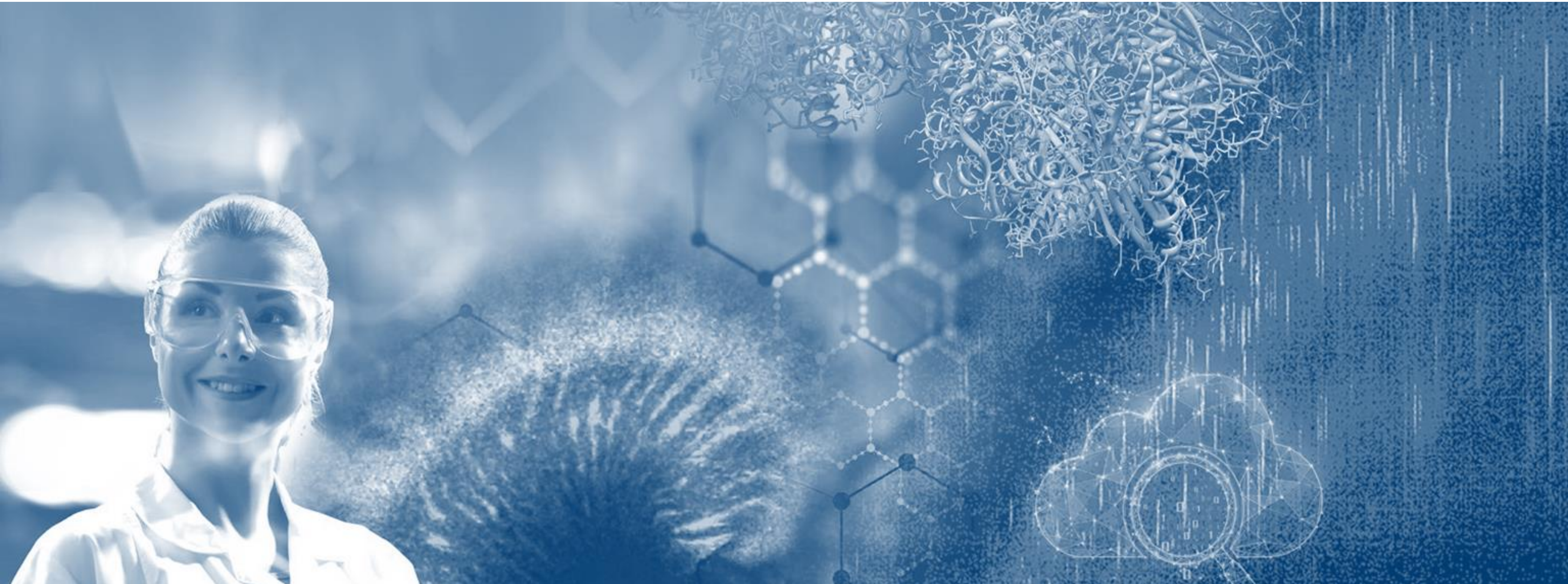

Compositional and Structural Continuum of Petroleum

Distillation series

A. McKenna et al., *Energy Fuels 2010, 24 (5), 2929–2938*.

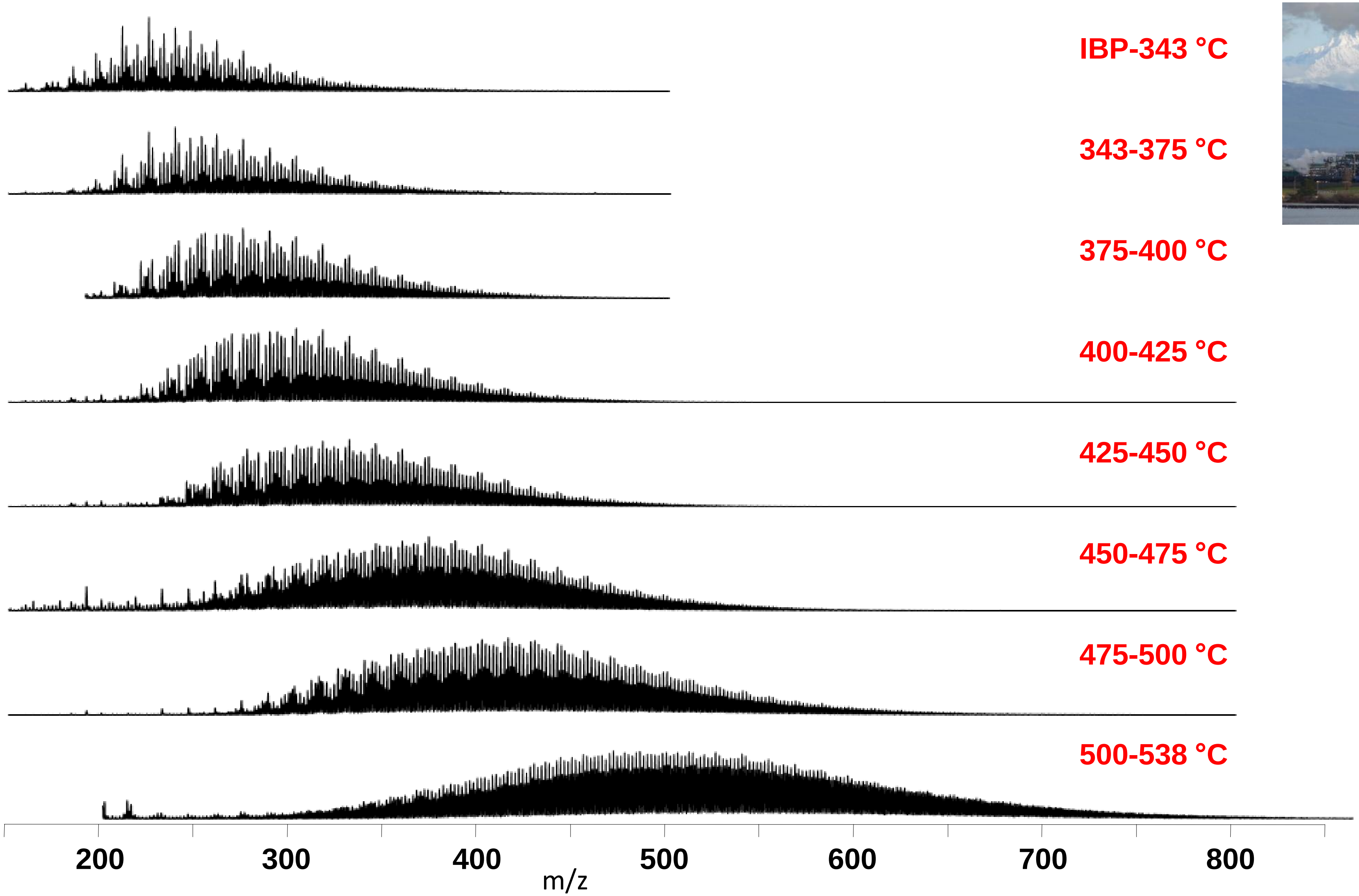

IBP: initial boiling point

Compositional and Structural Continuum of Petroleum

Distillation series – Boduszynski Continuum Model

A. McKenna et al., *Energy Fuels 2010, 24 (5), 2929–2938*.

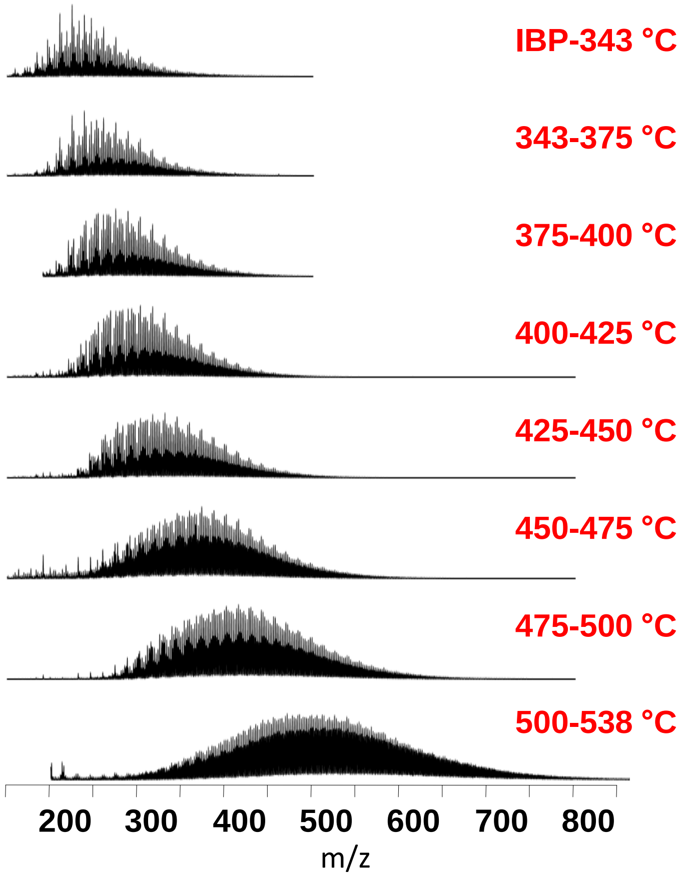

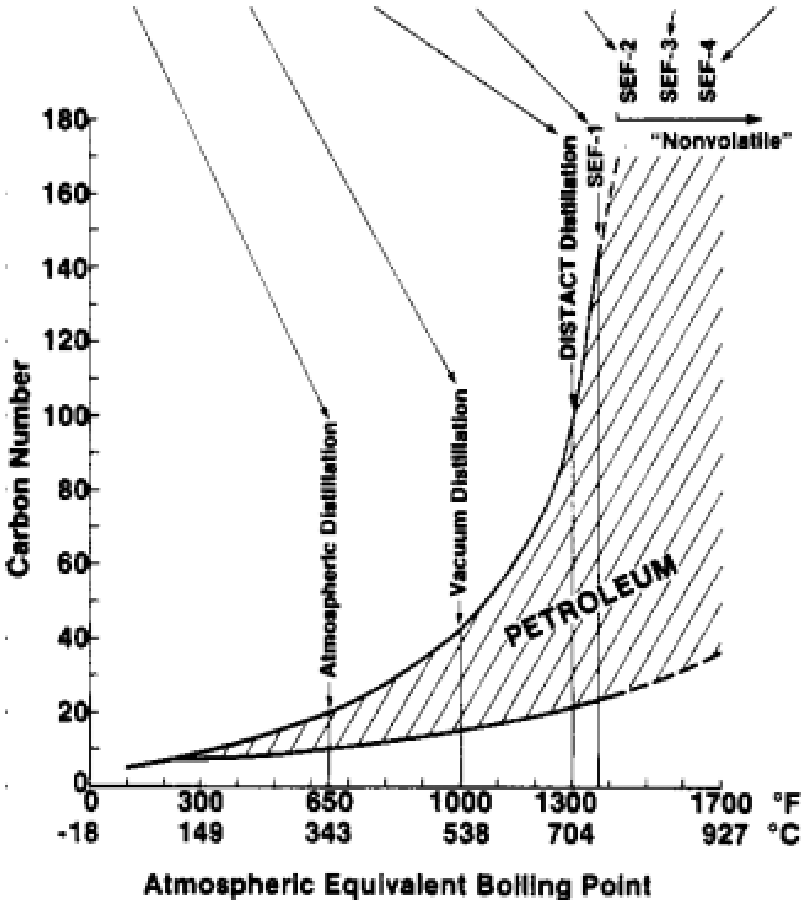

Boduszynski Continuum Model

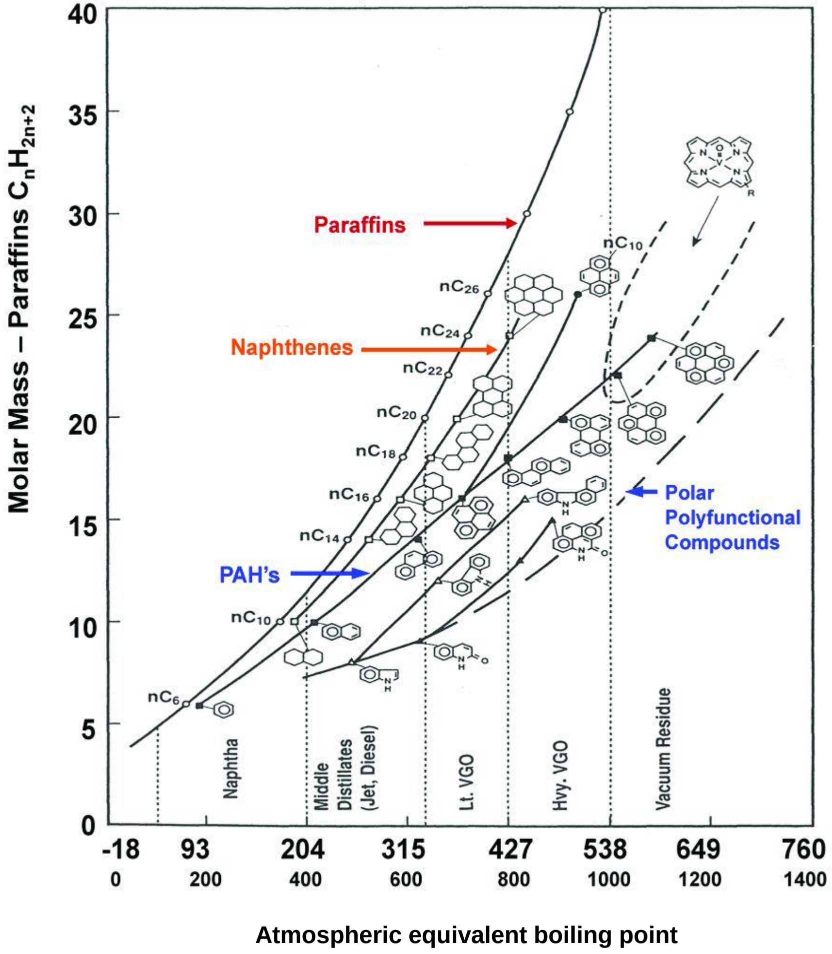

IBP: initial boiling point

Compositional and Structural Continuum of Petroleum

Distillation series

A. McKenna et al., *Energy Fuels 2010, 24 (5), 2929–2938.*

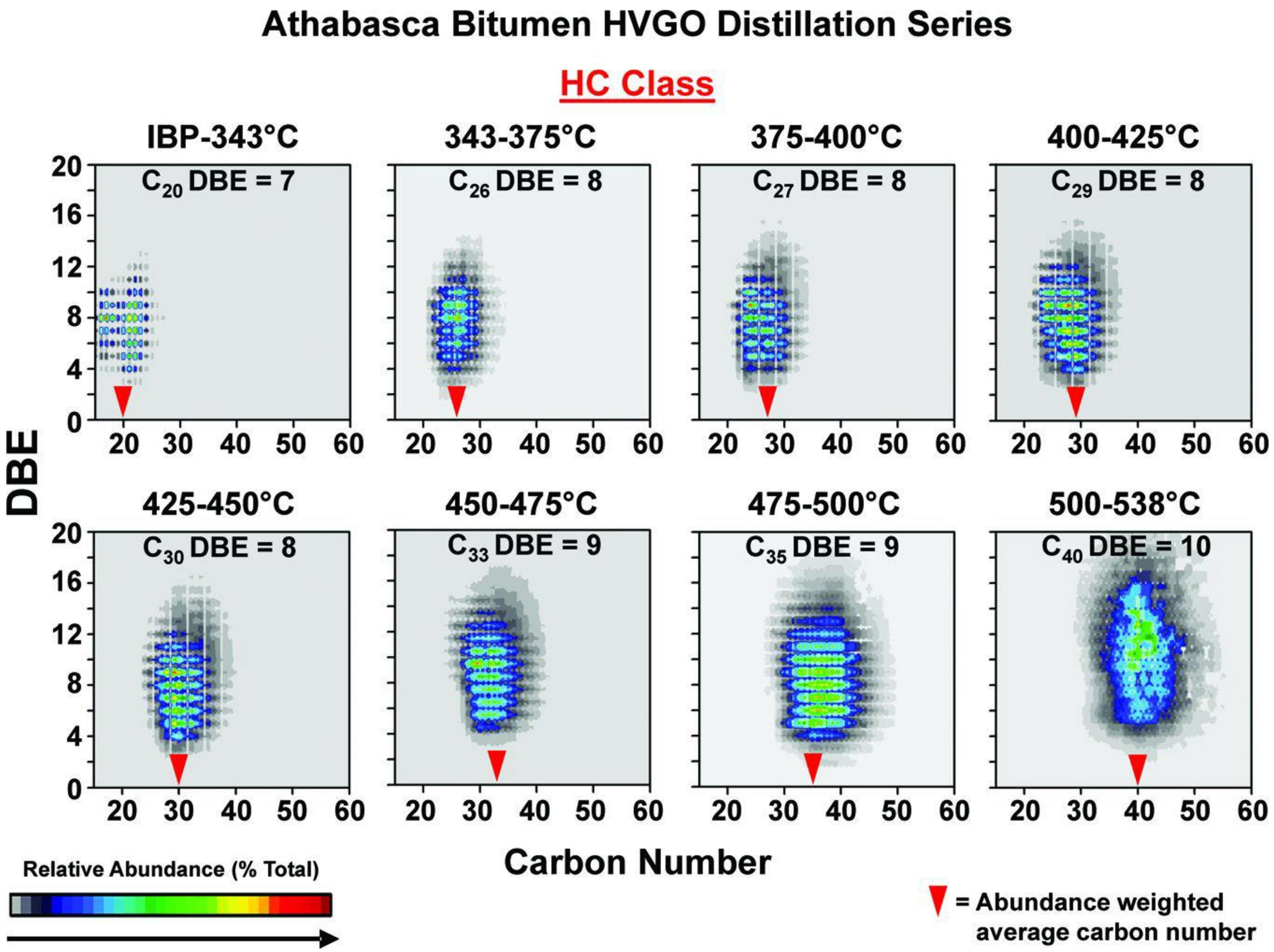

Compositional and Structural Continuum of Petroleum

Distillation series

A. McKenna et al., *Energy Fuels 2010, 24 (5), 2929–2938*.

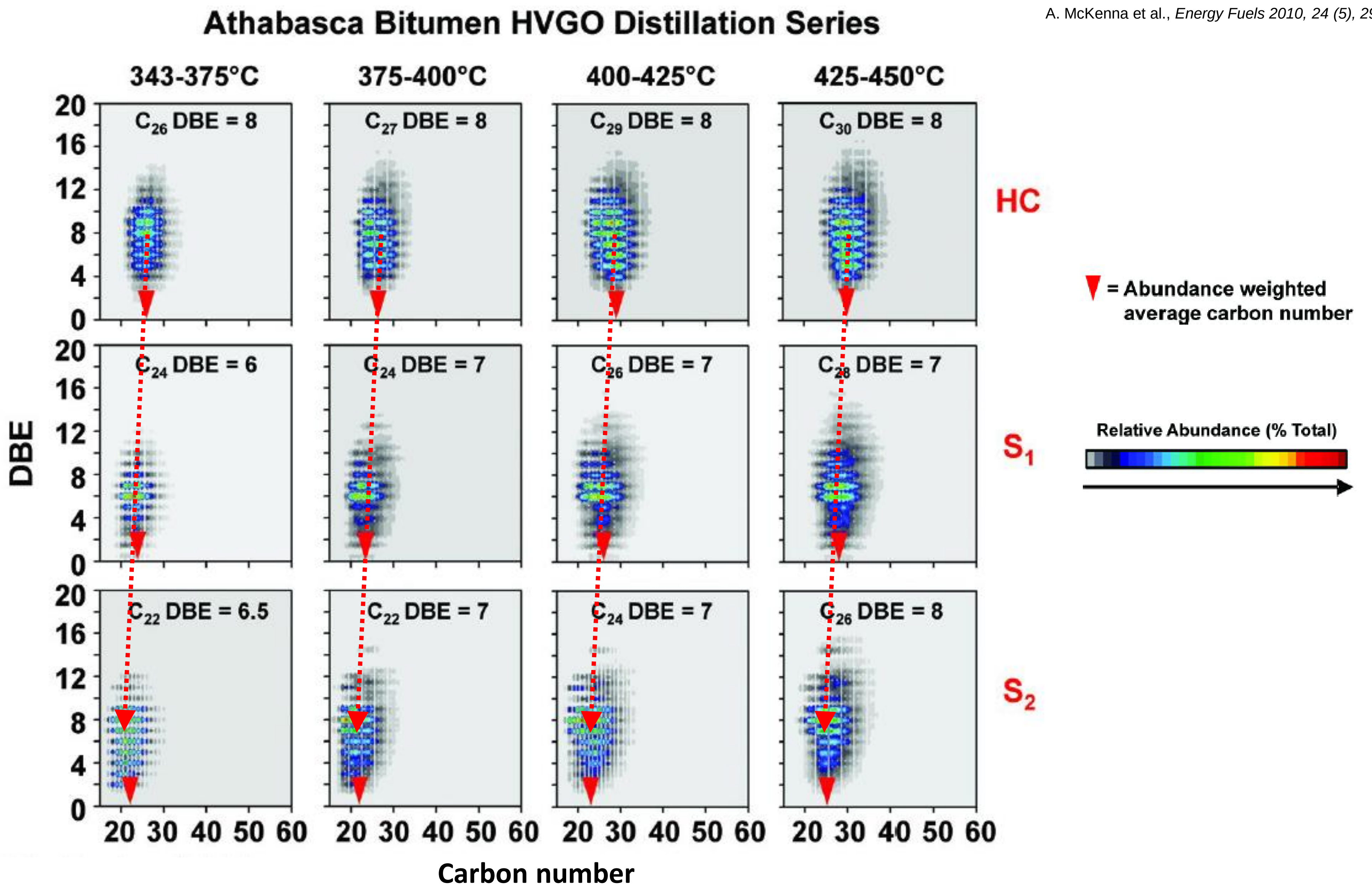

Compositional and Structural Continuum of Petroleum

Distillation series

A. McKenna et al., *Energy Fuels 2010, 24 (5), 2929–2938.*

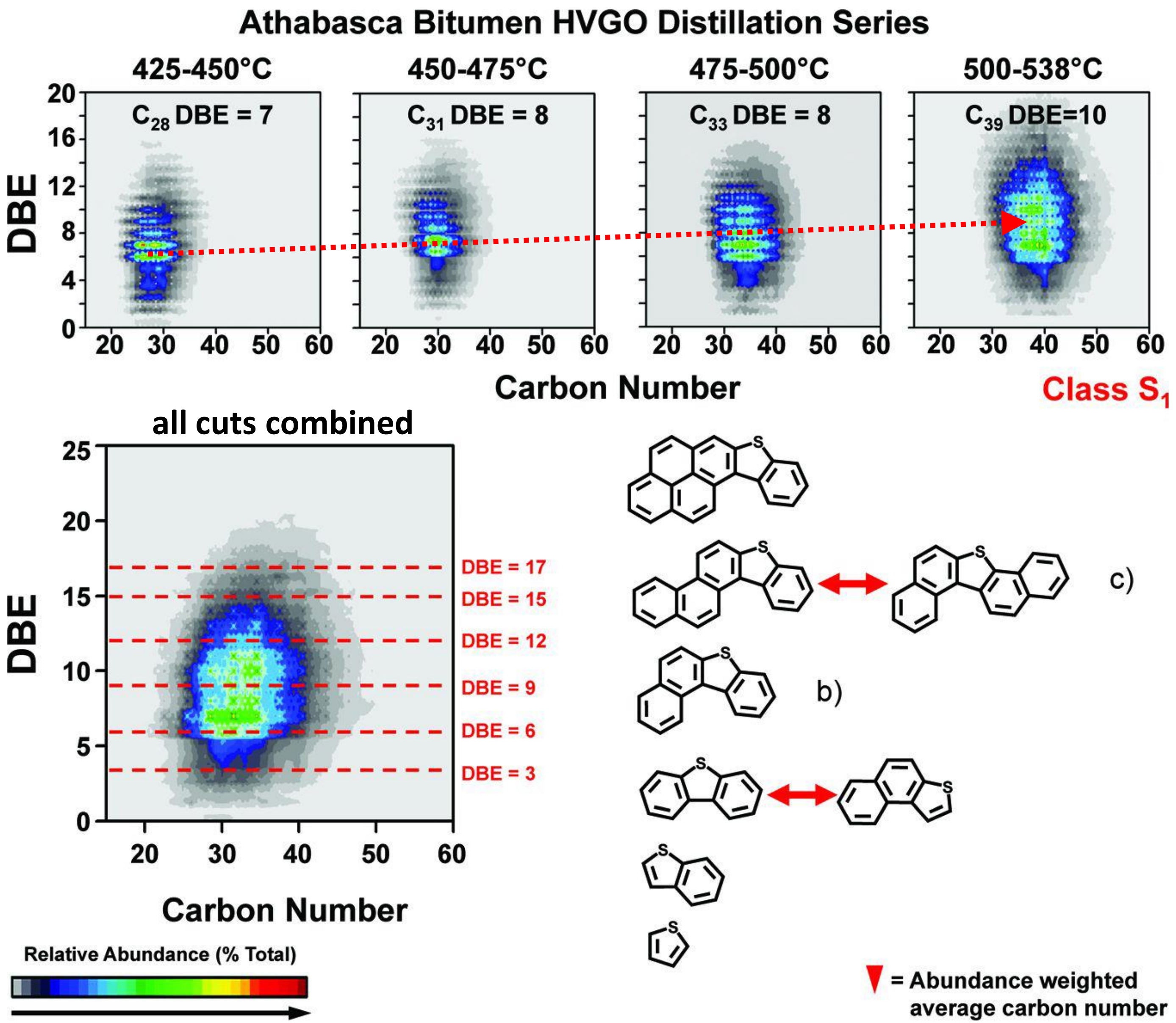

Compositional and Structural Continuum of Petroleum

Distillation series

A. McKenna et al., *Energy Fuels 2010, 24 (5), 2939–2946.*

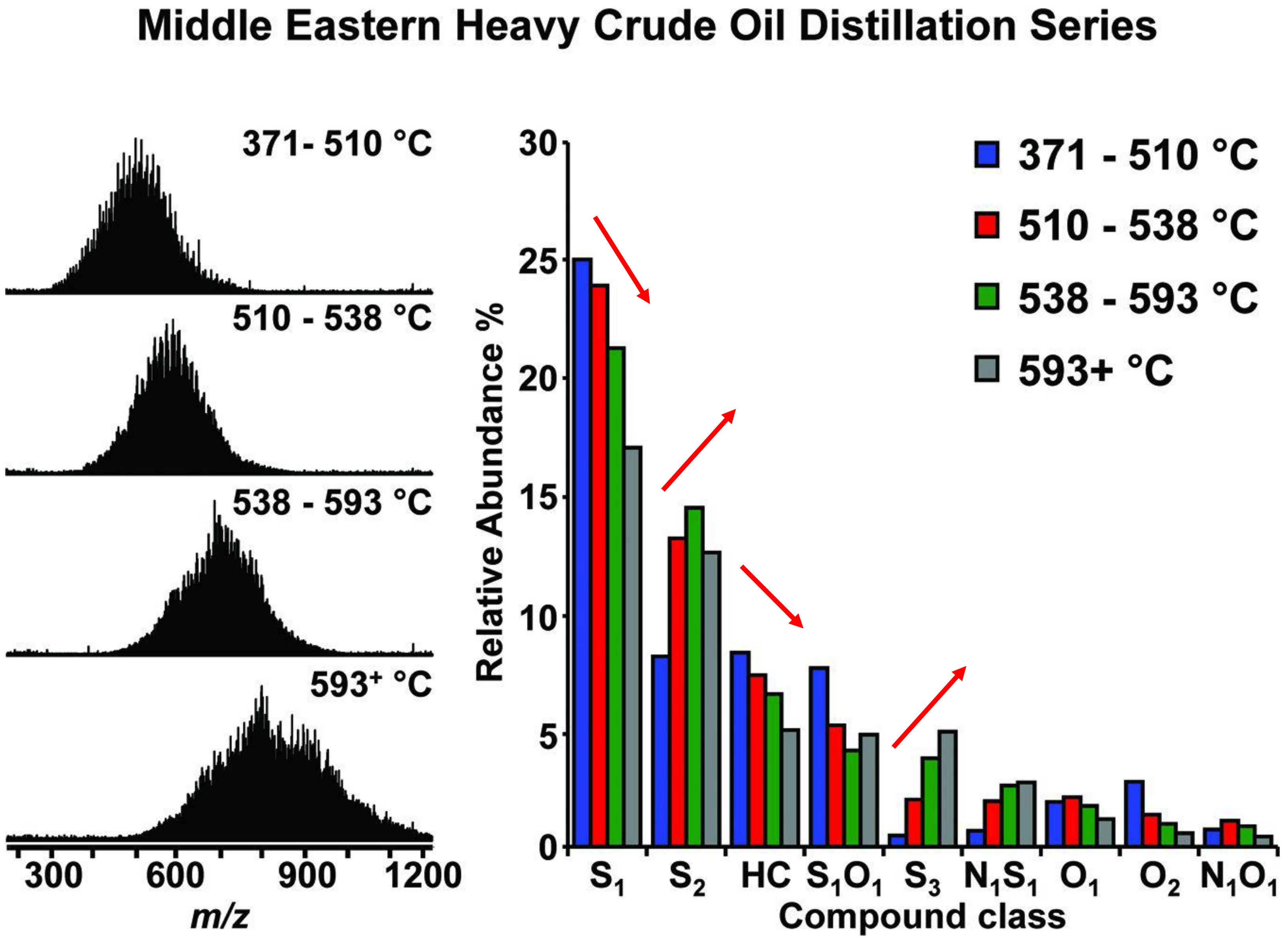

Fractionation of Material

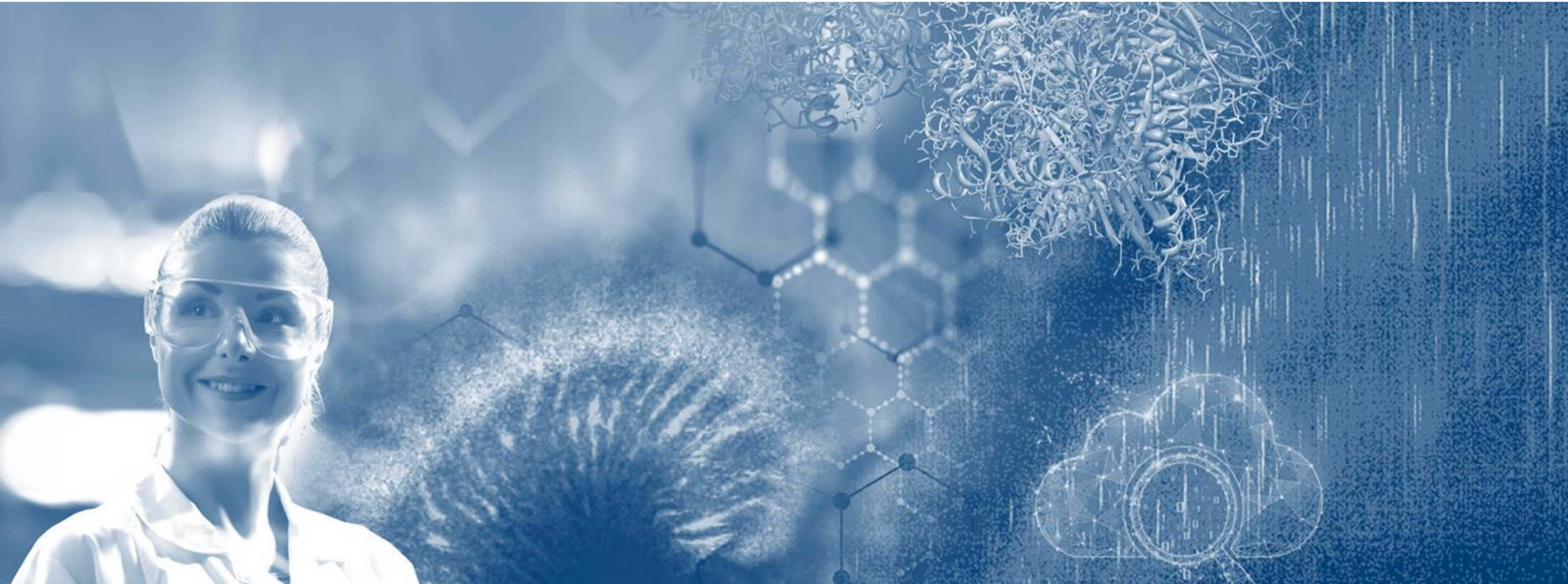

Fractionation of Naphthenic acids

MAPS fractionation (MAPS: modified aminopropyl silica)

S. Rowland et al., *Energy Fuels 2014, 28, 5043−5048*

APS Extraction

APS
Conditioned with DCM
↓
CN 1 (83.0 ± 0.4%)
(100%) DCM, 20 mL
↓
CN 2 (2.4 ± 1.0%)
(50/50) DCM:MeOH, 15 mL
↓
CA 1 (3.5 ± 0.4%)
(50/50/5) DCM:MeOH:FA, 10 mL

APS Extraction
Total % Recovery = 88.9 ± 1.1%

MAPS Extraction
Total % Recovery = 91.9 ± 0.8%

MAPS Extraction

APS
Conditioned with DCM
↓
MN 1 (87.2 ± 0.7%)
(100%) DCM, 20 mL
↓
MN 2 (1.3 ± 0.1%)
(50/50) DCM:MeOH, 15 mL
↓
MN 3 (N/A)
(100%) MeOH, 15 mL
↓
MN 4 (N/A)
(70/30) MeOH:H_2O, 15 mL
→
MA 1 (0.8 ± 0.1%)
(70/30/5) MeOH:H_2O:FA, 10 mL
↑
MA 2 (0.6 ± 0.1%)
(80/20/5) MeOH:H_2O:FA, 10 mL
↑
MA 3 (0.6 ± 0.1%)
(90/10/5) MeOH:H_2O:FA , 10 mL
↑
MA 4 (0.6 ± 0.1%)
(100/5) MeOH:FA , 10 mL
↑
MA 5 (0.1 ± 0.1%)
(5/95/5) DCM:MeOH:FA , 10 mL
↑
MA 6 (0.2 ± 0.1%)
(20/80/5) DCM:MeOH:FA , 10 mL
↑
MA 7 (0.5 ± 0.1%)
(50/50/5) DCM:MeOH:FA

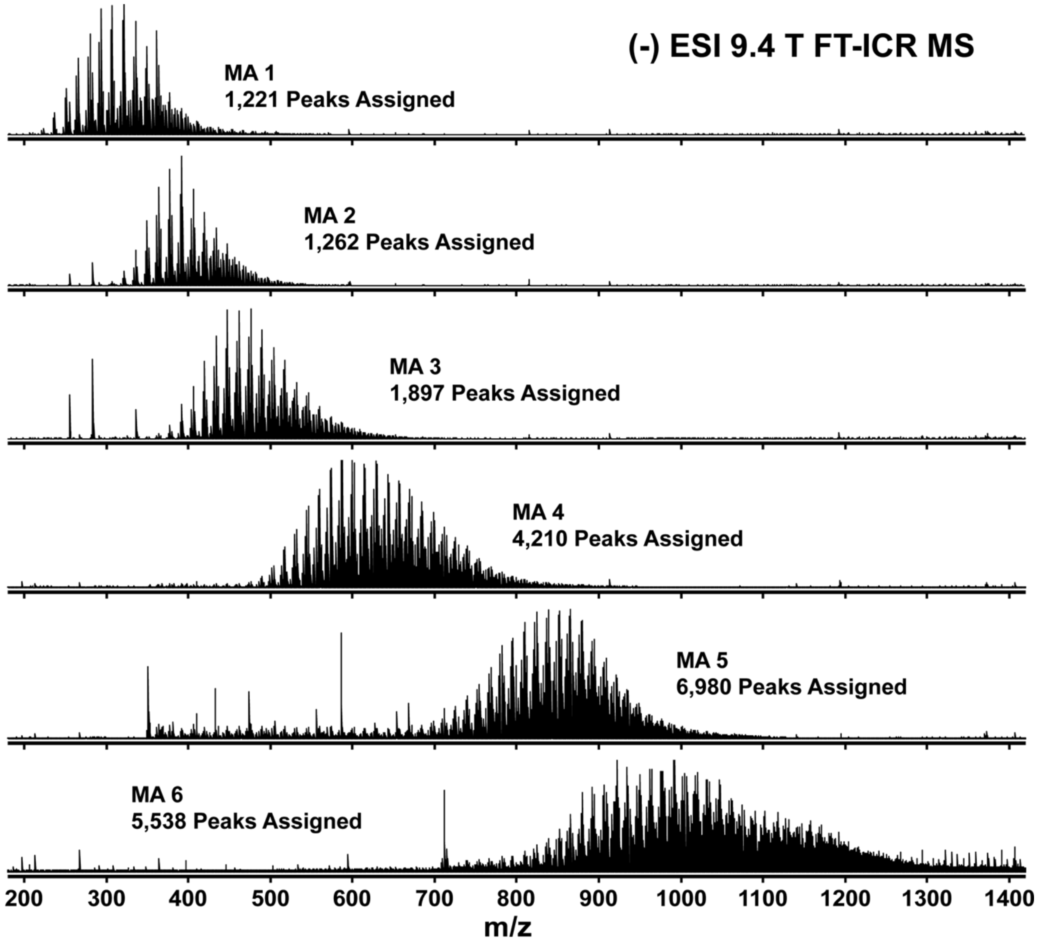

Fractionation of Naphthenic acids

MAPS fractionation (MAPS: modified aminopropyl silica)

S. Rowland et al., *Energy Fuels 2014, 28, 5043−5048*

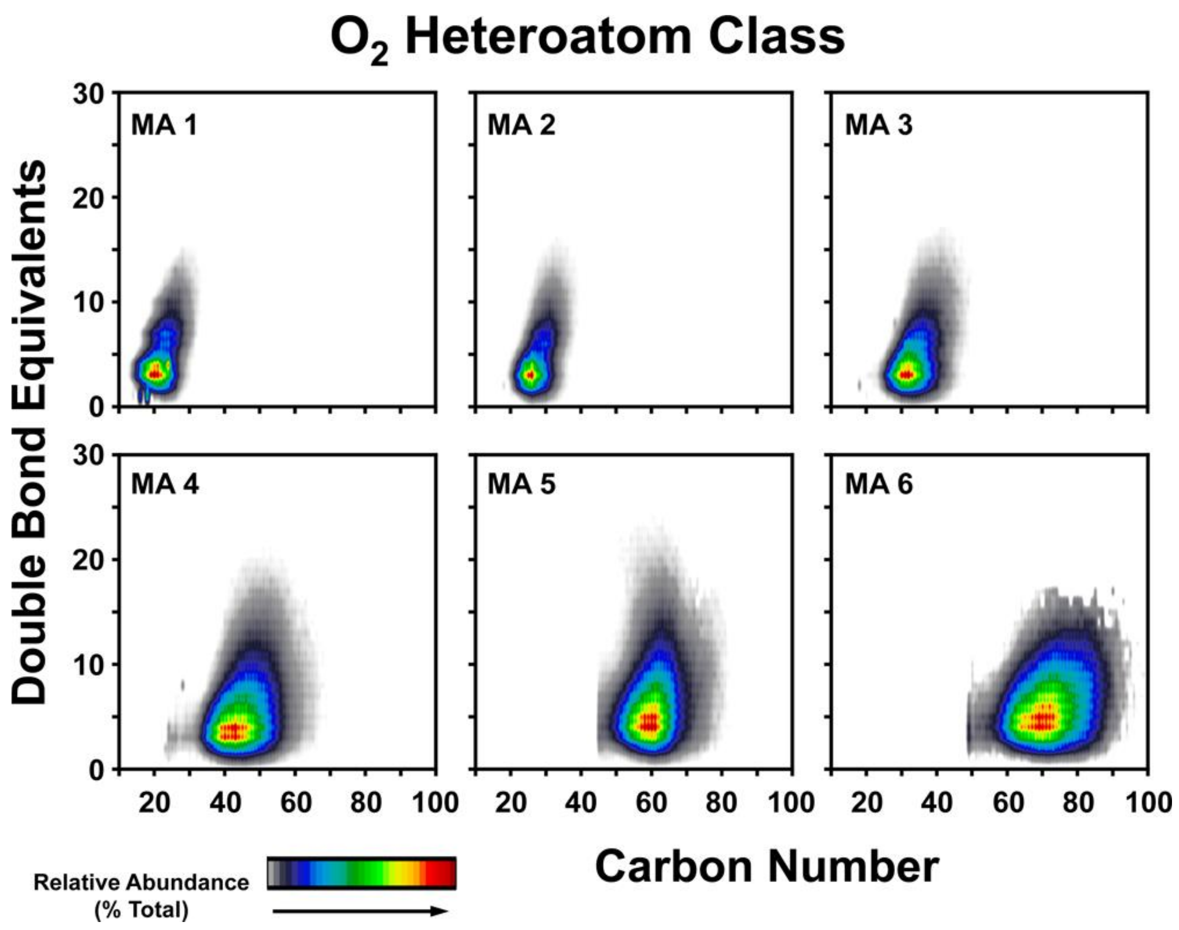

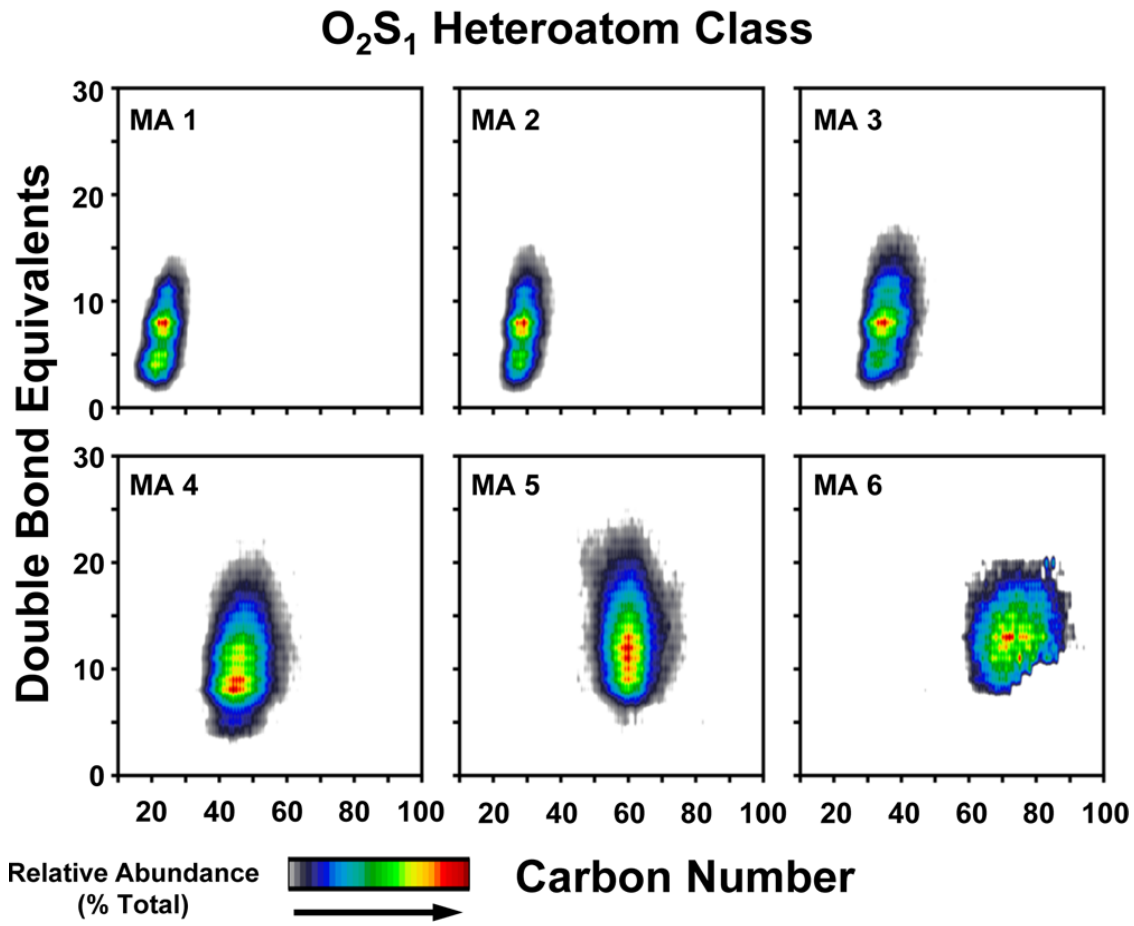

Fractionation of Interfacial Material

MAPS fractionation (MAPS: modified aminopropyl silica)

A. Klingenpeel et al., *Energy Fuels 2017, 31, 5933−5939.*

MAPS Extraction of Interfacial Material

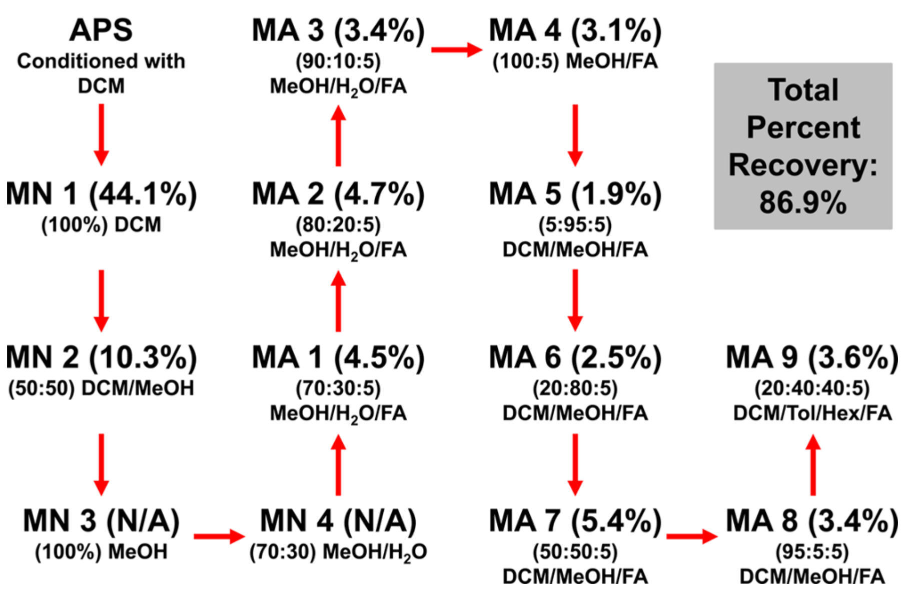

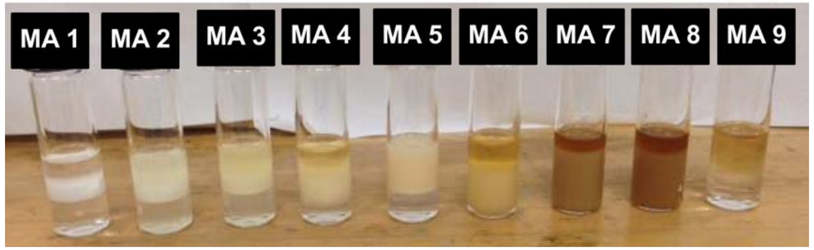

Emulsion test

Bitumen IM Singly-Charged Acids

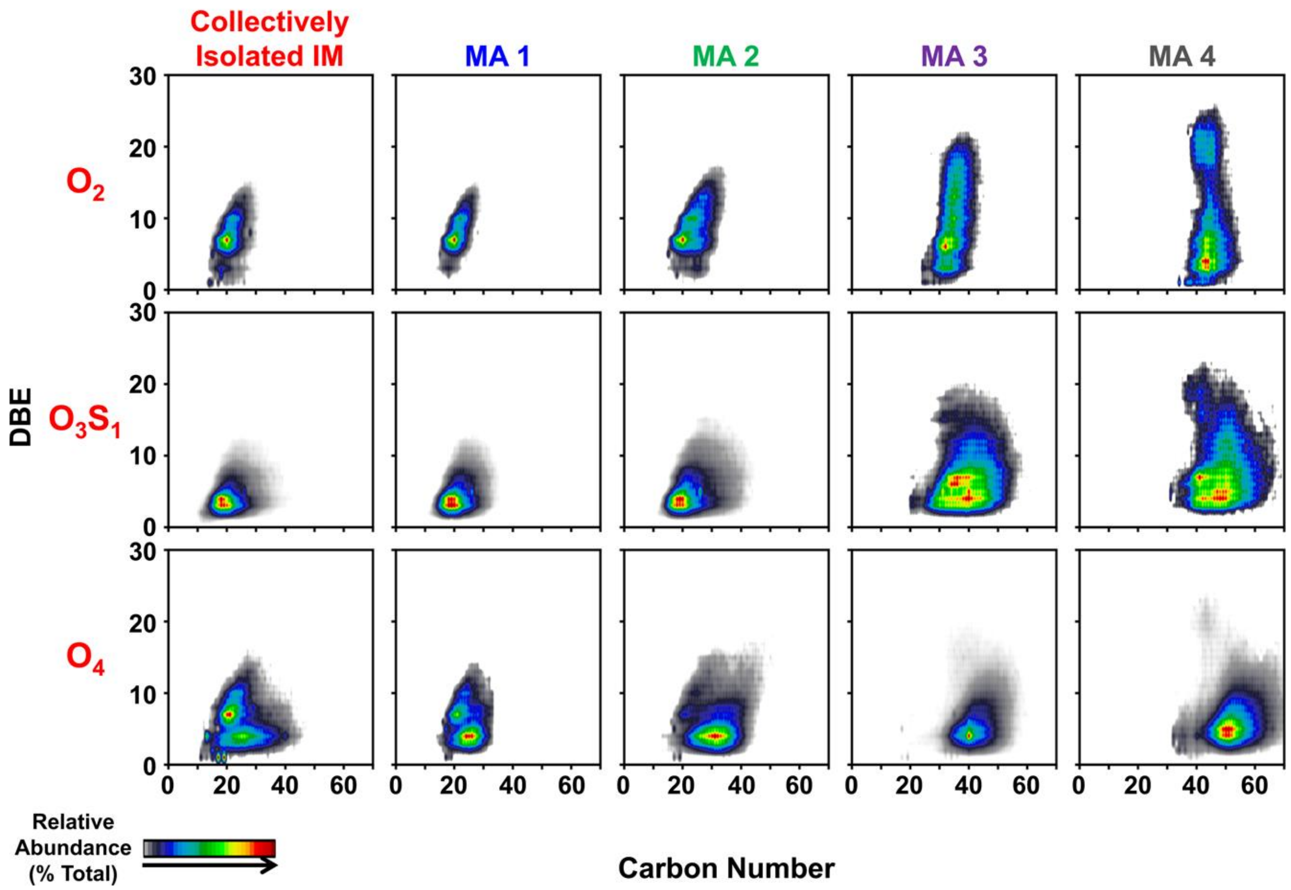

Island and archipelago structures of asphaltene molecules

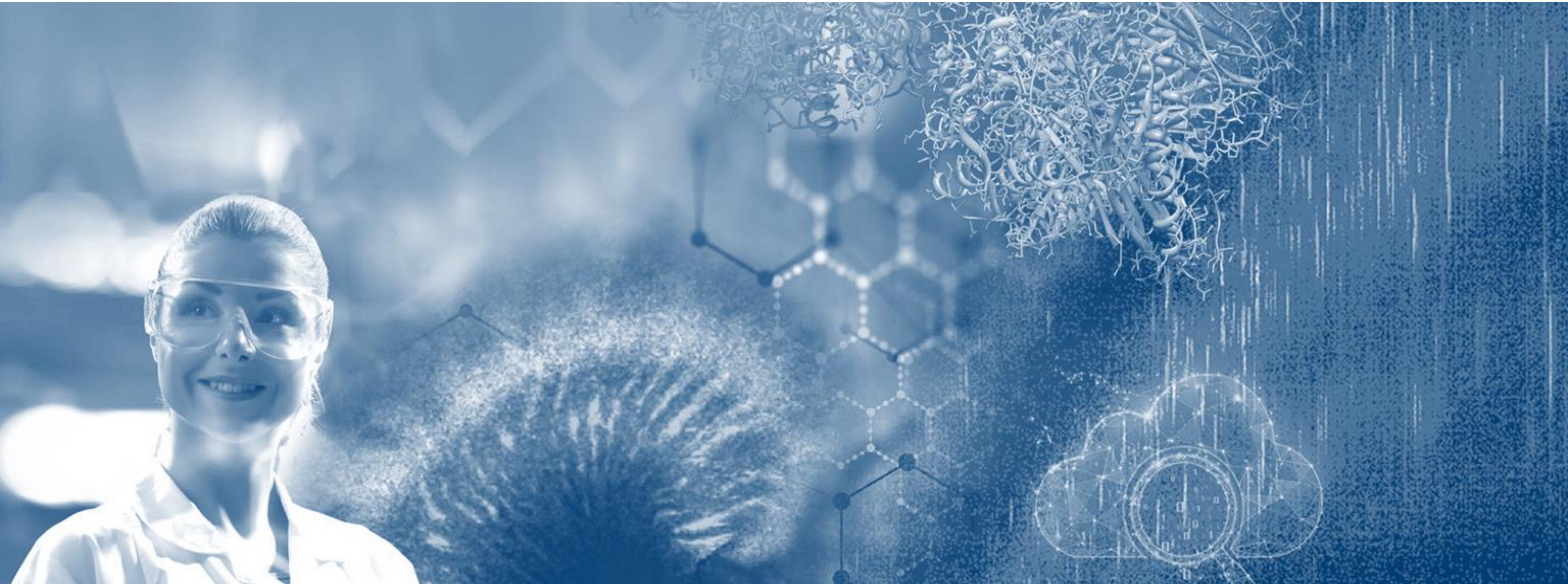

Structure of Asphaltene molecules

CID of an Asphaltene fractions (APPI pos)

M. Witt et al., Petrophase 2018.

Q-isolation with a small mass window of **10 Da**.

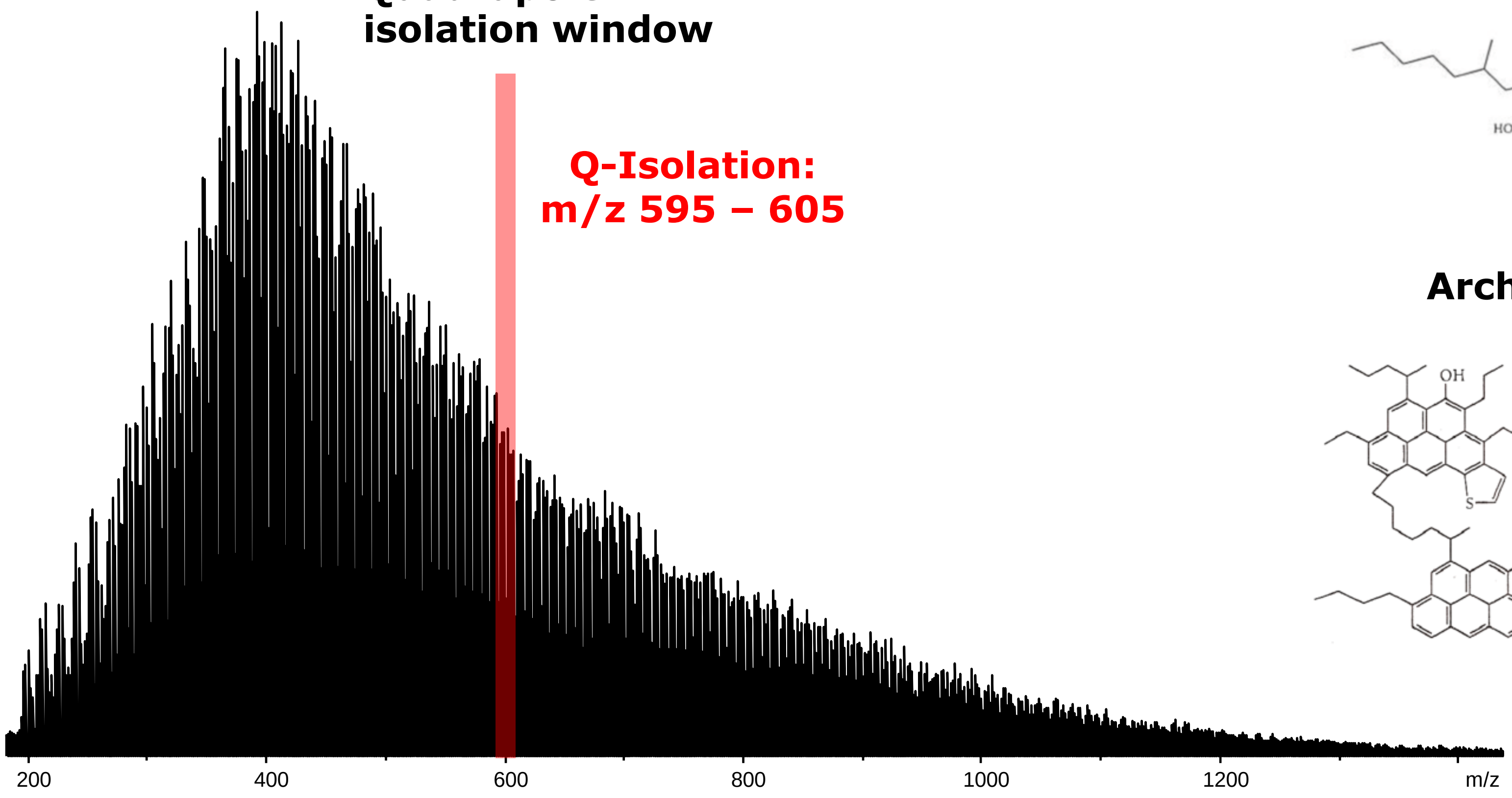

Island structurec

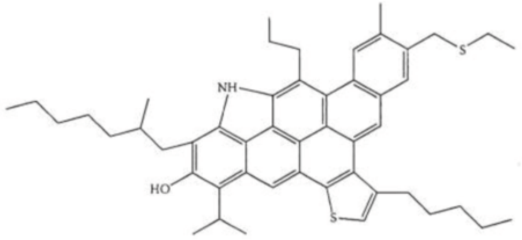

Archipelago structure

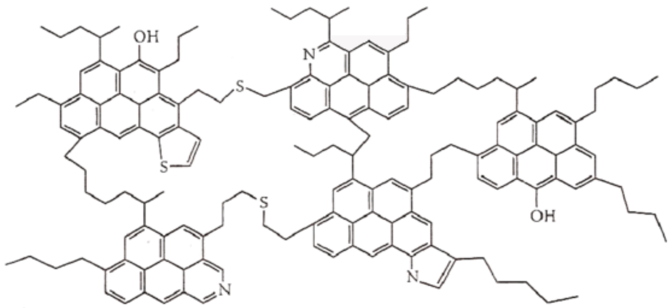

Structure of Asphaltene molecules

CID of an Asphaltene fractions (APPI pos)

M. Witt et al., Petrophase 2018.

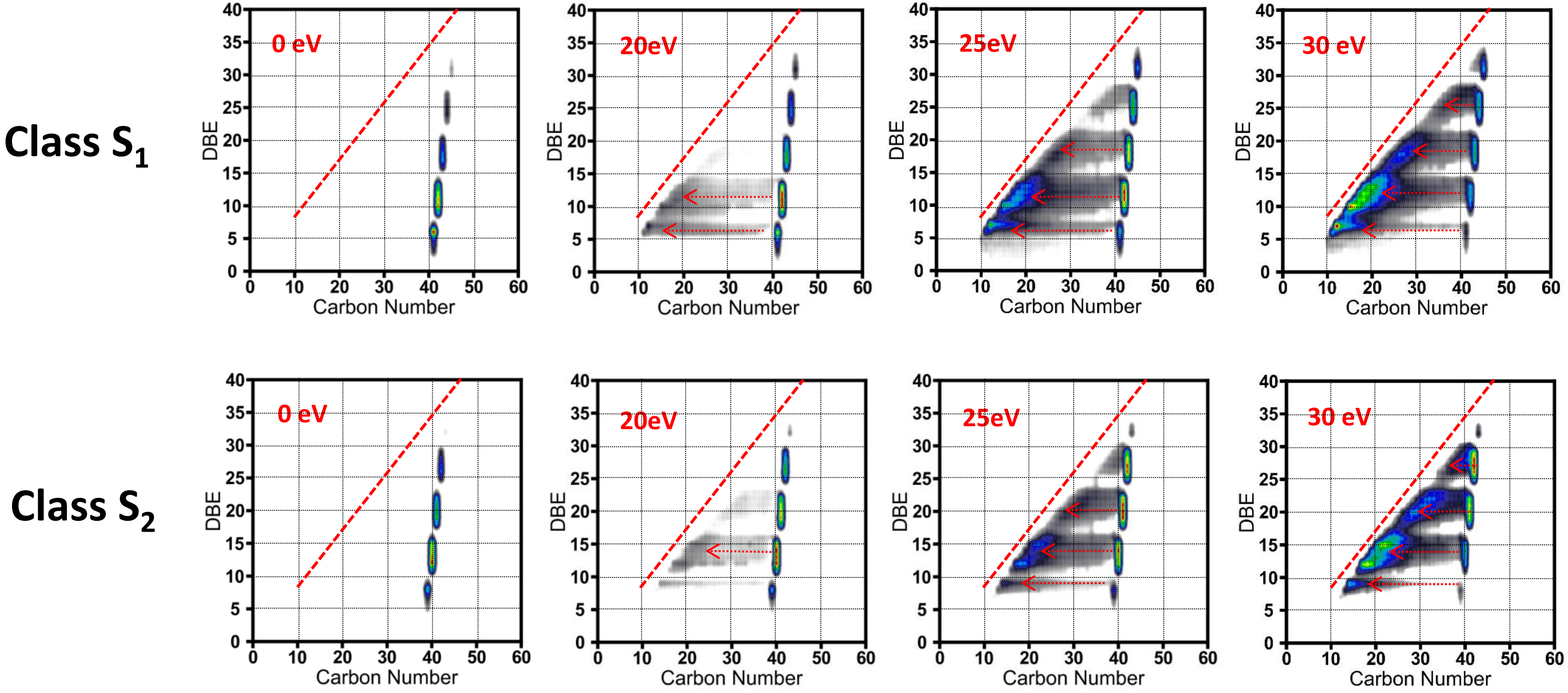

No loss is DBE ⇨ mainly island structures

Structure of Asphaltene molecules

Asphaltene fractions (APPI pos)

Martha L. Chacón-Patiño et al., *Energy & Fuels* 2018, 32, 314-328.

PetroPhase 2017 asphaltenes

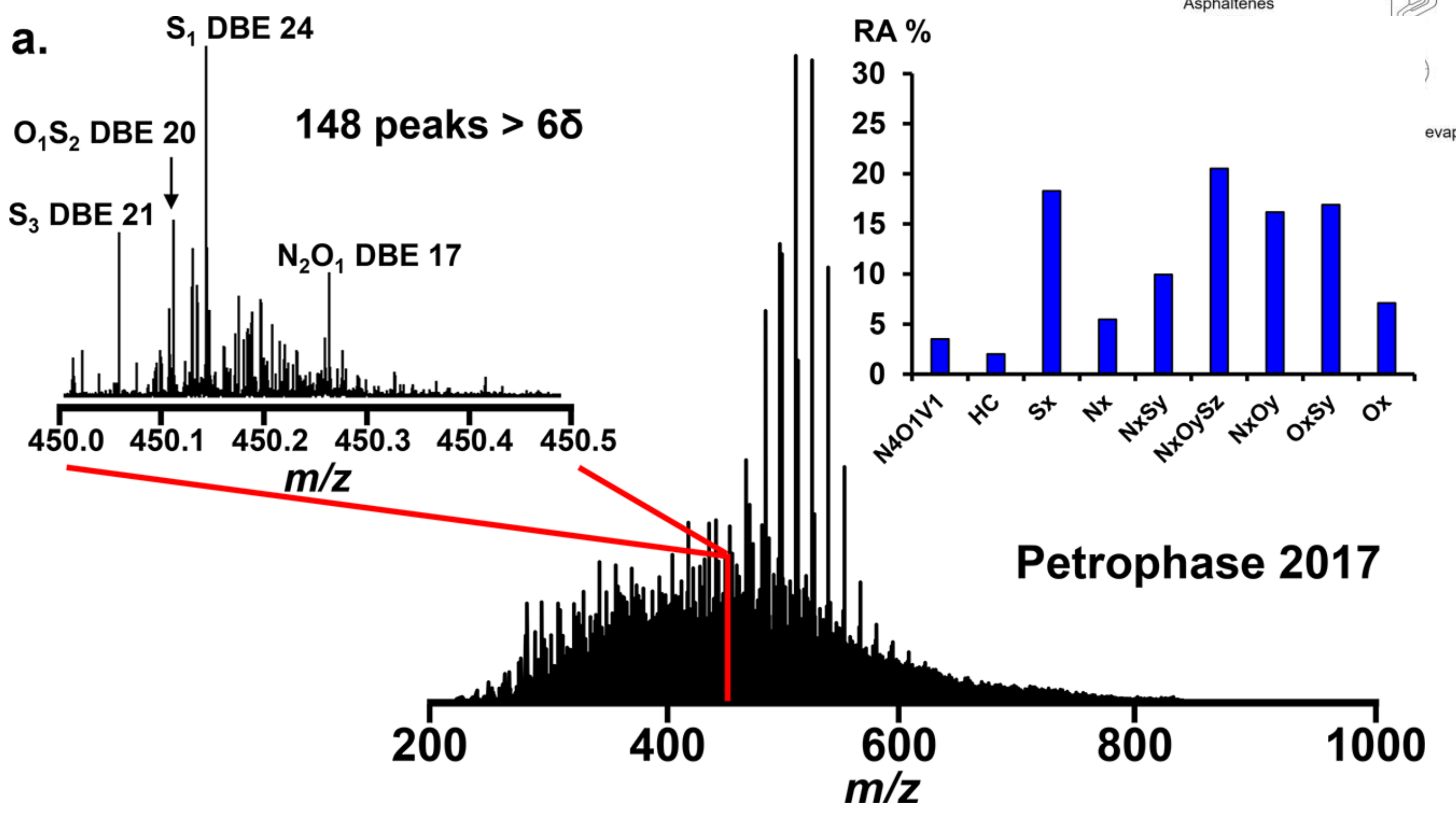

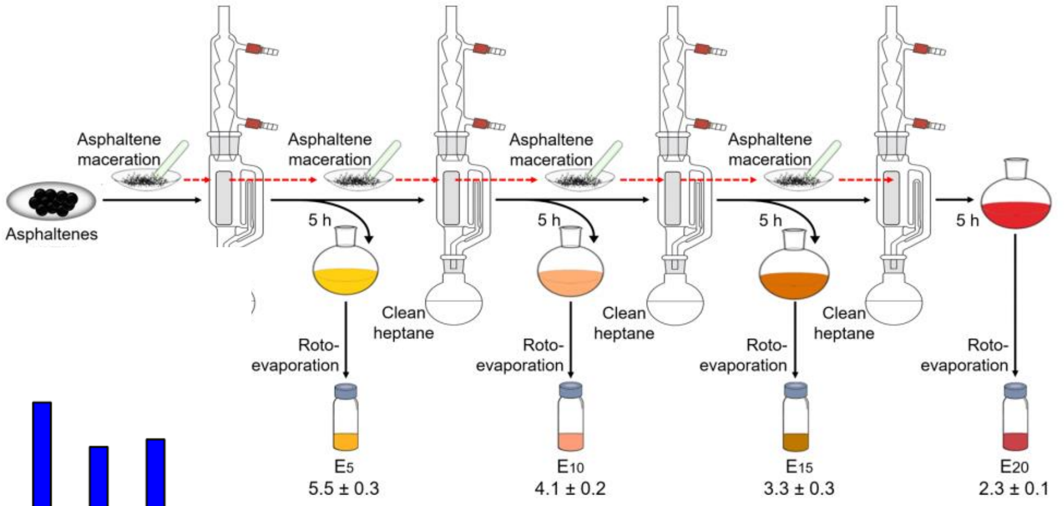

Structure of Asphaltene molecules

Asphaltene fractions (APPI pos)

Martha L. Chacón-Patiño et al., *Energy & Fuels* 2018, 32, 314-328.

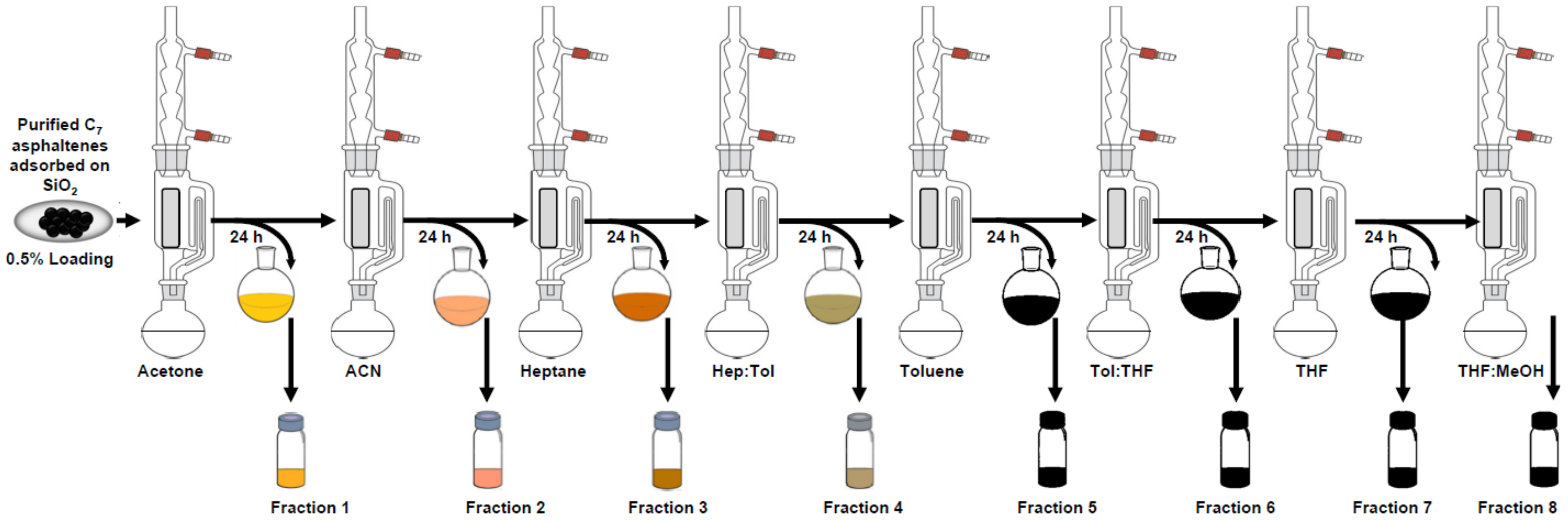

Petrophase 2017 wt.% Recovery 84.7%	17.4	0.2	6.9	11.3	8.7	19.7	7.5	13.0

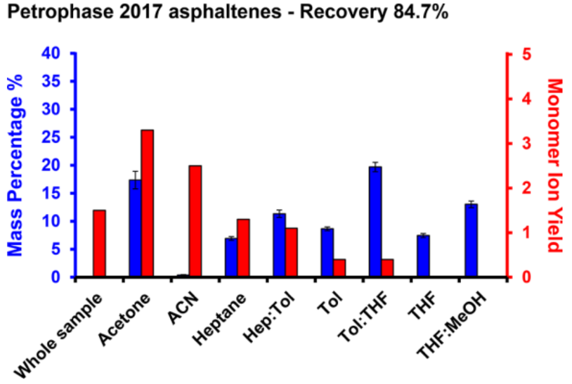

Structure of Asphaltene molecules

Asphaltene fractions (APPI pos)

Martha L. Chacón-Patiño et al., *Energy & Fuels* 2018, 32, 314-328.

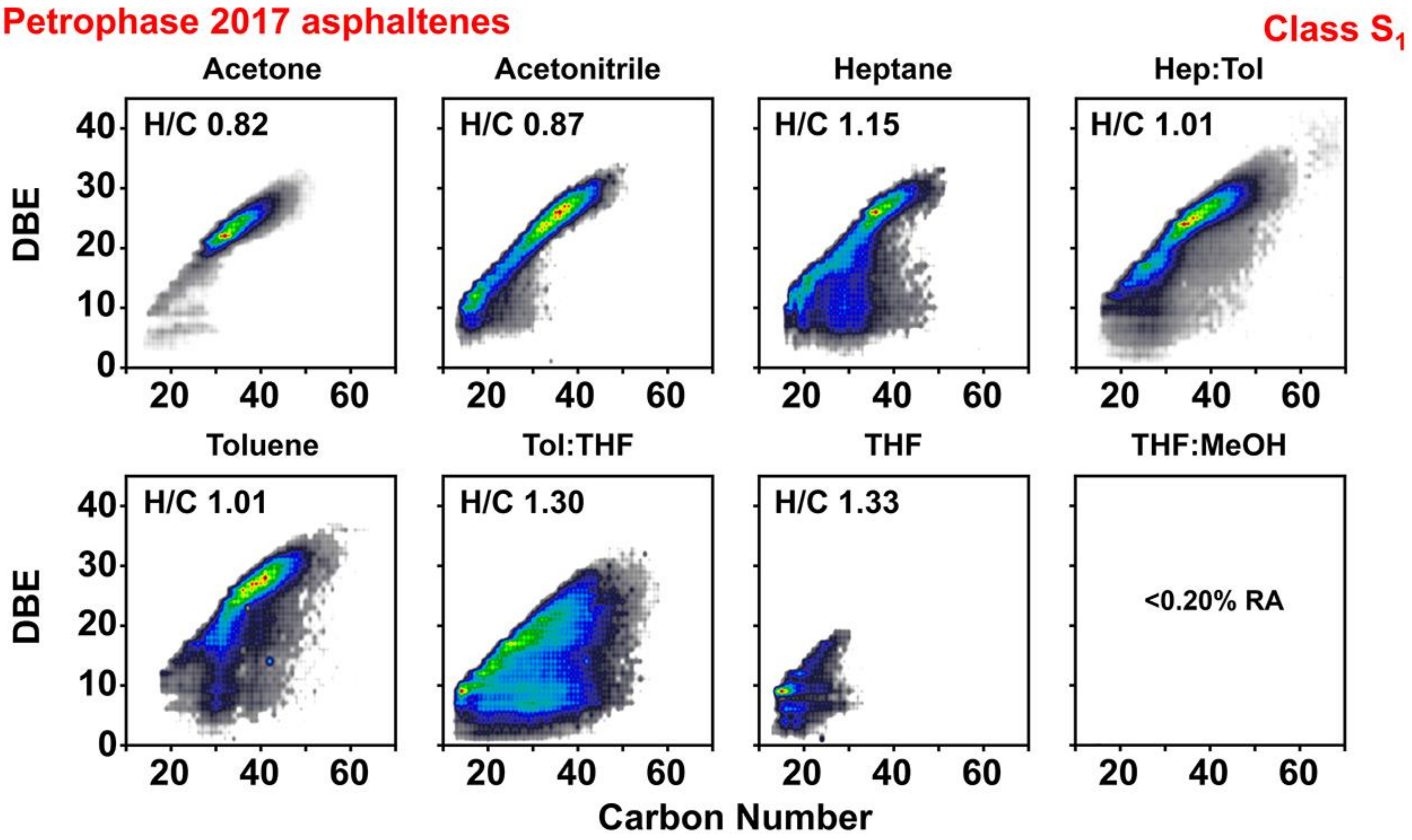

Structure of Asphaltene molecules

Asphaltene fractions (APPI pos)

Martha L. Chacón-Patiño et al., *Energy & Fuels* 2018, 32, 314-328.

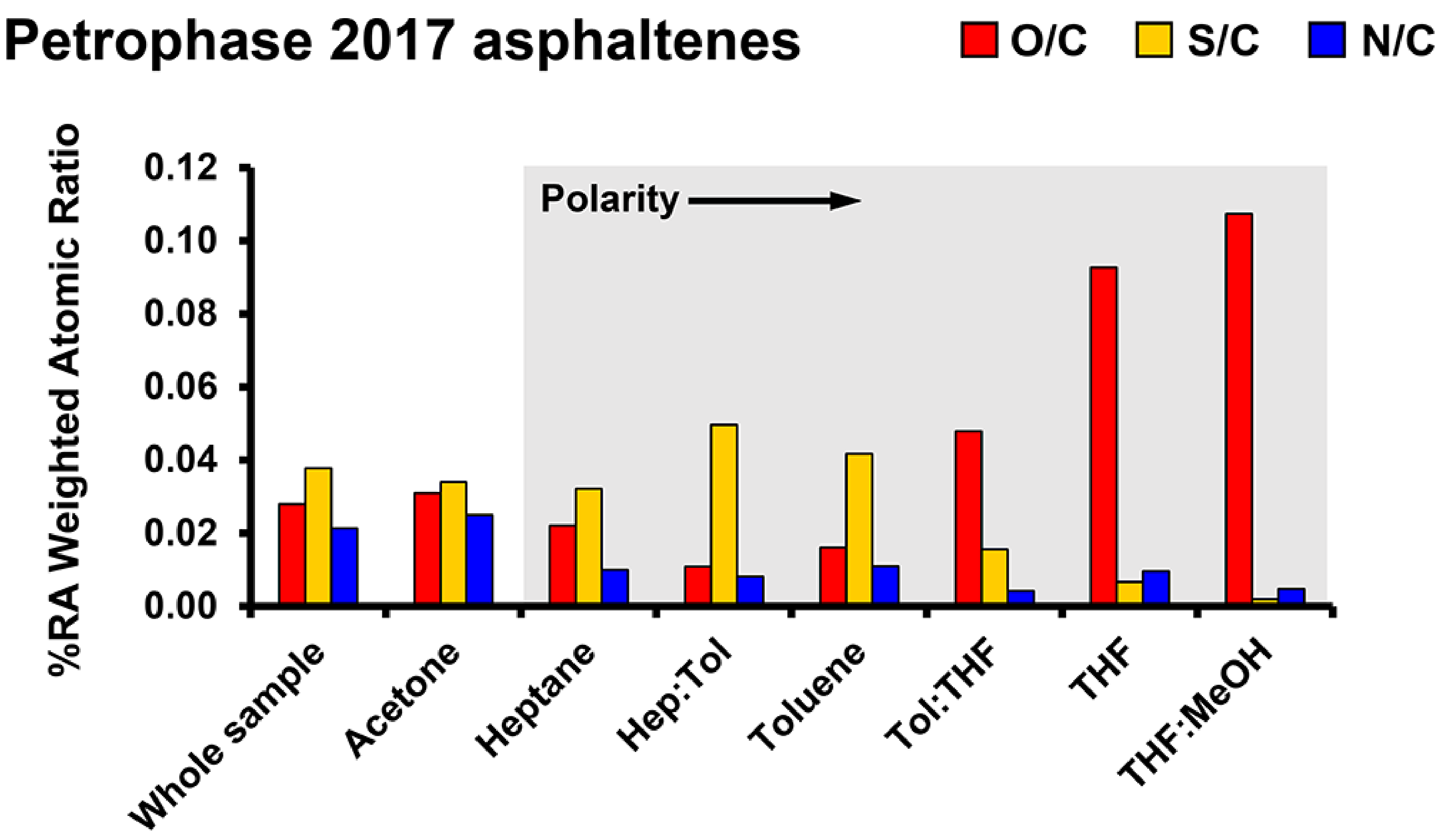

Structure of Asphaltene molecules

Asphaltene fractions (APPI pos)

Martha L. Chacón-Patiño et al., *Energy & Fuels* 2018, 32, 314-328.

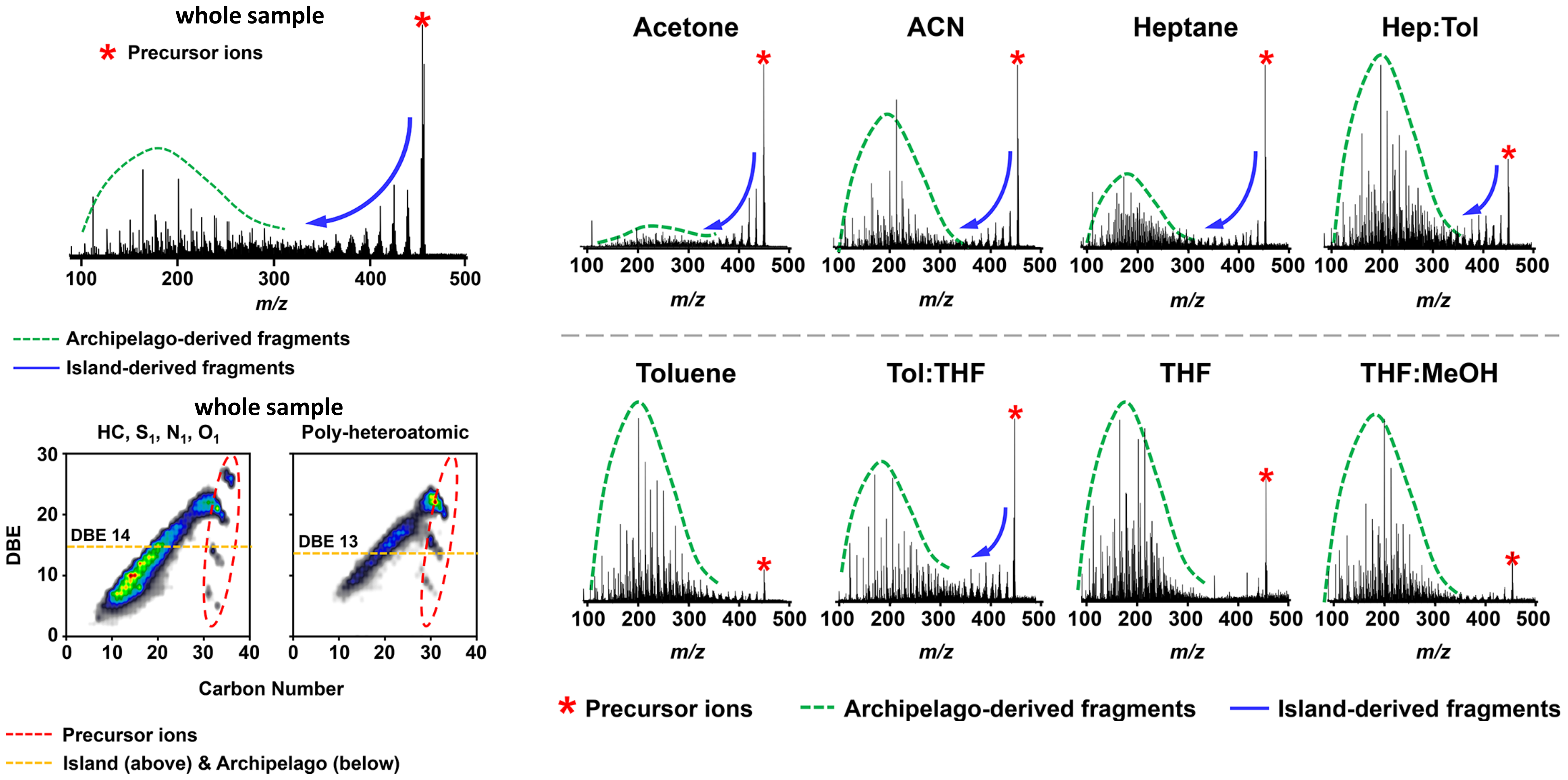

Structure of Asphaltene molecules

Asphaltene fractions (APPI pos)

Martha L. Chacón-Patiño et al., *Energy & Fuels* 2018, 32, 314-328.

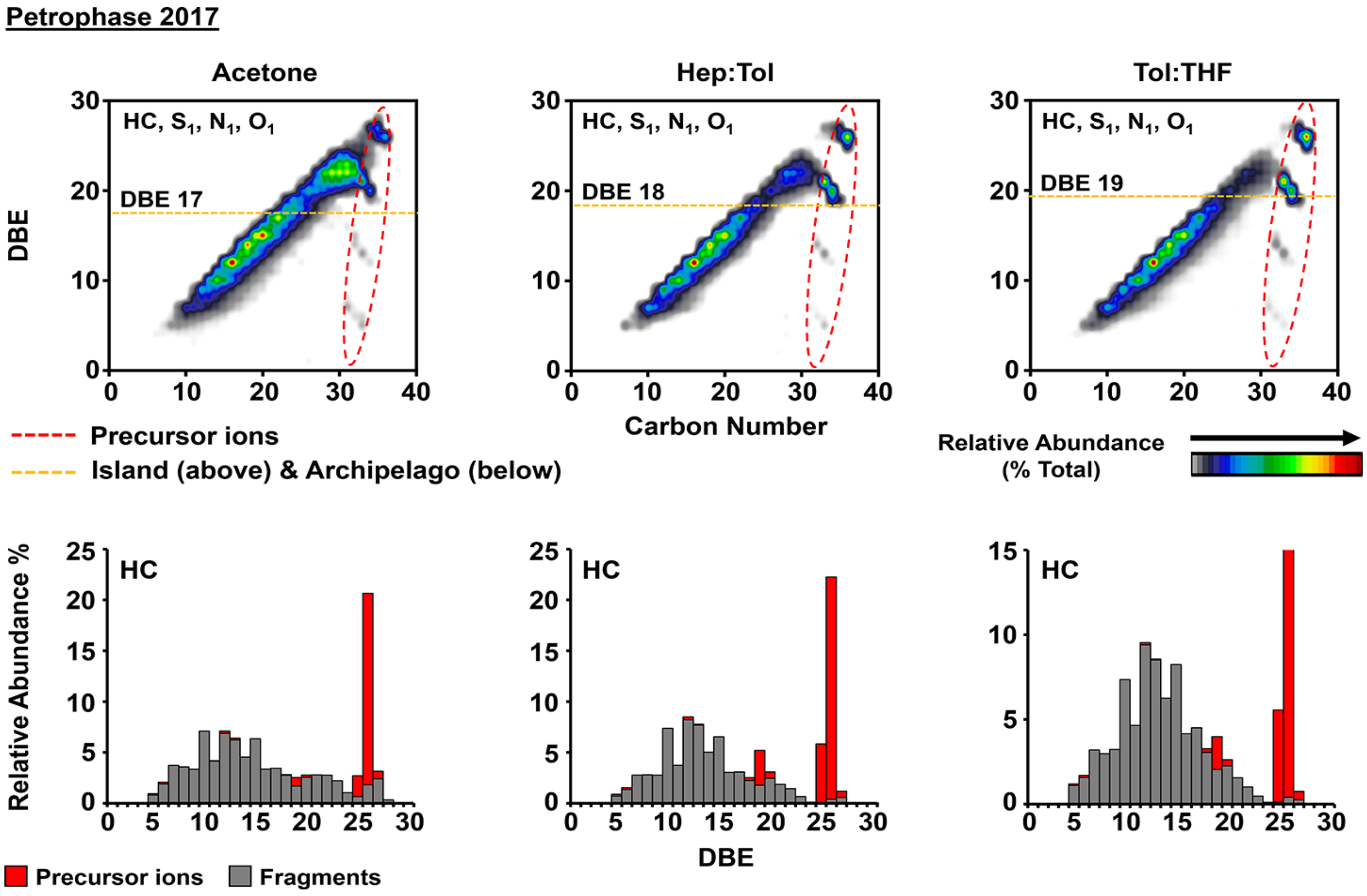

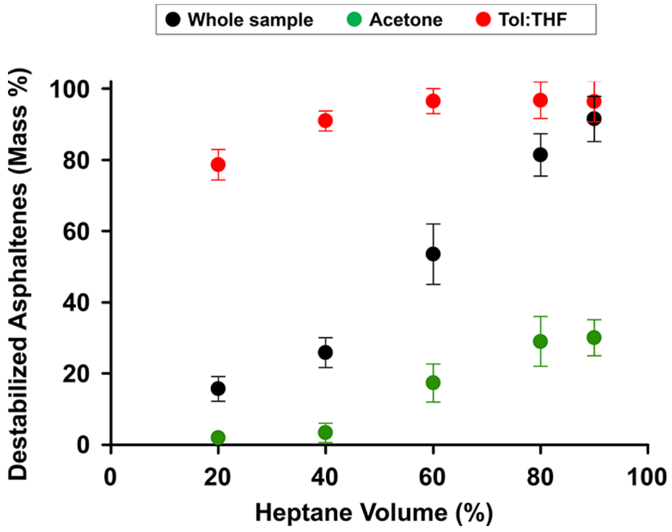

Structure of Asphaltene molecules

AFM – Atomic Force Microscopy

B. Schuler et al., *Energy Fuels* **2017**, *31*, 6856–6861

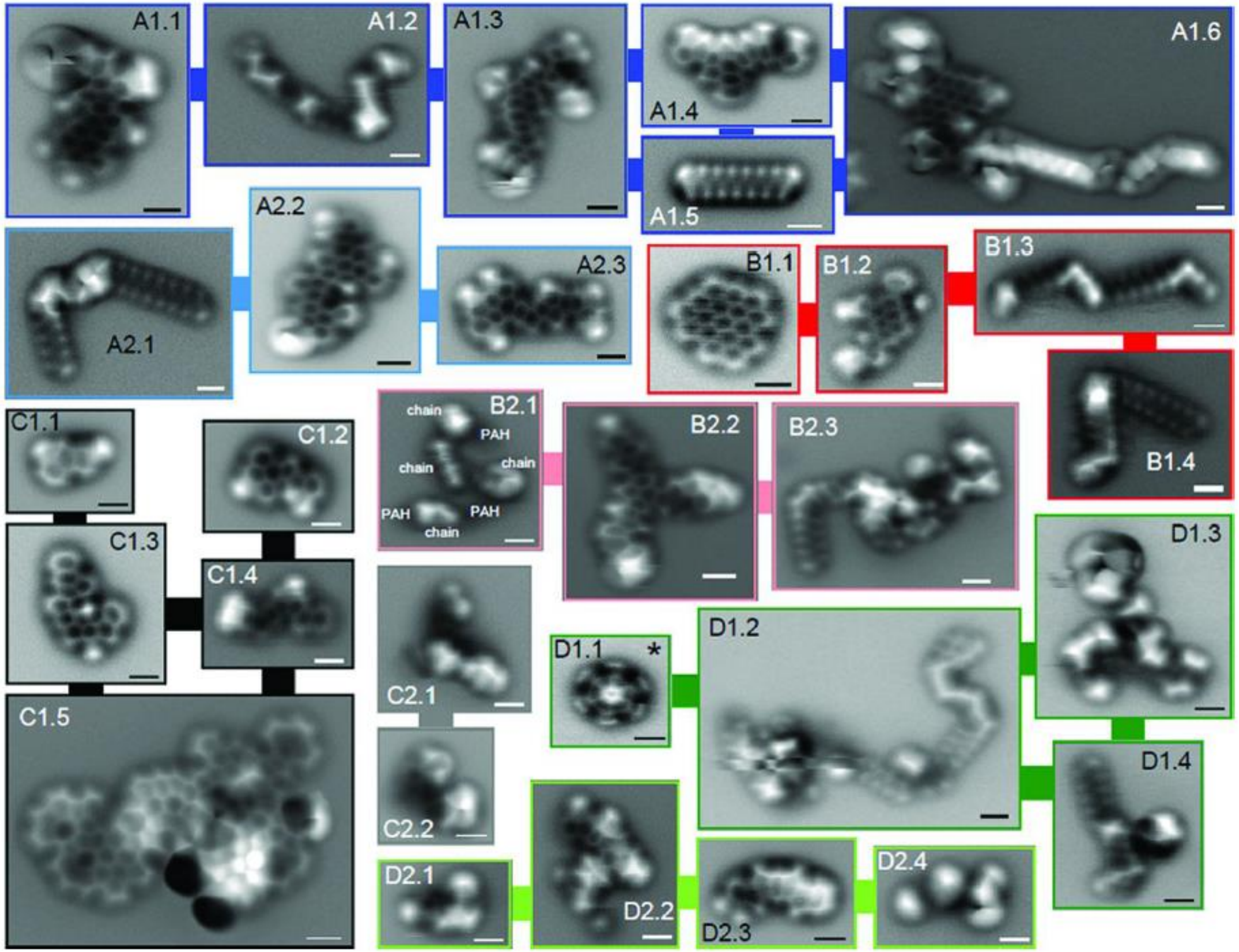

Bio-oil analysis

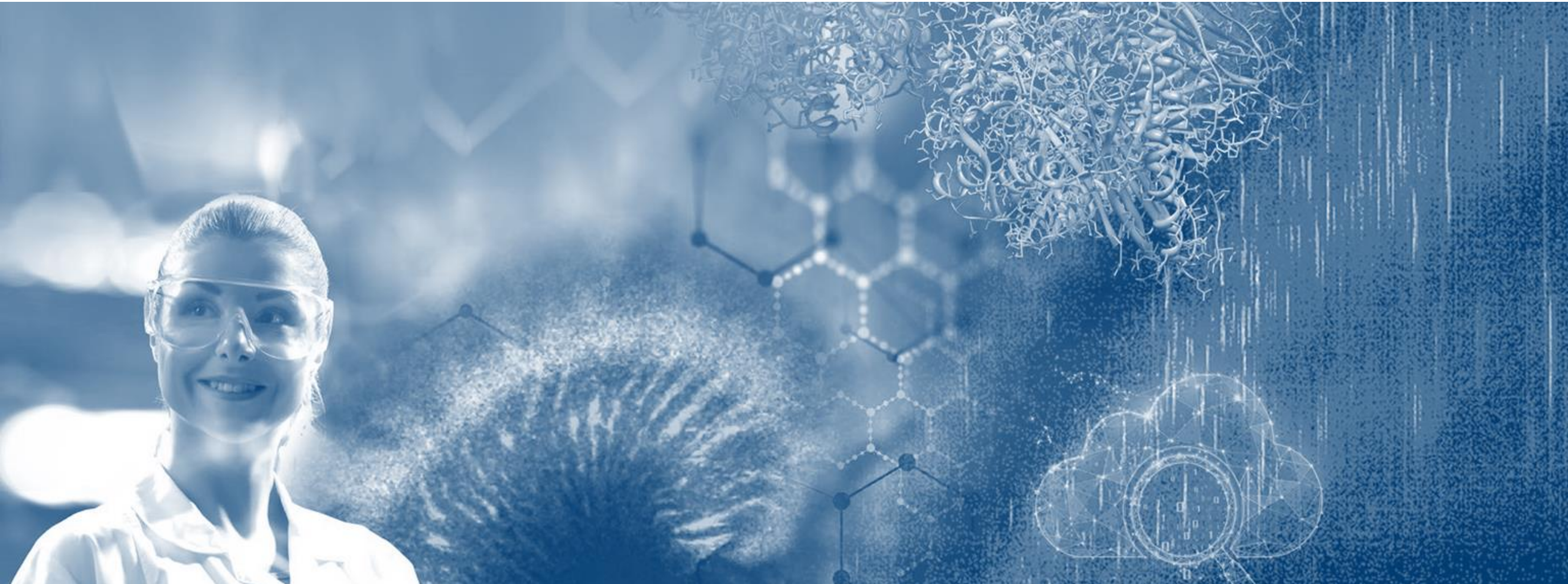

Bio-oil analysis

Pine pellet oily (red) and aqueous (blue) phase analysis

J. M. Jarvis et al., Energy Fuels 2012, 26, 3810−3815.

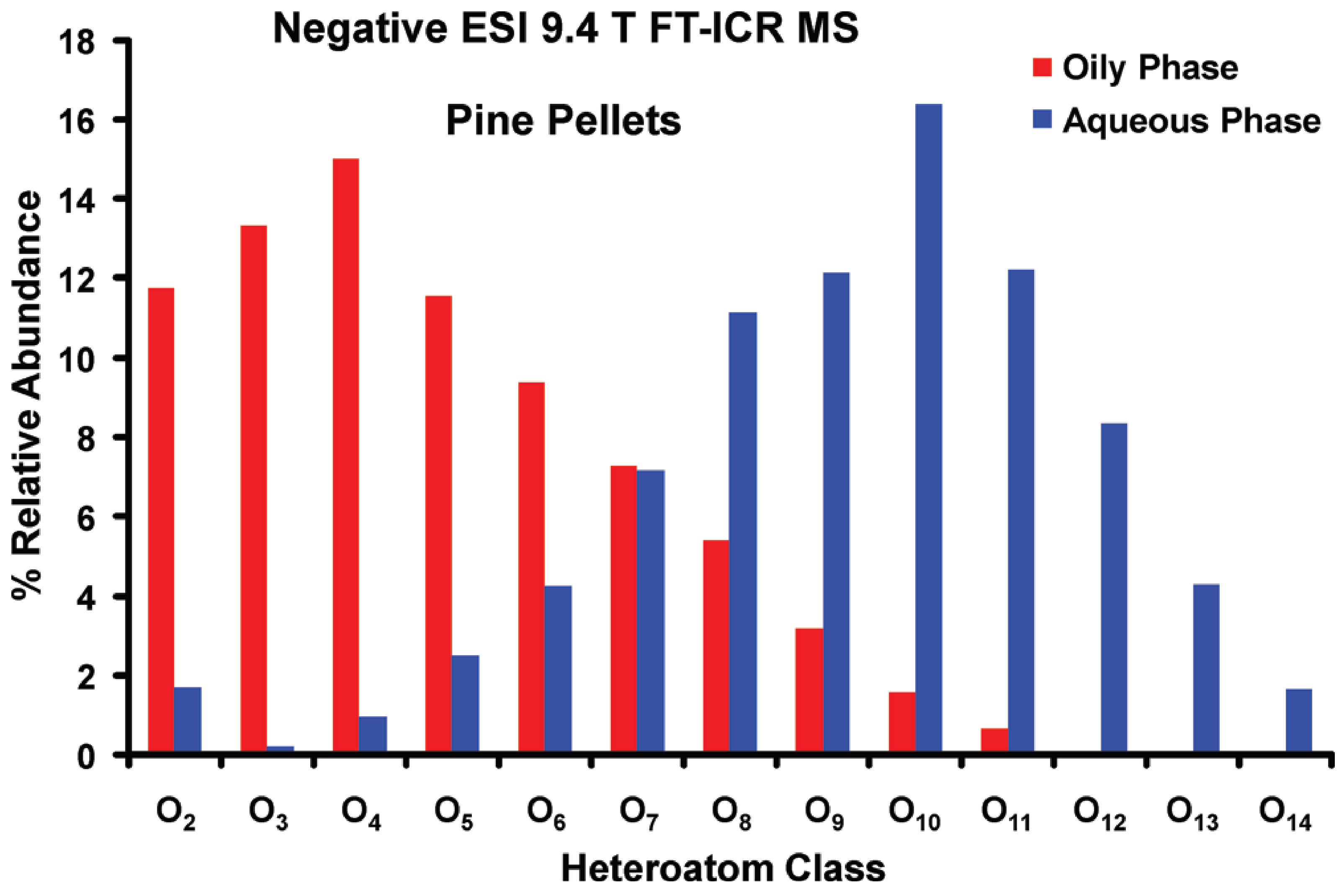

Bio-oil analysis

Pine pellet oily (red) and aqueous (blue) phase analysis

J. M. Jarvis et al., Energy Fuels 2012, 26, 3810−3815.

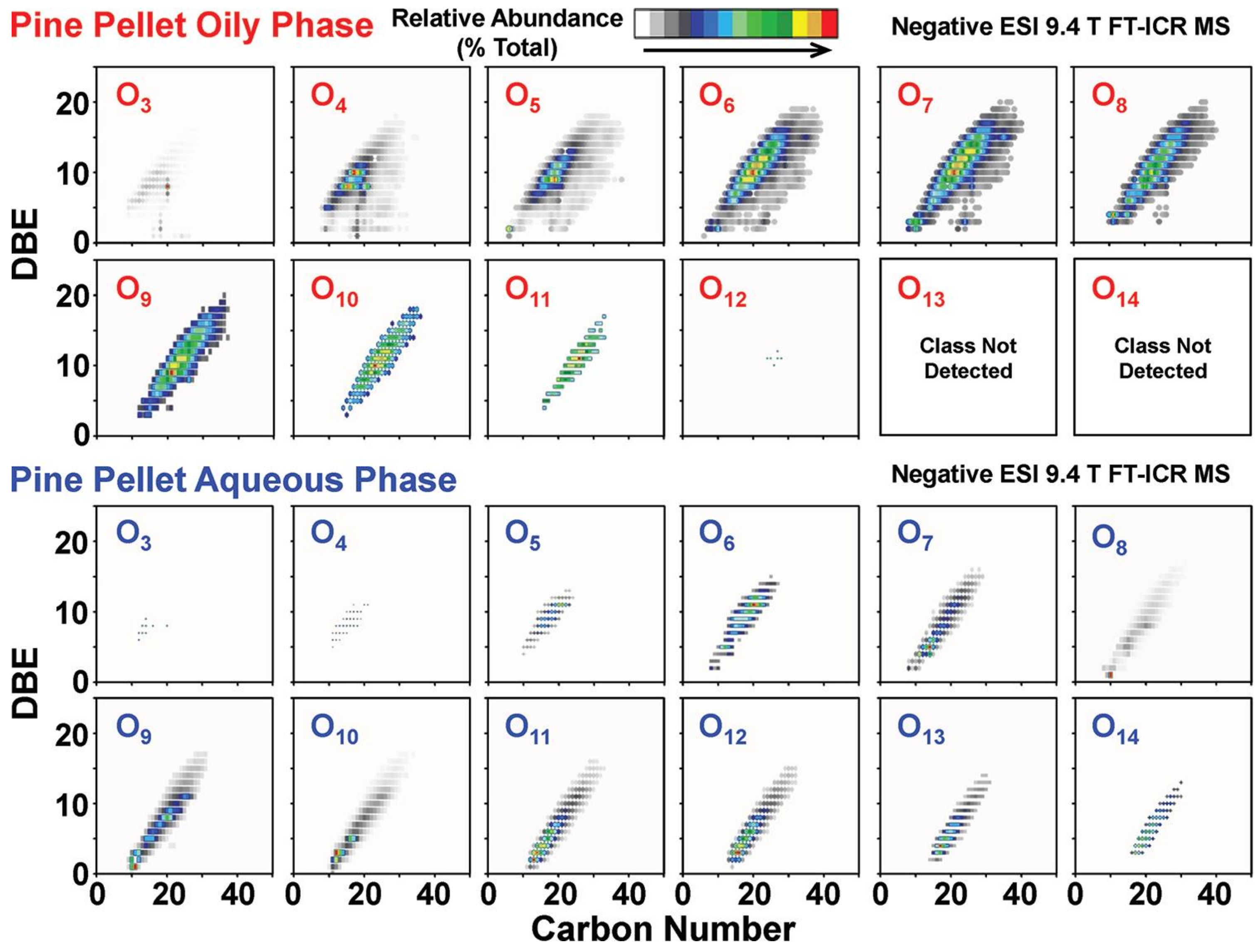

Effect of Maturity

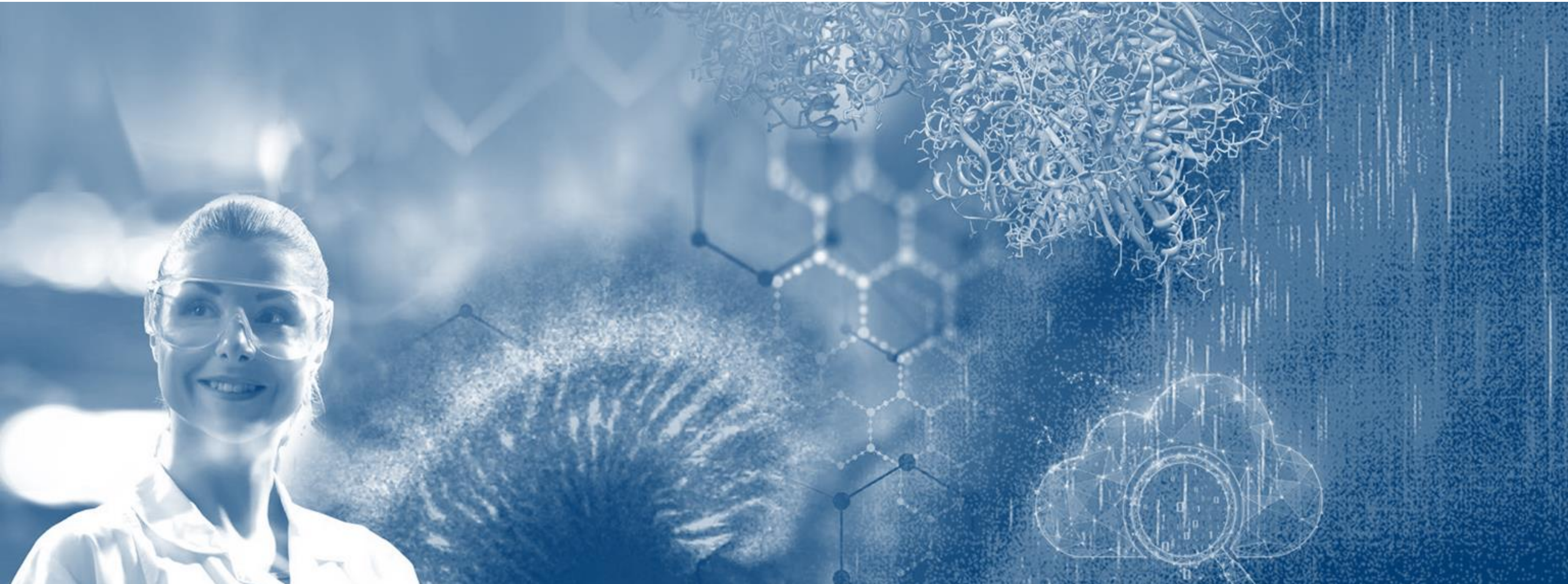

Effect of Maturity

Effect of Maturity on oil composition

S. Poetz et al, *Energy Fuels* 2014, 28, 4877–4888.

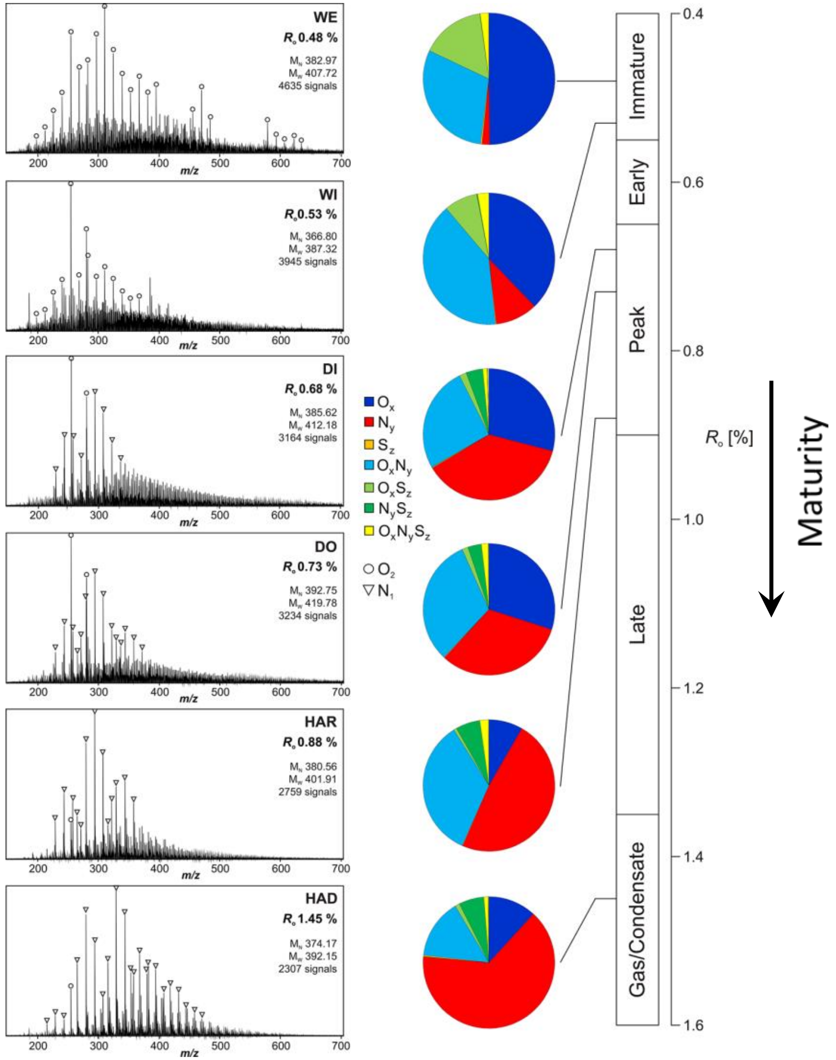

R_0: vitrinite reflectance

Transformation of Compounds in the Organic-Rich Posidonia Shale by Maturity

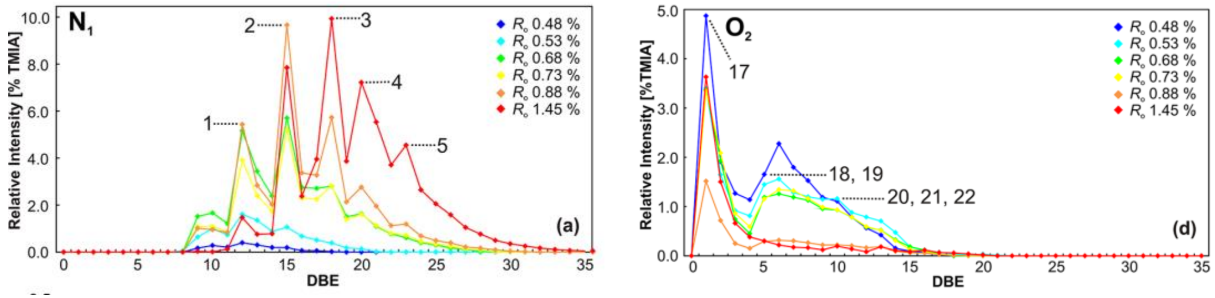

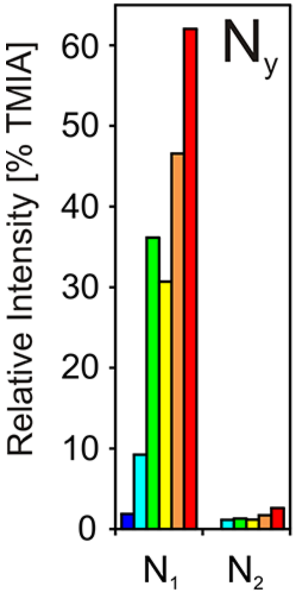

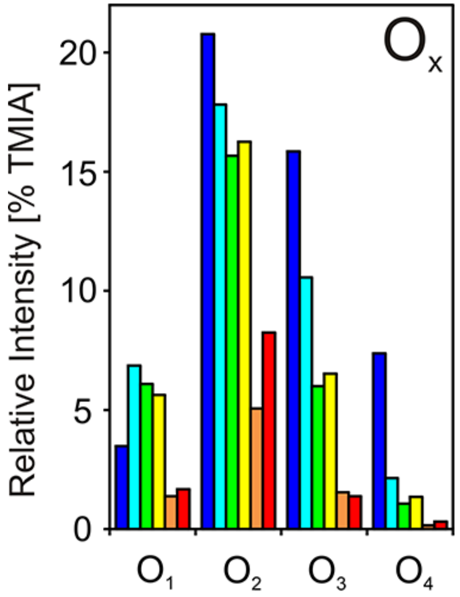

solariX 12T data, ESI(-)

Effect of Maturity

Effect of Maturity on oil composition

S. Poetz et al, *Energy Fuels* 2014, 28, 4877–4888.

Effect of Maturity of composition of N_1-containing compounds

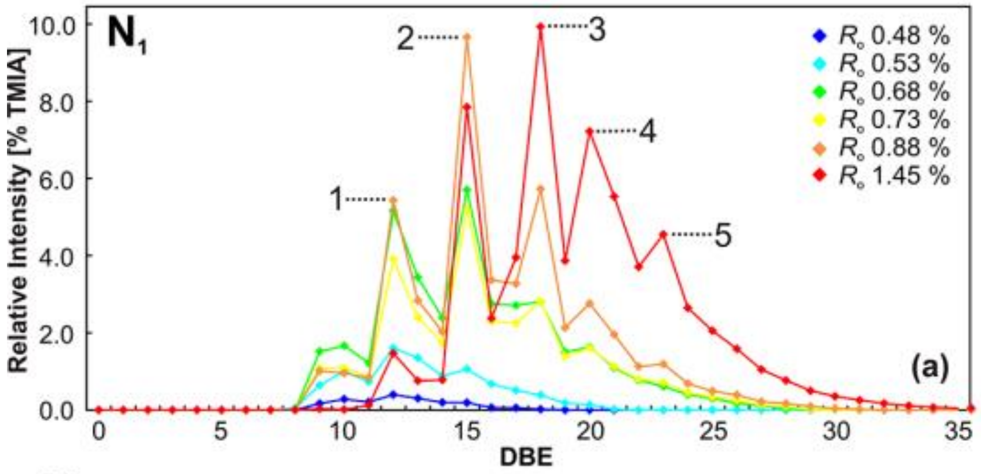

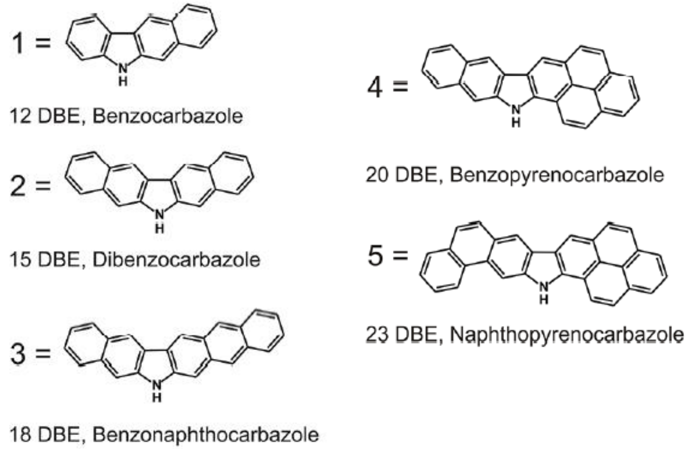

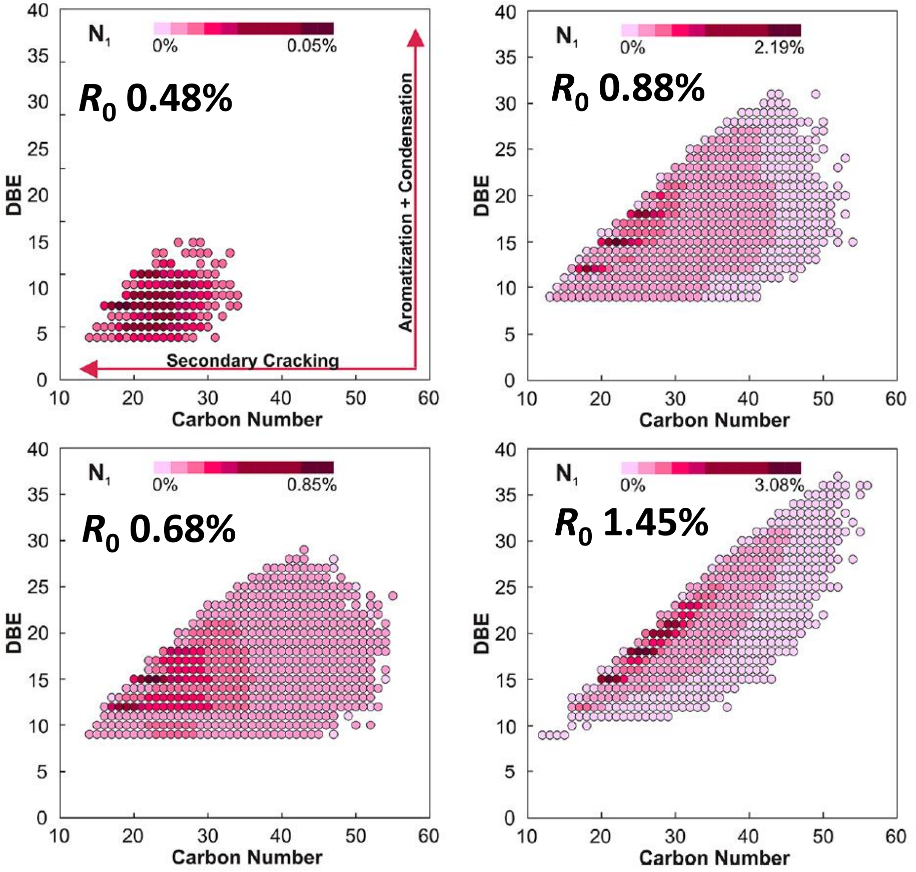

solariX 12T data, ESI(-)

Effect of Maturity

Effect of Maturity on oil composition

S. Poetz et al, *Energy Fuels* 2014, 28, 4877–4888.

Maturity-Driven Generation and Transformation of Compounds in the Organic-Rich Posidonia Shale

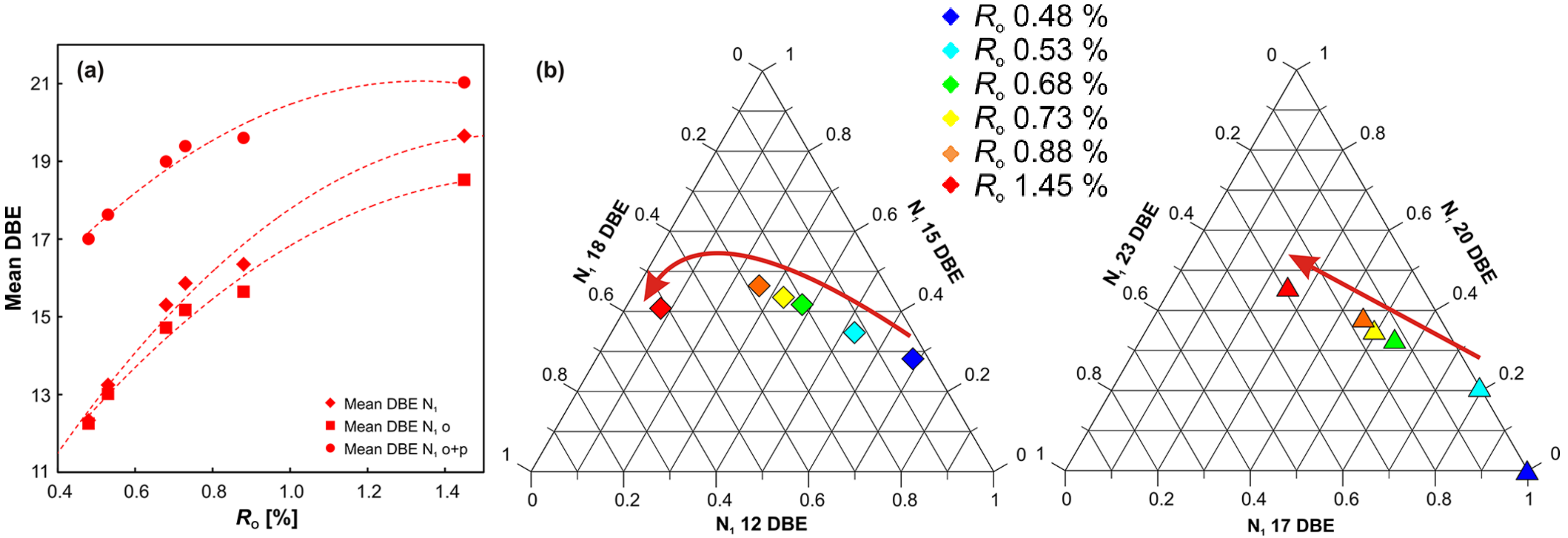

Possible Thermally-induced Reaction occurring during Maturation

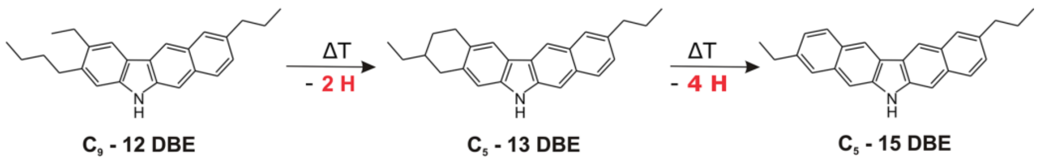

solariX 12T data, ESI(-)

Improving S/N and mass resolution

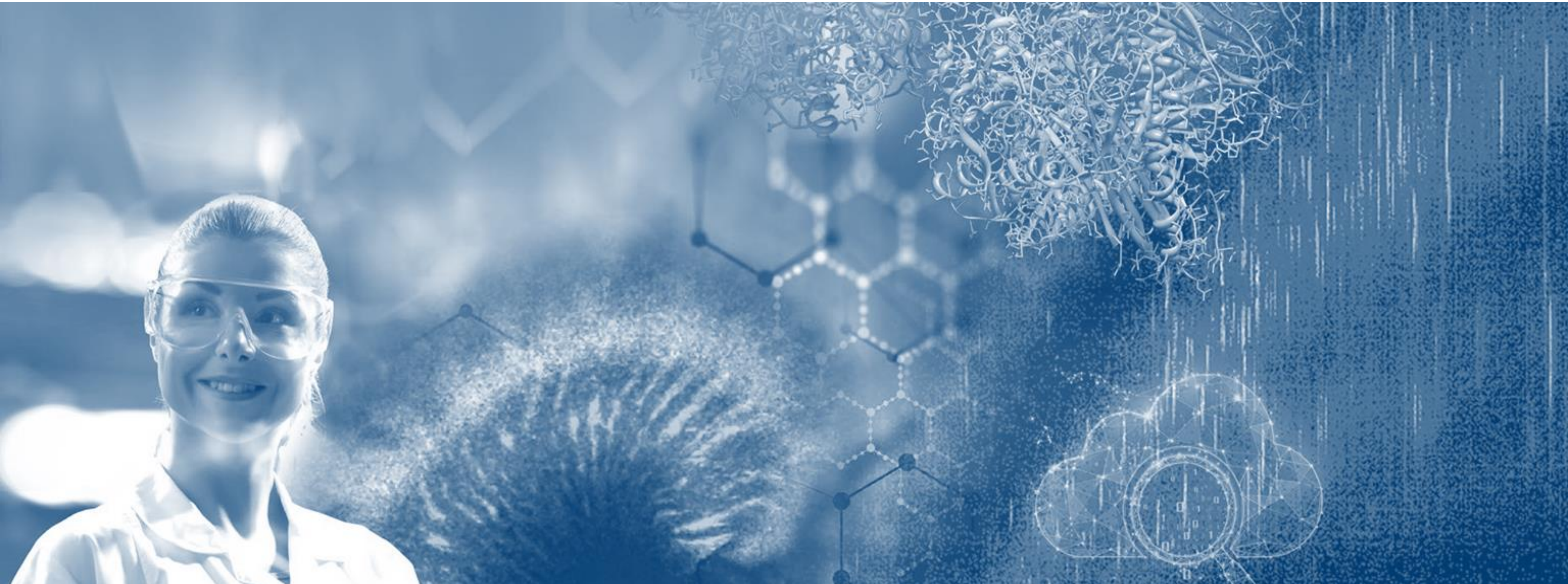

Improving S/N and mass resolution

Spectra stitching

L. C. Krajewski, Anal. Chem. 2017, 89, 21, 11318–11324.

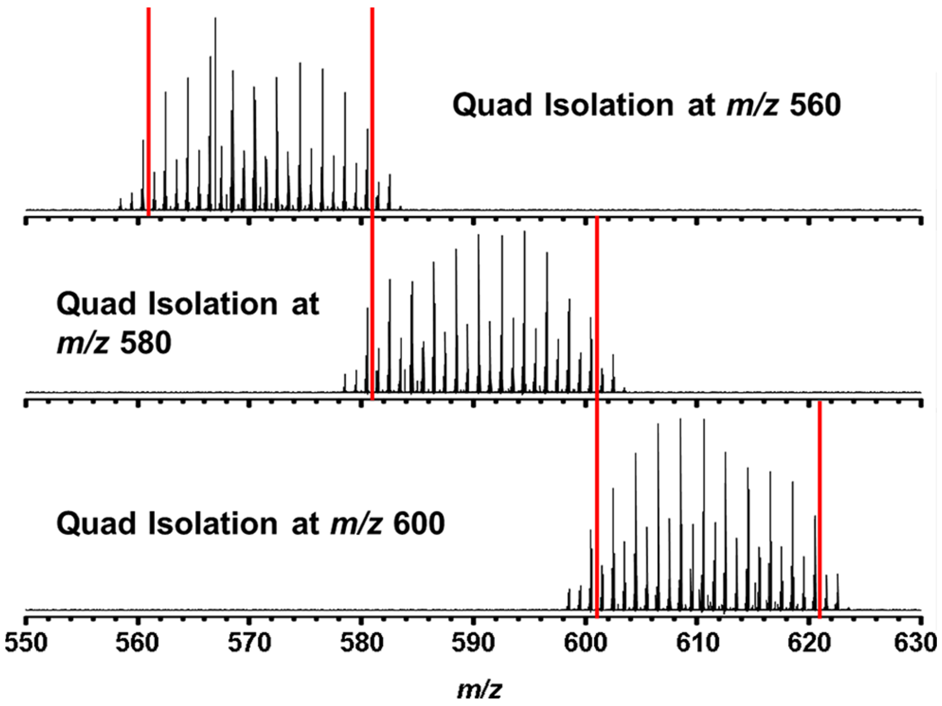

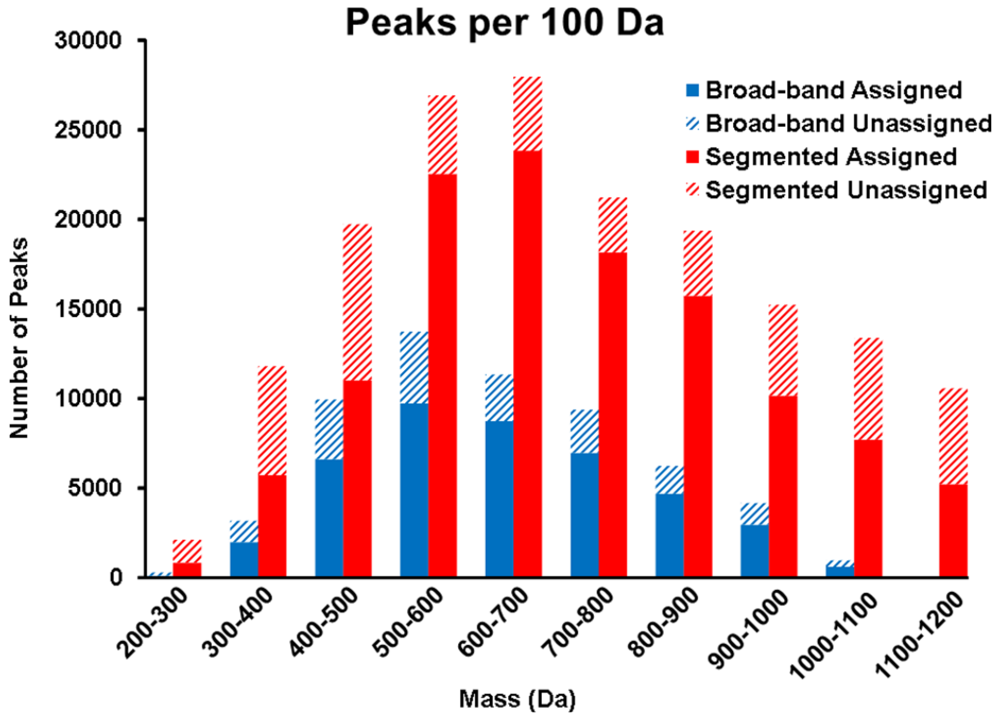

	broad band	segmented
no. of peaks	59 015	170 115
no. of assigned peaks/percentage of total	42 182 (71.5%)	126 264 (74.2%)
no. of monoisotopic peaks	23 946	67 237
rms mass error for assigned peaks (ppm)	0.19	0.13
number-average neutral mass (Da)	647.5	750.2
number-average carbon number	44.7	49.7
number-average neutral DBE	15.9	15.3
approximate total analysis time (s)	2000	37 500

Improving S/N and mass resolution

Spectra stitching and keeping mass resolution

D. C. Palacio Lozano, Chem. Sci., 2019, 10, 6966.

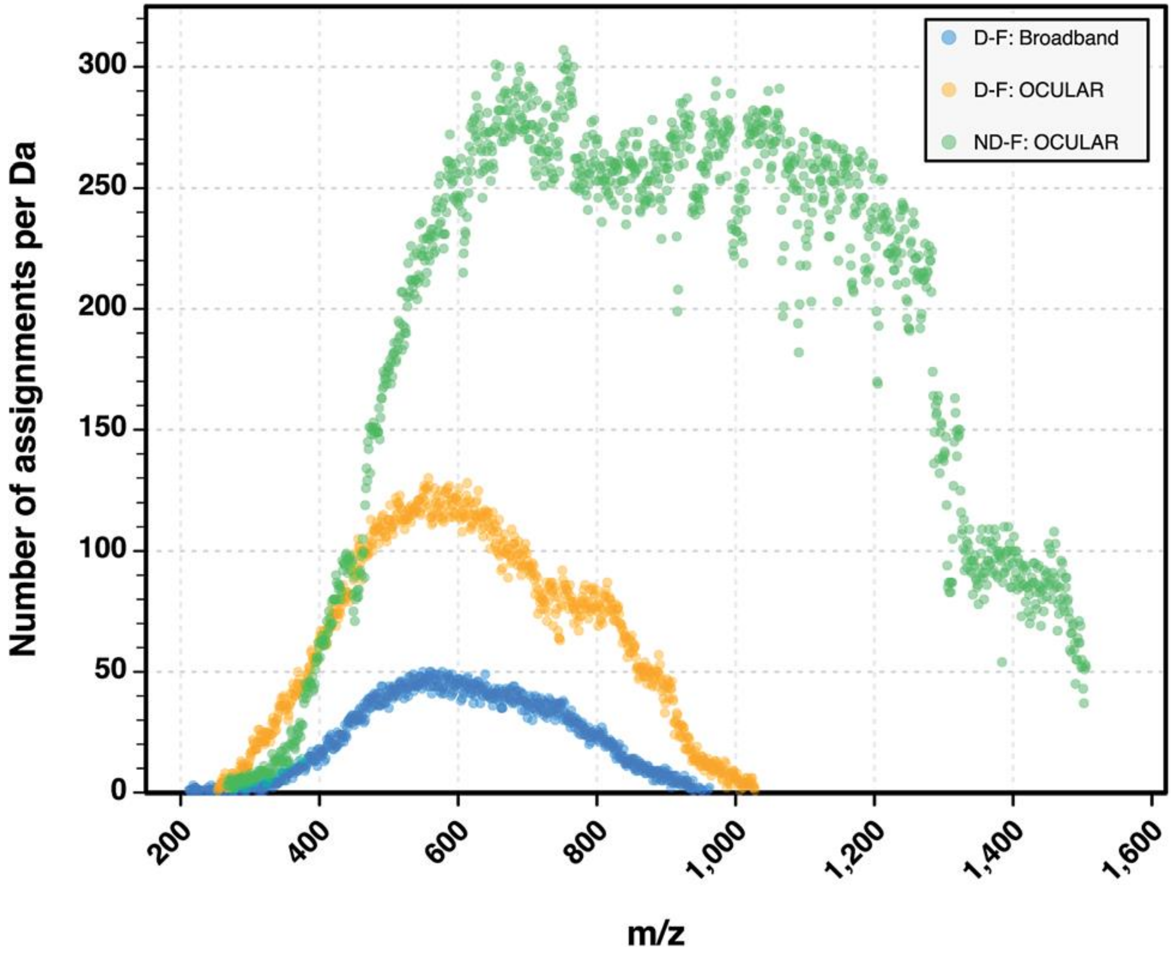

	Stitched
Average resolving power (*m/z* 260–1505)	3.12×10^6
Resolving power at *m/z* 400	3.07×10^6
Monoisotopic peaks assigned	106 871
Total peaks assigned	244 779
% Assigned	88.44%
RMS mass error for assigned peaks	0.11 ppm
Mean molecular weight	890.3 Da
Peaks with mass error ≤1 ppb	2305
Peaks with mass error ≤20 ppb	66 814
Peaks with mass error ≤50 ppb	122 911
Max. number of peaks assigned per Da	307

Improving S/N and mass resolution

Concept of dipolar and quadrupolar detection

Standard 1ω Dipole Detection

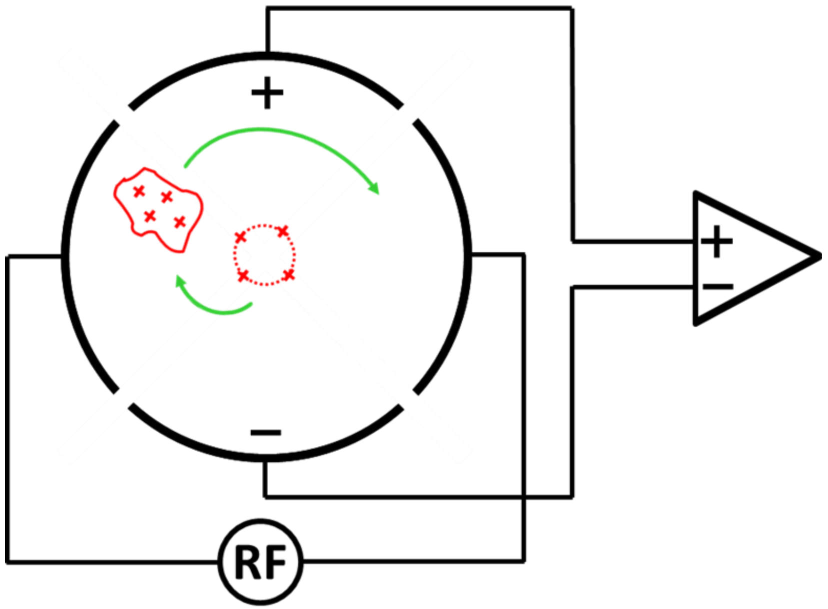

Direct detection of the cyclotron frequency ω_+

$$R_{Dipole} = \nu \cdot T$$

2ω Quadrupolar Detection (QPD)

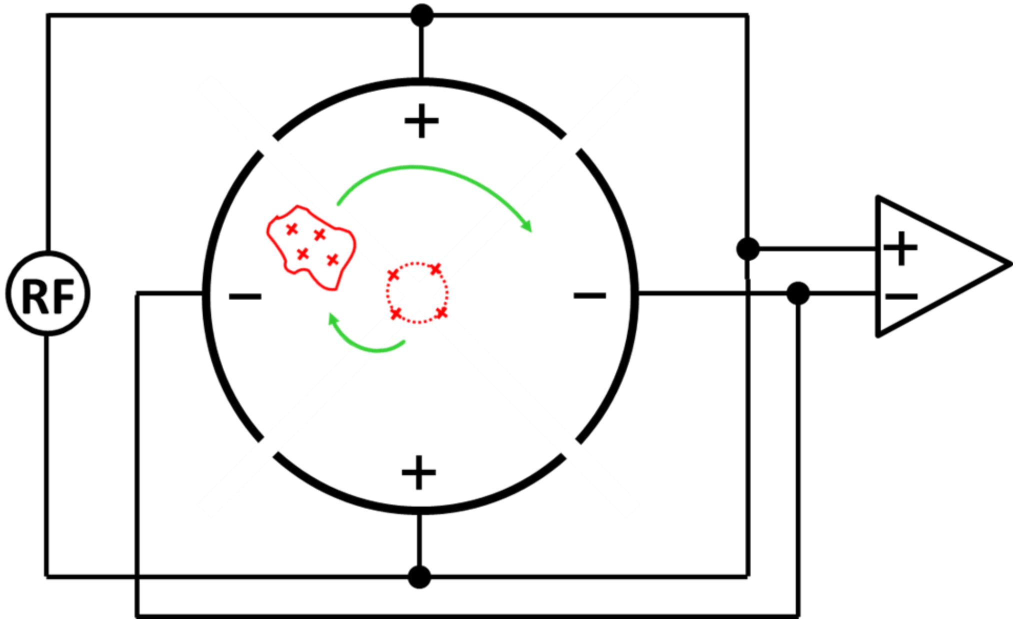

QUADRUPOLE–DETECTION FT-ICR MASS SPECTROMETRY*
L. SCHWEIKHARD, M. LINDINGER and H.-J. KLUGE published 1990

Direct detection of the **double** cyclotron frequency $2\omega_+$

$$R_{QPD} = 2 \cdot \nu \cdot T = 2 \cdot R_{Dipole}$$

→ **Double mass resolution**

Improving S/N and mass resolution

12T 1ω measurement with AMP, APPI, Oil Residue, m/z 250-800

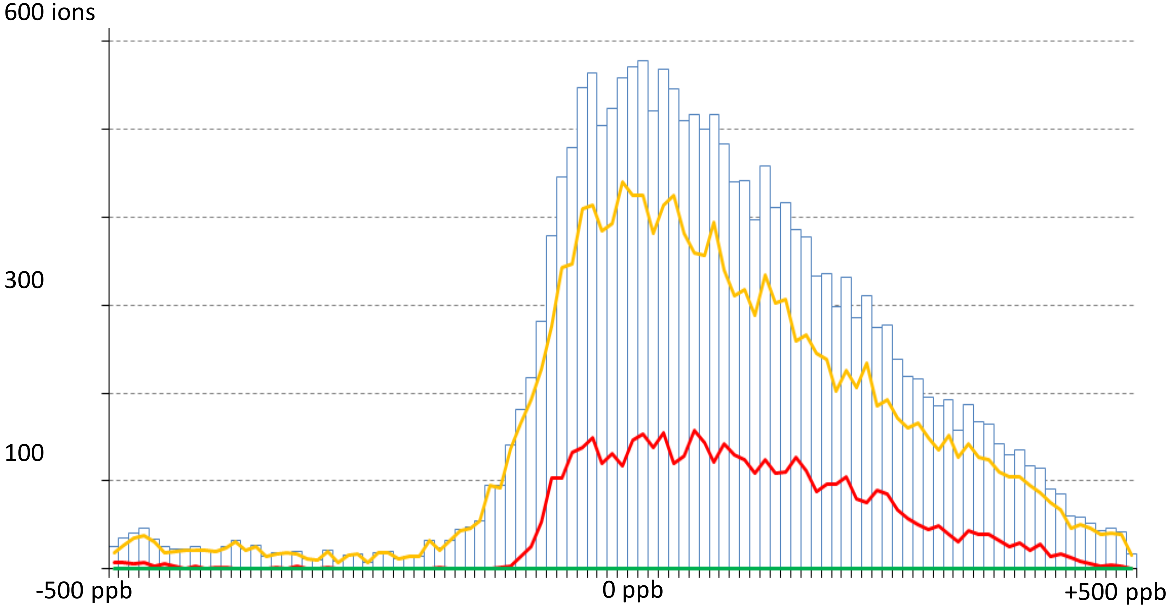

Mass resolution (m/z 400): **1,400,000**
Mass accuracy: **93 ± 161 ppb**
Compounds: **19847**

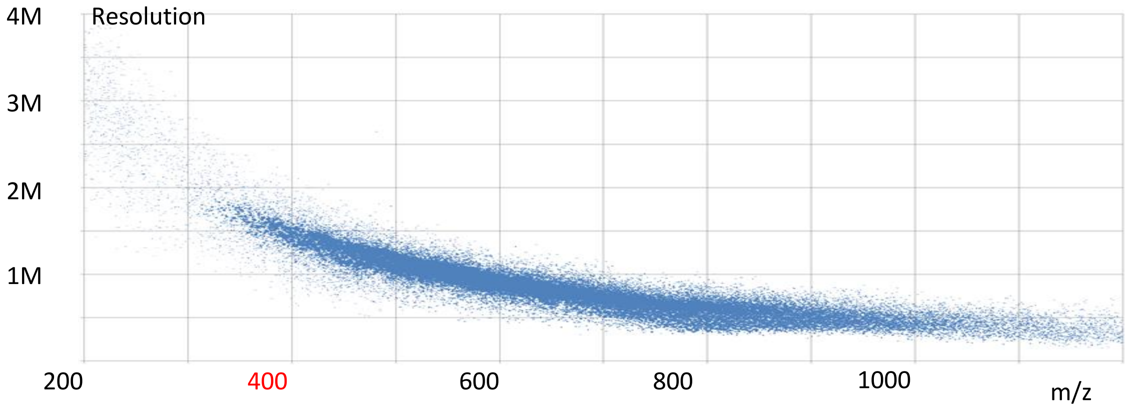

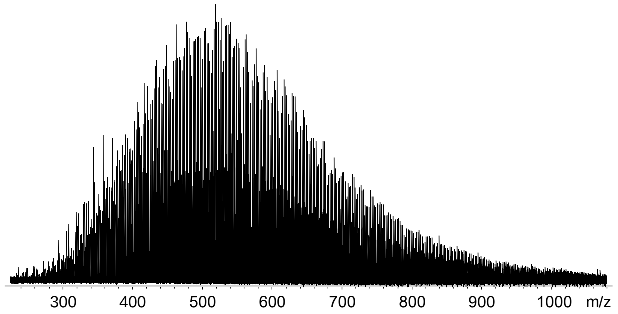

Improving S/N and mass resolution

7T 2ω measurement with AMP, APPI, Oil Residue, m/z 250-800

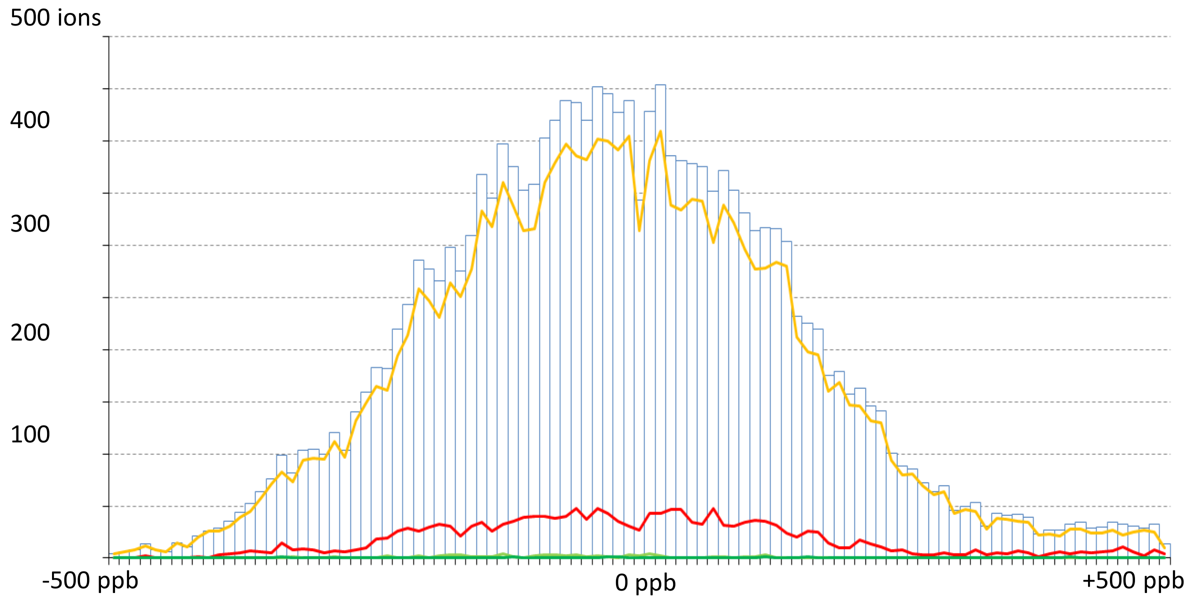

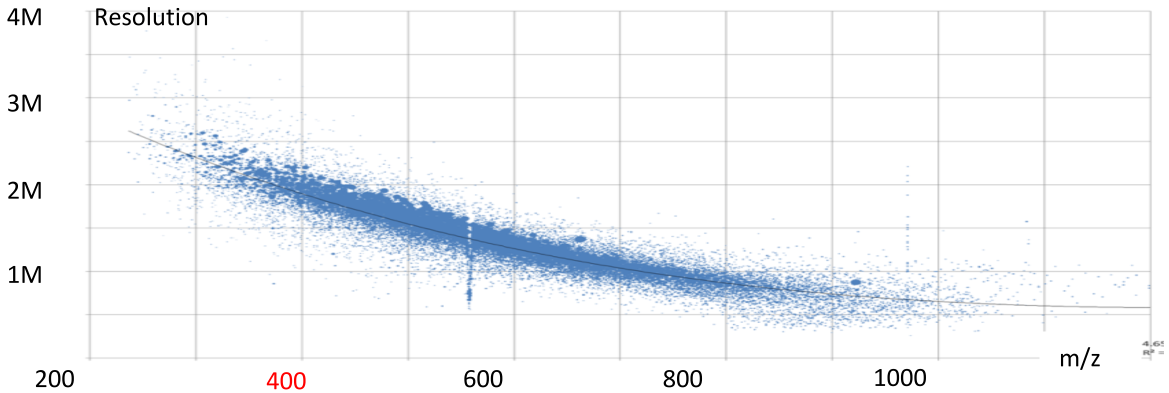

Mass resolution (m/z 400): **1,950,000**
Mass accuracy: **-20 ± 168 ppb**
Compounds: **18200**

m/z	Calc. Res.
300	2368970
400	1950080
500	1600250
600	1313480
700	1083770
800	905120
900	771530
1000	677000

Improving S/N and mass resolution

7T 2ω measurement with AMP, APPI, Oil Residue, m/z 200-800

CASI with 55 Da isolation windows

Isolation mass: m/z 325
Resolution at m/z 325: 3.300.000

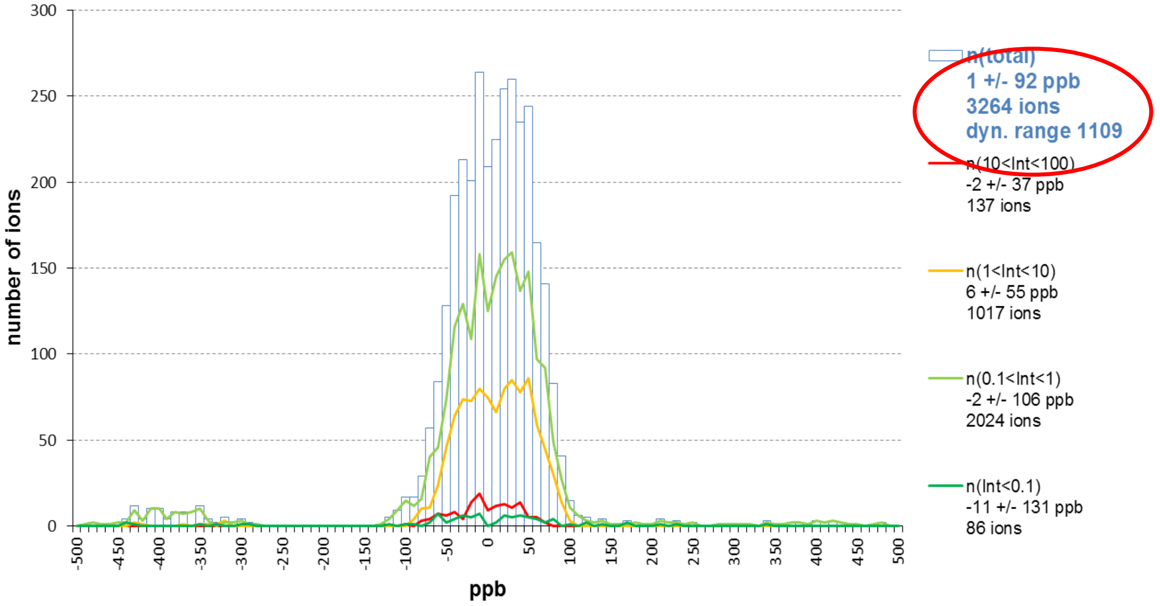

Isolation mass: m/z 525
Resolution at m/z 525: 2.100.000

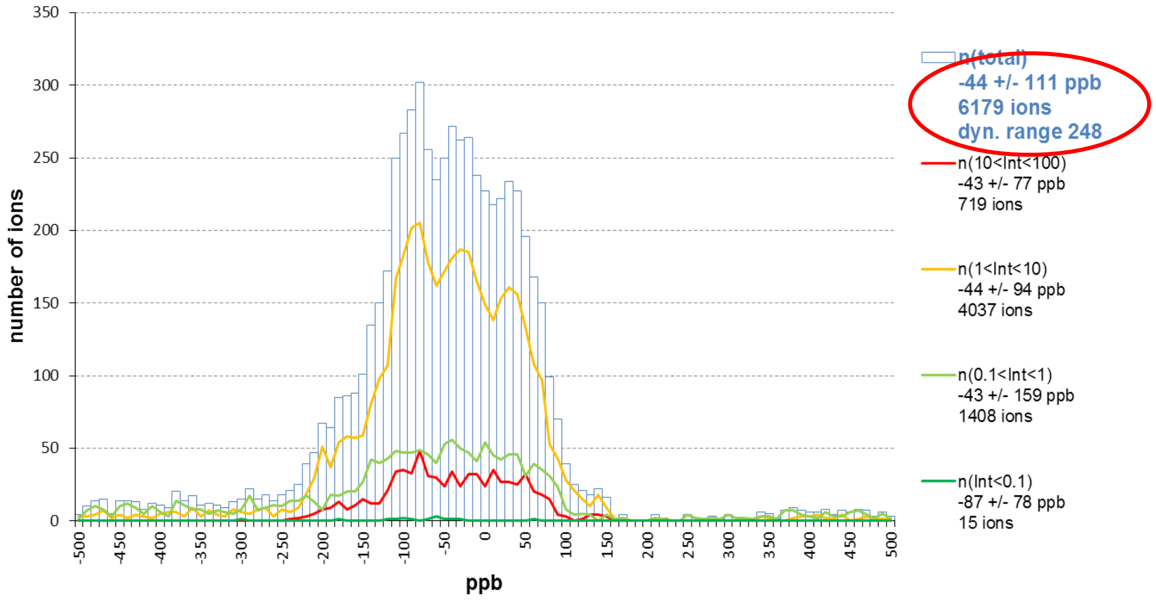

Improving S/N and mass resolution

7T 2ω measurement with AMP, APPI, Oil Residue, m/z 200-800

CASI with 55 Da isolation windows

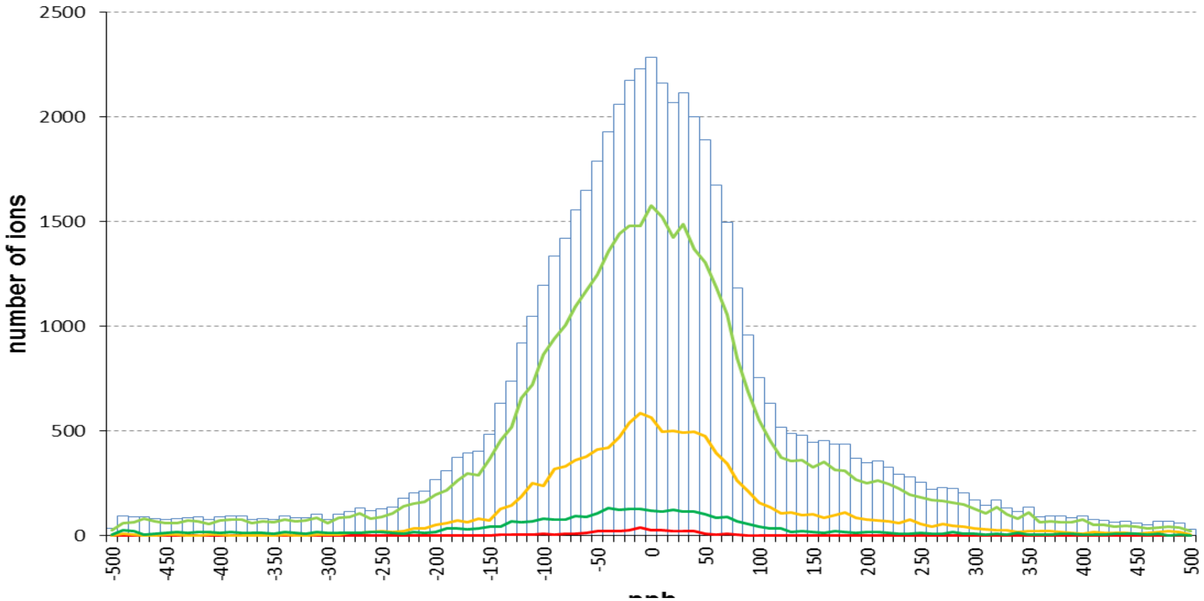

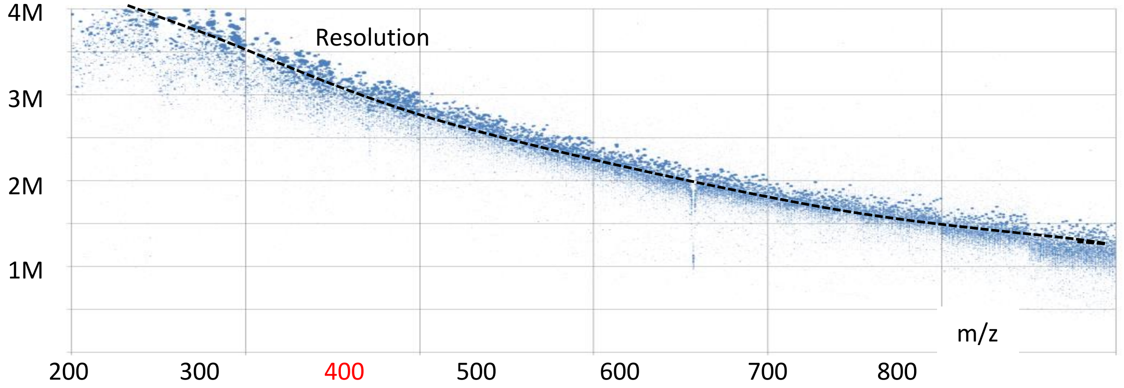

Resolution (m/z 400): **2,750,000**

Mass accuracy: ~~7± 138 ppb~~

Compounds: **52370**

Petrophase 2017 asphaltene

7T solariX 2xR, quadrupolar detection, AMP

Compound classes plot

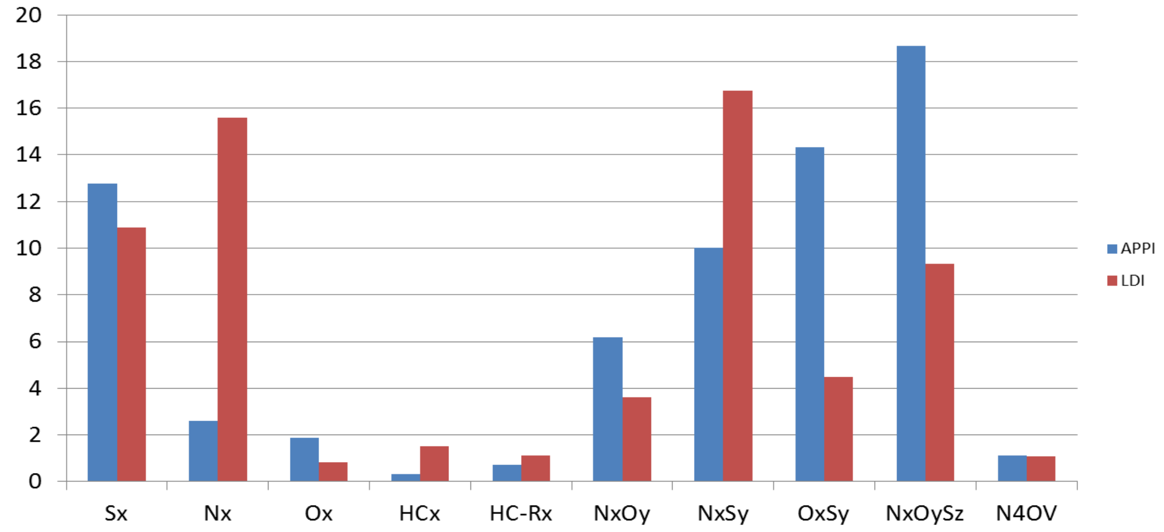

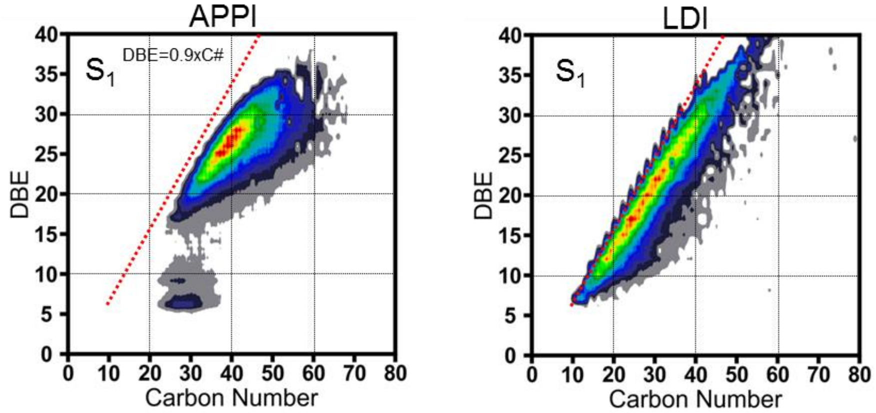

APPI: RMS mass error of 207 ppb (53000 molecular formulae)
LDI: RMS mass error of 248 ppb (42000 molecular formulae)

Resolving power: 1,200,000 @ m/z 400

C (wt. %)	H (wt. %)	N (wt. %)	S (wt. %)
81.78	7.06	1.17	6.82

Hetero atom content

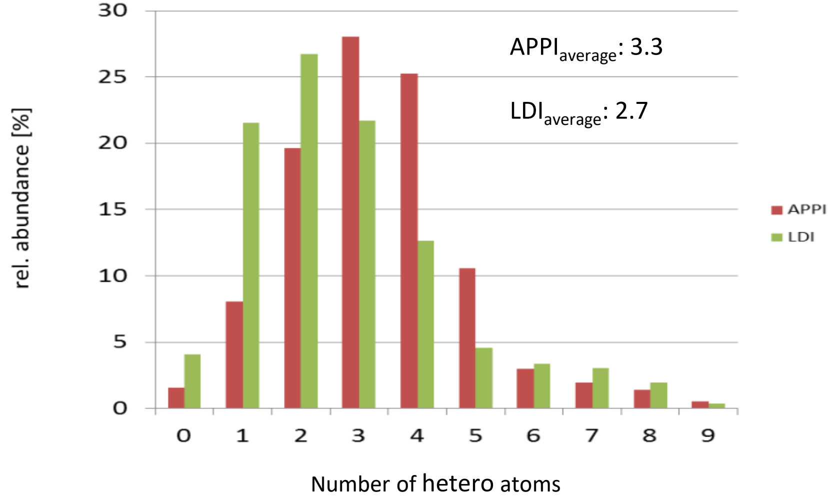

Petroleomics with scimaX

Petroleomics with scimaX

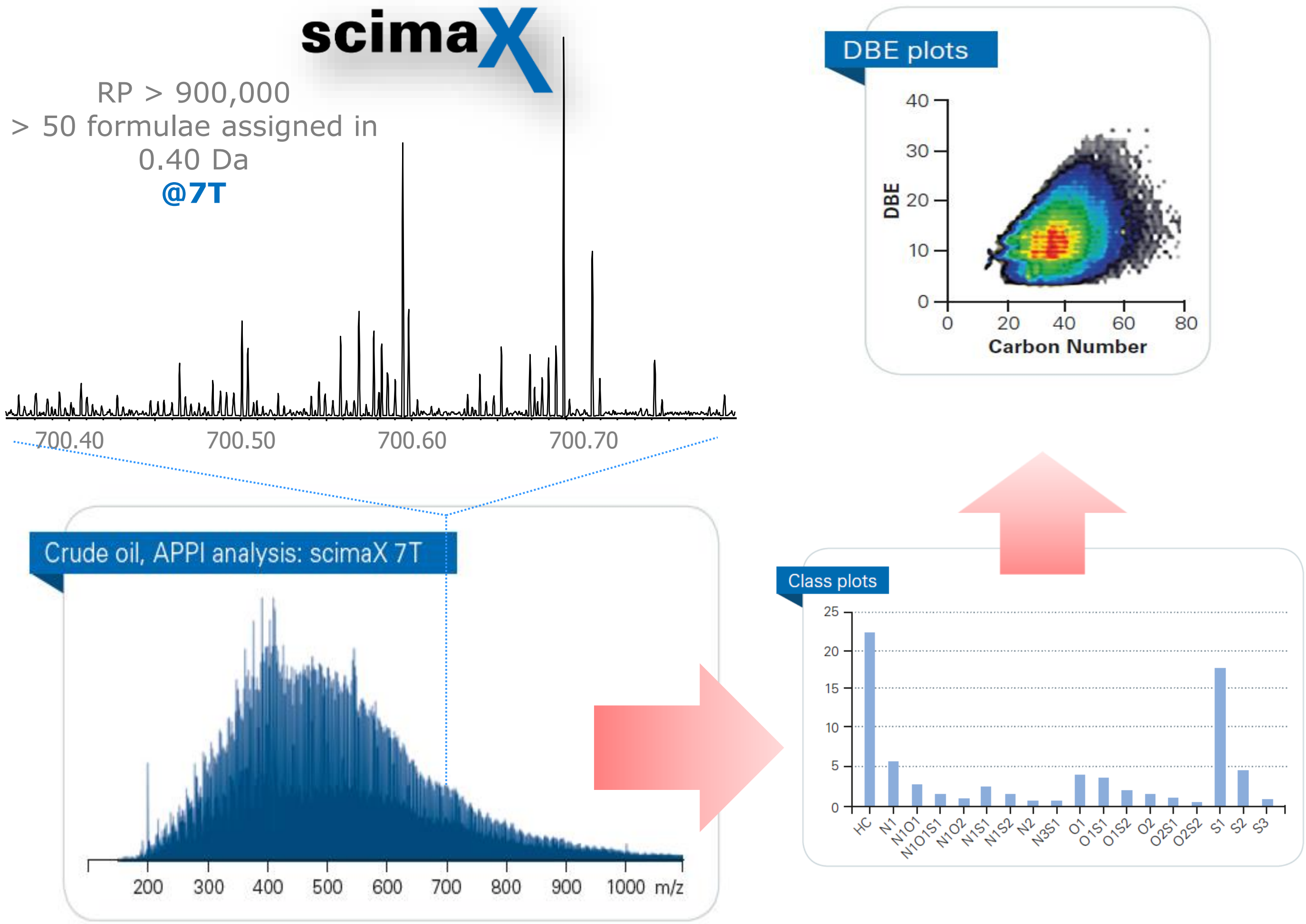

Petroleomics with scimaX

- Study of TAN, corrosion, fouling processes
- 2xR technology
- Easy import of data in Petroleomics software (PetroOrg/Composer) to generate classical plots
- compatible ionization sources to access different molecular species:
  - ESI for basic and acidic compounds
  - LDI, APCI and APPI to access aromatic and non-polar compounds

Summary and Acknowledgements

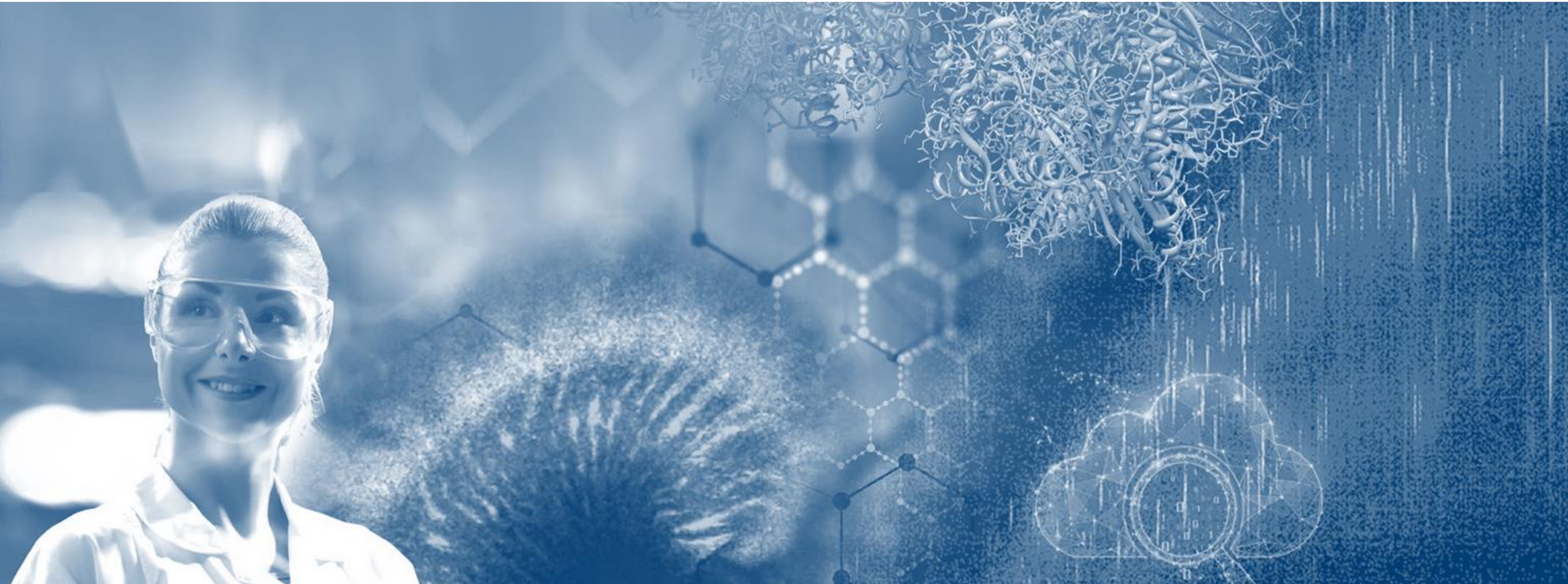

Summary

- LDI of crude oil, shale oil (correlation with acidity, detection of metallo porphyrins)
- Analysis of TLC fractions of crude oil by LDI
- Fingerprint of crude oils by LDI
- Analysis of oil mixtures
- Asphaltene fractions: - different solvent fractions
  - fractions at different solvent power
  - time effects on precipitation
  - island and archipelago structures
- Effect of hydroprocessing
- Continuum of Petroleum
- Fractionation of interfacial material and naphthenic acids
- Bio-oil analysis
- Effect of Maturity
- Improving data quality - Spectra stitching and quadrupolar detection

Acknowledgements

Kyungpook National University, Korea
Shungwan Kim
Yunju Cho

SINTEF, Norway
Kolbjørn Zahlsen
Anders Brunsvik

Chevron, Richmond, CA, USA
Estrella Rogel
Michael Moir

Bruker Daltonics
Jochen Friedrich
Roland Jertz

EU FT-ICR MS